

Radiation-Induced Apoptosis in Mouse Embryonic
Limb Bud Cells *in vivo* and *in vitro*

マウス胚肢芽細胞の生体内および
試験管内放射線誘発アポトーシス

東京大学大学院理学系研究科
生物科学専攻

王 冰

①

学 位 論 文

Radiation-Induced Apoptosis in Mouse Embryonic
Limb Bud Cells *in vivo* and *in vitro*

マウス胚肢芽細胞の生体内および
試験管内放射線誘発アポトーシス

平成8年12月博士(理学)申請

東京大学大学院理学系研究科
生物科学専攻

王 冰

**Radiation-Induced Apoptosis in Mouse
Embryonic Limb Bud Cells**

In Vitro and In Vivo

by

Bing WANG

**Department of Biological Sciences, Graduate School of
Science, The University of Tokyo**

**A Thesis Submitted in a Partial Fulfillment
of the Requirements for the Degree of
Doctor of Science**

December 1996

Introduction	1
Chapter I	1
Chapter II	2
Chapter III	3
Chapter IV	4
Chapter V	5
Chapter VI	6
Chapter VII	7
Chapter VIII	8
Chapter IX	9
Chapter X	10
Chapter XI	11
Chapter XII	12
Chapter XIII	13
Chapter XIV	14
Chapter XV	15
Chapter XVI	16
Chapter XVII	17
Chapter XVIII	18
Chapter XIX	19
Chapter XX	20
Chapter XXI	21
Chapter XXII	22
Chapter XXIII	23
Chapter XXIV	24
Chapter XXV	25
Chapter XXVI	26
Chapter XXVII	27
Chapter XXVIII	28
Chapter XXIX	29
Chapter XXX	30
Chapter XXXI	31
Chapter XXXII	32
Chapter XXXIII	33
Chapter XXXIV	34
Chapter XXXV	35
Chapter XXXVI	36
Chapter XXXVII	37
Chapter XXXVIII	38
Chapter XXXIX	39
Chapter XL	40
Chapter XLI	41
Chapter XLII	42
Chapter XLIII	43
Chapter XLIV	44
Chapter XLV	45
Chapter XLVI	46
Chapter XLVII	47
Chapter XLVIII	48
Chapter XLIX	49
Chapter L	50
Chapter LI	51
Chapter LII	52
Chapter LIII	53
Chapter LIV	54
Chapter LV	55
Chapter LVI	56
Chapter LVII	57
Chapter LVIII	58
Chapter LIX	59
Chapter LX	60
Chapter LXI	61
Chapter LXII	62
Chapter LXIII	63
Chapter LXIV	64
Chapter LXV	65
Chapter LXVI	66
Chapter LXVII	67
Chapter LXVIII	68
Chapter LXIX	69
Chapter LXX	70
Chapter LXXI	71
Chapter LXXII	72
Chapter LXXIII	73
Chapter LXXIV	74
Chapter LXXV	75
Chapter LXXVI	76
Chapter LXXVII	77
Chapter LXXVIII	78
Chapter LXXIX	79
Chapter LXXX	80
Chapter LXXXI	81
Chapter LXXXII	82
Chapter LXXXIII	83
Chapter LXXXIV	84
Chapter LXXXV	85
Chapter LXXXVI	86
Chapter LXXXVII	87
Chapter LXXXVIII	88
Chapter LXXXIX	89
Chapter LXXXX	90
Chapter LXXXXI	91
Chapter LXXXXII	92
Chapter LXXXXIII	93
Chapter LXXXXIV	94
Chapter LXXXXV	95
Chapter LXXXXVI	96
Chapter LXXXXVII	97
Chapter LXXXXVIII	98
Chapter LXXXXIX	99
Chapter LXXXXX	100
Chapter LXXXXXI	101
Chapter LXXXXXII	102
Chapter LXXXXXIII	103
Chapter LXXXXXIV	104
Chapter LXXXXXV	105
Chapter LXXXXXVI	106
Chapter LXXXXXVII	107
Chapter LXXXXXVIII	108
Chapter LXXXXXIX	109
Chapter LXXXXXX	110
Chapter LXXXXXXI	111
Chapter LXXXXXXII	112
Chapter LXXXXXXIII	113
Chapter LXXXXXXIV	114
Chapter LXXXXXXV	115
Chapter LXXXXXXVI	116
Chapter LXXXXXXVII	117
Chapter LXXXXXXVIII	118
Chapter LXXXXXXIX	119
Chapter LXXXXXXX	120
Chapter LXXXXXXXI	121
Chapter LXXXXXXXII	122
Chapter LXXXXXXXIII	123
Chapter LXXXXXXXIV	124
Chapter LXXXXXXXV	125
Chapter LXXXXXXXVI	126
Chapter LXXXXXXXVII	127
Chapter LXXXXXXXVIII	128
Chapter LXXXXXXXIX	129
Chapter LXXXXXXXI	130
Chapter LXXXXXXXII	131
Chapter LXXXXXXXIII	132
Chapter LXXXXXXXIV	133
Chapter LXXXXXXXV	134
Chapter LXXXXXXXVI	135
Chapter LXXXXXXXVII	136
Chapter LXXXXXXXVIII	137
Chapter LXXXXXXXIX	138
Chapter LXXXXXXXI	139
Chapter LXXXXXXXII	140
Chapter LXXXXXXXIII	141
Chapter LXXXXXXXIV	142
Chapter LXXXXXXXV	143
Chapter LXXXXXXXVI	144
Chapter LXXXXXXXVII	145
Chapter LXXXXXXXVIII	146
Chapter LXXXXXXXIX	147
Chapter LXXXXXXXI	148
Chapter LXXXXXXXII	149
Chapter LXXXXXXXIII	150
Chapter LXXXXXXXIV	151
Chapter LXXXXXXXV	152
Chapter LXXXXXXXVI	153
Chapter LXXXXXXXVII	154
Chapter LXXXXXXXVIII	155
Chapter LXXXXXXXIX	156
Chapter LXXXXXXXI	157
Chapter LXXXXXXXII	158
Chapter LXXXXXXXIII	159
Chapter LXXXXXXXIV	160
Chapter LXXXXXXXV	161
Chapter LXXXXXXXVI	162
Chapter LXXXXXXXVII	163
Chapter LXXXXXXXVIII	164
Chapter LXXXXXXXIX	165
Chapter LXXXXXXXI	166
Chapter LXXXXXXXII	167
Chapter LXXXXXXXIII	168
Chapter LXXXXXXXIV	169
Chapter LXXXXXXXV	170
Chapter LXXXXXXXVI	171
Chapter LXXXXXXXVII	172
Chapter LXXXXXXXVIII	173
Chapter LXXXXXXXIX	174
Chapter LXXXXXXXI	175
Chapter LXXXXXXXII	176
Chapter LXXXXXXXIII	177
Chapter LXXXXXXXIV	178
Chapter LXXXXXXXV	179
Chapter LXXXXXXXVI	180
Chapter LXXXXXXXVII	181
Chapter LXXXXXXXVIII	182
Chapter LXXXXXXXIX	183
Chapter LXXXXXXXI	184
Chapter LXXXXXXXII	185
Chapter LXXXXXXXIII	186
Chapter LXXXXXXXIV	187
Chapter LXXXXXXXV	188
Chapter LXXXXXXXVI	189
Chapter LXXXXXXXVII	190
Chapter LXXXXXXXVIII	191
Chapter LXXXXXXXIX	192
Chapter LXXXXXXXI	193
Chapter LXXXXXXXII	194
Chapter LXXXXXXXIII	195
Chapter LXXXXXXXIV	196
Chapter LXXXXXXXV	197
Chapter LXXXXXXXVI	198
Chapter LXXXXXXXVII	199
Chapter LXXXXXXXVIII	200
Chapter LXXXXXXXIX	201
Chapter LXXXXXXXI	202
Chapter LXXXXXXXII	203
Chapter LXXXXXXXIII	204
Chapter LXXXXXXXIV	205
Chapter LXXXXXXXV	206
Chapter LXXXXXXXVI	207
Chapter LXXXXXXXVII	208
Chapter LXXXXXXXVIII	209
Chapter LXXXXXXXIX	210
Chapter LXXXXXXXI	211
Chapter LXXXXXXXII	212
Chapter LXXXXXXXIII	213
Chapter LXXXXXXXIV	214
Chapter LXXXXXXXV	215
Chapter LXXXXXXXVI	216
Chapter LXXXXXXXVII	217
Chapter LXXXXXXXVIII	218
Chapter LXXXXXXXIX	219
Chapter LXXXXXXXI	220
Chapter LXXXXXXXII	221
Chapter LXXXXXXXIII	222
Chapter LXXXXXXXIV	223
Chapter LXXXXXXXV	224
Chapter LXXXXXXXVI	225
Chapter LXXXXXXXVII	226
Chapter LXXXXXXXVIII	227
Chapter LXXXXXXXIX	228
Chapter LXXXXXXXI	229
Chapter LXXXXXXXII	230
Chapter LXXXXXXXIII	231
Chapter LXXXXXXXIV	232
Chapter LXXXXXXXV	233
Chapter LXXXXXXXVI	234
Chapter LXXXXXXXVII	235
Chapter LXXXXXXXVIII	236
Chapter LXXXXXXXIX	237
Chapter LXXXXXXXI	238
Chapter LXXXXXXXII	239
Chapter LXXXXXXXIII	240
Chapter LXXXXXXXIV	241
Chapter LXXXXXXXV	242
Chapter LXXXXXXXVI	243
Chapter LXXXXXXXVII	244
Chapter LXXXXXXXVIII	245
Chapter LXXXXXXXIX	246
Chapter LXXXXXXXI	247
Chapter LXXXXXXXII	248
Chapter LXXXXXXXIII	249
Chapter LXXXXXXXIV	250
Chapter LXXXXXXXV	251
Chapter LXXXXXXXVI	252
Chapter LXXXXXXXVII	253
Chapter LXXXXXXXVIII	254
Chapter LXXXXXXXIX	255
Chapter LXXXXXXXI	256
Chapter LXXXXXXXII	257
Chapter LXXXXXXXIII	258
Chapter LXXXXXXXIV	259
Chapter LXXXXXXXV	260
Chapter LXXXXXXXVI	261
Chapter LXXXXXXXVII	262
Chapter LXXXXXXXVIII	263
Chapter LXXXXXXXIX	264
Chapter LXXXXXXXI	265
Chapter LXXXXXXXII	266
Chapter LXXXXXXXIII	267
Chapter LXXXXXXXIV	268
Chapter LXXXXXXXV	269
Chapter LXXXXXXXVI	270
Chapter LXXXXXXXVII	271
Chapter LXXXXXXXVIII	272
Chapter LXXXXXXXIX	273
Chapter LXXXXXXXI	274
Chapter LXXXXXXXII	275
Chapter LXXXXXXXIII	276
Chapter LXXXXXXXIV	277
Chapter LXXXXXXXV	278
Chapter LXXXXXXXVI	279
Chapter LXXXXXXXVII	280
Chapter LXXXXXXXVIII	281
Chapter LXXXXXXXIX	282
Chapter LXXXXXXXI	283
Chapter LXXXXXXXII	284
Chapter LXXXXXXXIII	285
Chapter LXXXXXXXIV	286
Chapter LXXXXXXXV	287
Chapter LXXXXXXXVI	288
Chapter LXXXXXXXVII	289
Chapter LXXXXXXXVIII	290
Chapter LXXXXXXXIX	291
Chapter LXXXXXXXI	292
Chapter LXXXXXXXII	293
Chapter LXXXXXXXIII	294
Chapter LXXXXXXXIV	295
Chapter LXXXXXXXV	296
Chapter LXXXXXXXVI	297
Chapter LXXXXXXXVII	298
Chapter LXXXXXXXVIII	299
Chapter LXXXXXXXIX	300
Chapter LXXXXXXXI	301
Chapter LXXXXXXXII	302
Chapter LXXXXXXXIII	303
Chapter LXXXXXXXIV	304
Chapter LXXXXXXXV	305
Chapter LXXXXXXXVI	306
Chapter LXXXXXXXVII	307
Chapter LXXXXXXXVIII	308
Chapter LXXXXXXXIX	309
Chapter LXXXXXXXI	310
Chapter LXXXXXXXII	311
Chapter LXXXXXXXIII	312
Chapter LXXXXXXXIV	313
Chapter LXXXXXXXV	314
Chapter LXXXXXXXVI	315
Chapter LXXXXXXXVII	316
Chapter LXXXXXXXVIII	317
Chapter LXXXXXXXIX	318
Chapter LXXXXXXXI	319
Chapter LXXXXXXXII	320
Chapter LXXXXXXXIII	321
Chapter LXXXXXXXIV	322
Chapter LXXXXXXXV	323
Chapter LXXXXXXXVI	324
Chapter LXXXXXXXVII	325
Chapter LXXXXXXXVIII	326
Chapter LXXXXXXXIX	327
Chapter LXXXXXXXI	328
Chapter LXXXXXXXII	329
Chapter LXXXXXXXIII	330
Chapter LXXXXXXXIV	331
Chapter LXXXXXXXV	332
Chapter LXXXXXXXVI	333
Chapter LXXXXXXXVII	334
Chapter LXXXXXXXVIII	335
Chapter LXXXXXXXIX	336
Chapter LXXXXXXXI	337
Chapter LXXXXXXXII	338
Chapter LXXXXXXXIII	339
Chapter LXXXXXXXIV	340
Chapter LXXXXXXXV	341
Chapter LXXXXXXXVI	342
Chapter LXXXXXXXVII	343
Chapter LXXXXXXXVIII	344
Chapter LXXXXXXXIX	345
Chapter LXXXXXXXI	346
Chapter LXXXXXXXII	347
Chapter LXXXXXXXIII	348
Chapter LXXXXXXXIV	349
Chapter LXXXXXXXV	350
Chapter LXXXXXXXVI	351
Chapter LXXXXXXXVII	352
Chapter LXXXXXXXVIII	353
Chapter LXXXXXXXIX	354
Chapter LXXXXXXXI	355
Chapter LXXXXXXXII	356
Chapter LXXXXXXXIII	357
Chapter LXXXXXXXIV	358
Chapter LXXXXXXXV	359
Chapter LXXXXXXXVI	360
Chapter LXXXXXXXVII	361
Chapter LXXXXXXXVIII	362
Chapter LXXXXXXXIX	363
Chapter LXXXXXXXI	364
Chapter LXXXXXXXII	365
Chapter LXXXXXXXIII	366
Chapter LXXXXXXXIV	367
Chapter LXXXXXXXV	368
Chapter LXXXXXXXVI	369
Chapter LXXXXXXXVII	370
Chapter LXXXXXXXVIII	371
Chapter LXXXXXXXIX	372
Chapter LXXXXXXXI	373
Chapter LXXXXXXXII	374
Chapter LXXXXXXXIII	375
Chapter LXXXXXXXIV	376
Chapter LXXXXXXXV	377
Chapter LXXXXXXXVI	378
Chapter LXXXXXXXVII	379
Chapter LXXXXXXXVIII	380
Chapter LXXXXXXXIX	381
Chapter LXXXXXXXI	382
Chapter LXXXXXXXII	383
Chapter LXXXXXXXIII	384
Chapter LXXXXXXXIV	385
Chapter LXXXXXXXV	386
Chapter LXXXXXXXVI	387
Chapter LXXXXXXXVII	388
Chapter LXXXXXXXVIII	389
Chapter LXXXXXXXIX	390
Chapter LXXXXXXXI	391
Chapter LXXXXXXXII	392
Chapter LXXXXXXXIII	393
Chapter LXXXXXXXIV	394
Chapter LXXXXXXXV	395
Chapter LXXXXXXXVI	396
Chapter LXXXXXXXVII	397
Chapter LXXXXXXXVIII	398
Chapter LXXXXXXXIX	399
Chapter LXXXXXXXI	400
Chapter LXXXXXXXII	401
Chapter LXXXXXXXIII	402
Chapter LXXXXXXXIV	403
Chapter LXXXXXXXV	404
Chapter LXXXXXXXVI	405
Chapter LXXXXXXXVII	406
Chapter LXXXXXXXVIII	407
Chapter LXXXXXXXIX	408
Chapter LXXXXXXXI	409
Chapter LXXXXXXXII	410
Chapter LXXXXXXXIII	411
Chapter LXXXXXXXIV	412
Chapter LXXXXXXXV	413
Chapter LXXXXXXXVI	414
Chapter LXXXXXXXVII	415
Chapter LXXXXXXXVIII	416
Chapter LXXXXXXXIX	417
Chapter LXXXXXXXI	418
Chapter LXXXXXXXII	419
Chapter LXXXXXXXIII	420
Chapter LXXXXXXXIV	421
Chapter LXXXXXXXV	422
Chapter LXXXXXXXVI	423
Chapter LXXXXXXXVII	424
Chapter LXXXXXXXVIII	425
Chapter LXXXXXXXIX	426
Chapter LXXXXXXXI	427
Chapter LXXXXXXXII	428
Chapter LXXXXXXXIII	429
Chapter LXXXXXXXIV	430
Chapter LXXXXXXXV	431
Chapter LXXXXXXXVI	432
Chapter LXXXXXXXVII	433
Chapter LXXXXXXXVIII	434
Chapter LXXXXXXXIX	435
Chapter LXXXXXXXI	436
Chapter LXXXXXXXII	437
Chapter LXXXXXXXIII	438
Chapter LXXXXXXXIV	439
Chapter LXXXXXXXV	440
Chapter LXXXXXXXVI	441
Chapter LXXXXXXXVII	442
Chapter LXXXXXXXVIII	443
Chapter LXXXXXXXIX	444
Chapter LXXXXXXXI	445
Chapter LXXXXXXXII	446
Chapter LXXXXXXXIII	447
Chapter LXXXXXXXIV	448
Chapter LXXXXXXXV	449
Chapter LXXXXXXXVI	450
Chapter LXXXXXXXVII	451
Chapter LXXXXXXXVIII	452
Chapter LXXXXXXXIX	453
Chapter LXXXXXXXI	454
Chapter LXXXXXXXII	455
Chapter LXXXXXXXIII	456
Chapter LXXXXXXXIV	457
Chapter LXXXXXXXV	458
Chapter LXXXXXXXVI	459
Chapter LXXXXXXXVII	460
Chapter LXXXXXXXVIII	461
Chapter LXXXXXXXIX	462
Chapter LXXXXXXXI	463
Chapter LXXXXXXXII	464
Chapter LXXXXXXXIII	465
Chapter LXXXXXXXIV	466
Chapter LXXXXXXXV	4

Contents

Acknowledgements	---	1
Abbreviation	---	2
General Introduction	---	4
Chapter I. Effects of radiation on the cellular proliferation, differentiation and apoptosis in the mouse limb bud cell micromass culture system		
Summary	---	13
Introduction	---	15
Materials and Methods	---	18
Results and Discussion	---	25
Figures	---	31
References	---	50
Chapter II. Localization of apoptosis in the limb buds irradiated <i>in utero</i>		
Summary	---	56
Introduction	---	58
Materials and Methods	---	61
Results and Discussion	---	67
Figures and Tables	---	76
References	---	109
Chapter III. Further analysis of the localization of apoptosis in the mouse limb buds in the organ culture system		
Summary	---	114
Introduction	---	116
Materials and Methods	---	118
Results and Discussion	---	122
Figures	---	129
References	---	147
General Discussion and Conclusion	---	149

Acknowledgments

I wish to express my greatest appreciation to Prof. Akihiro Shima of The University of Tokyo and Prof. Takeshi Yamada of Toho University for their supervision and encouragement throughout the course of this study.

I thank Dr. Hiroshi Mitani of The University of Tokyo and Dr. Harumi Ohyama of the National Institute of Radiological Sciences for their experimental instruction and encouragement throughout the course of this study.

I am also indebted to Dr. I. Hayata and Dr. M. Uchiyama of the National Institute of Radiological Sciences for their kind permission to use their machines. I am very grateful to Dr. S. Tone of Tokyo Metropolitan Institute of Medical Science; Dr. H. Takeda, Dr. M. Koike and Dr. S. Tokonami of the National Institute of Radiological Sciences for their valuable instruction, discussion, and kind permission for machine usage.

I deeply appreciate the contributions of Dr. K. Fujita, Ms. K. Watanabe, Ms. C. Ohhira of Toho University for their excellent technical assistance throughout the study. The results presented in the study could not have been obtained without their devoted efforts.

I am thankful to Dr. S. Takayanagi, Dr. K. Oka and Dr. K. Sugimori of Toho University, Prof. O. Nikaido of Kanazawa University, Dr. I. Ishikawa of the National Institute of Radiological Sciences, Dr. T. Shimokawa and Dr. N. Uchida of The University of Tokyo, Mr. S. Hashimoto, Ms. K. Abe and Mr. T. Matsushima of Toho University, for kindly providing me with experimental reagents and technical help.

I also would like to express my sincere gratitude to Dr. Julie Geng of The University of Tokyo for her critically reading this manuscript and kind corrections of English.

Abbreviation

- Aba: Abasophalangy (Absence of proximal phalanx).
- AER: Apical ectodermal ridge.
- Ame: Amesophalangy (Absence of middle phalanx).
- ANZ: Anterior necrotic zone.
- Aph: Aphlangy (Missing digit, but metacarpal or metatarsal is present).
- Ate: Atelephalangy (Absence of distal phalanx).
- Biotin-dUTP: Biotin-16-2'-deoxyuridine-5'-triphosphate.
- Bra: Brachydactyly (General classification for shortness of finger or toe).
- CPDs: Cyclobutane pyrimidine dimers.
- D1 and E1: The day when copulatory plug was found was designated day 1 of gestation for the pregnant mice (D1) or embryonic age day 1 for the embryo (E1).
- DAB: 3,3'-diaminobenzidine.
- Dh: Dominant hemimelia.
- DMEM10: Dulbecco's modified eagle medium, supplemented with 10% fetal calf serum, penicillin 100 IU/ml and streptomycin 100mg/ml.
- DMEM10L: Dulbecco's Modified Eagle Medium, supplemented with 10% fetal calf serum, ascorbic acid (150 ng/ml), L-glutamine (200 ng/ml), penicillin 100 IU/ml and streptomycin 100mg/ml.
- Ect: Ectrodactyly (Missing digit or metacarpal or metatarsal).
- ELISA: Enzyme-linked immunosorbent assay.
- FM: Fluorescence microscopy.
- Free-DNA: low molecular weight DNA.
- HE staining: Heamatoxylin and Eosin staining.

ID50: Inhibitory doses that reduced the value by 50% of the control.

LBC: Limb bud cells.

LM: Light microscopy.

NB: Nile Blue sulphate staining.

p53LI: p53 labelling index (The mean number of p53 positive nuclei per graticule recorded).

PBS: Phosphate buffered saline.

PG: Chondrogenic proteoglycan.

PNZ: Posterior necrotic zone.

(6-4)PPs: (6-4) photoproducts.

Ps: Polysyndactyly.

PZ: Progress zone.

SD: Standard deviation.

SDS-PAGE: 7.5% SDS-polyacrylamide gel electrophoresis.

SDS: 10% sodium dodecyl sulfate.

Syn: Syndactyly (Cutaneous or osseous fusion of adjacent digits).

TDT: Terminal deoxynucleotidyl transferase.

TEM: Transmission electron microscopy.

TUNEL: Terminal deoxynucleotidyl transferase mediated dUTP nick end labeling.

UVC: UVC-irradiation.

WS: The wingless mutation.

ZPA: Zone of polarizing activity.

General introduction

Organogenesis requires a precise maintenance of the balance between cell proliferation, differentiation and loss. Until recently, most of researches were focused on the roles of cell proliferation and differentiation, and the importance of the controlled cell loss, named the programmed cell death, has been ignored. In 1972, the concept of apoptosis, including a programmed process, was first coined out by Kerr *et al.* Detection of cell death throughout embryogenesis demonstrates its importance in the normal organogenesis and function of the organism.

Combining the conclusions by Walker *et al.* (1988), Arends *et al.* (1990) and Bursch *et al.* (1990), histological and morphological changes of apoptosis could be broken down into four steps. (1) The pre-condensation stage during which the genes necessary for apoptosis are induced or recruited from other functions. (2) The condensation stage during which the interactions between the dying cells and their neighbors *in vivo* are lost. Condensation of chromatin into crescent-shaped caps at the nuclear periphery, disintegration of the nucleoli, and reduction of nuclear size and cytoplasmic volumes occur. Also observed are an increase in cell density, compacting of some cytoplasmic organelles, and dilatation of the endoplasmic reticulum. The mitochondria however, remain morphologically normal. (3) The fragmentation phase during which there is blebbing and constriction of both the nucleus and the cytoplasm into multiple, small, membrane-bound apoptotic bodies. And (4) the final stage of phagocytosis and degradation, during which the apoptotic bodies are shed *in vivo* from epithelial surfaces or phagocytosed by neighboring cells. There is progressive degeneration of the residual nuclear and cytoplasmic structures by the lysosomal enzymes

activated in the host cells without the invoking of a complement-based immune response.

Apoptosis is centrally involved in morphogenesis and in the regulation of cell populations in embryos (Sanders and Wride 1995). To date, cell death is known as an important aspect of developmental biology that defines the form of many structures. Its significance is highlighted by alterations of cell death that create numerous developmental abnormalities.

There has been concern in teratogenesis since the beginning of the 20th century. As one of the teratogens, radiation has its unique significance compared to the other biological and chemical factors in experimental study on mechanisms of congenital malformations. Radiation exposure could be administered at any "time point" during development, while most of the biological and chemical teratogens function chronically, and often through metabolic effects.

Radiation effects on the embryo have been of great concern to the public as well as the academic sphere (ICRP 1986; NCRP 1994). Investigation of radiation effects could lead to a more direct explanation to prenatal teratogenic mechanisms during organogenesis. The well-known rule of Bergonié and Tribondeau that radiation killing of cells relates proportionally to cellular proliferation activity and inversely to degree of cellular differentiation. Together with this rule, the concept of "critical period" by Russell is now of great significance (Koneremann 1987). The critical period differs considerably depending on morphogenetic period of each organ concerned.

It has been known that radiation exposure *in utero* at the critical period induces malformation of various organs. Although much attention was paid to the radiation-induced apoptosis in organs and established cell lines

(Potten 1992; Lee *et al.* 1994; Levine *et al.* 1994; Stewart 1994; Montenarch 1995; Reed 1995), few research on how apoptosis functions in the radiation-induced malformation has been conducted (Norimura 1996; Norimura *et al.* 1996).

Cell death is particularly prominent in limb bud development. The most dramatic features of cell death during limb bud morphogenesis are that cell death shapes and contours the digital palettes. The cell death is apoptosis, presumably under pattern-forming controls that related to the normal trophic support encountered throughout life. The normal development of mouse limbs and spontaneous cell death during morphogenesis have been widely studied, and the spontaneous apoptosis demonstrated its decided relation to limb bud pattern formation (Zakeri and Ahuja 1994). The mutant mice are also helpful to understand the important role that apoptotic cell death plays in morphogenesis. Reduction of interdigital cell death during limb bud morphogenesis in the mouse with a transgene insertion in the D region of chromosome 8 finally results in congenital fused toes (van der Hoeven *et al.* 1994).

Establishment of limb bud staging system, success of the limb bud organ culture and the micromass cell culture make it possible to standardize and compare the normal developmental process *in vivo* and *in vitro* (Milaire and Mulnard 1984; Wanek *et al.* 1989; Ide 1990; Flint 1993). Thus the limb is an excellent model to study the mechanisms of radiation teratogenesis. Understanding how radiation exerts its damaging effects on development could (1) provide clues to understand the mechanisms of teratogenesis by other environmental factors, and (2) help us to utilize radiation most effectively in the treatment of disease as well as to provide effective protection against its hazards (Alper 1979; Tubiana *et al.* 1990).

The expression of some genes has been associated with the induction of apoptosis induced by radiation (Hendry *et al.* 1995). The p53 tumor suppressor gene product is induced by a number of DNA damage agents including radiation, and the p53 is involved in both growth arrest and apoptotic cell death in certain mammalian cells. Most cells showed the p53 dependent way for radiation induced apoptosis (Lowe *et al.* 1993a and 1993b; Milas 1994).

Studies using p53 "knock out" mouse revealed that radiation-induced apoptosis in several cells, such as thymocytes and intestinal crypt cells occurred depending on p53, whereas spontaneous physiological apoptosis was independent from p53. Further, the knockout mice gave a good explanation for the relationship between p53 expression and radiation induced apoptosis and resultant phenotypic anomalies (Merritt *et al.* 1994; Norimura *et al.* 1996).

The amount of p53 protein normally is so low as to be virtually undetectable in the cells from adult animals. The p53 is detectable in the embryonic tissues (Schmid *et al.* 1991), but no relation is shown between the increased p53 protein level and spontaneous apoptosis in the embryo of early stages (Norimura 1996). Norimura *et al.* (1996) reported that p53-dependent apoptosis by radiation caused an increase of prenatal death in the early period of organogenesis, which eventually lead to decrease in congenital malformation, such as poly- or megadactyly.

Present study was conducted to clarify the role and mechanisms of apoptosis in the radiation-induced teratogenesis in ICR mouse limb bud. Examinations of limb buds irradiated at the "critical period of the morphogenesis", namely at the embryonic day 11 and 11.5 were done. At this stage, the limb buds are small protrusions consisted of the cellular

masses, which are known to be highly radiosensitive. In the subsequent stage, spontaneous cell death is observed in limb buds, especially in interdigital mesenchymal cells. Three different systems; (1) *in vitro* micromass limb bud cell culture, (2) limb buds irradiated *in utero*, and (3) limb bud organ and tissue culture, were used in this study.

In Chapter I, using the limb bud cell micromass culture system, (1) Radiation inhibitory effects on cellular proliferation and differentiation were observed. (2) Induction of apoptosis in the limb bud cells was identified and quantitated. (3) Changes of p53 protein level in the limb bud cells after irradiation was analyzed.

Data shown in Chapter II were obtained from the limb bud irradiated *in utero* system. (1) Localization of radiation induced apoptosis in limb buds was observed. (2) Difference of limb bud cell radiosensitivity was investigated. (3) Radiation-induced malformation was also examined. Radiation-induced limb bud teratogenesis was thought to be via radiation-induced apoptosis.

Data reported in Chapter III were obtained using the limb bud organ and limb bud tissue-culture system. (1) Results of the limb bud organ cultures were consistent with those obtained from the limb bud *in situ in vivo* study on apoptosis induction by radiation and distribution of radiation-induced apoptosis. (2) Results of the limb bud tissue culture study showed that cells from different anatomic portions had different radiosensitivities. All these data supported the results obtained from both micromass culture study and limb bud *in situ in vivo* study.

References

- Alper T. The significance of cell death. In: Cellular Radiobiology. Ed. T. Alper. Cambridge University Press. 1979. London. pp. 1-5.
- Arends M. J., Morris R. G., and A. H. Wyllie. Apoptosis. The role of endonuclease. *Am. J. Pathol.*, 1990; 136, 593-608.
- Bursch W., Lleine L., and M. P. Tenniswood. The biochemistry of cell death by apoptosis. *Biochem. Cell Biol.*, 1990; 68(9): 1071-1074.
- Flint O. P. In vitro tests for teratogens: desirable endpoints, test batteries and current status of the micromass teratogen test. *Reprod. Toxicol.*, 1993; 7: 103-111.
- Hendry J. H., Potten C. S., and A. Merritt. Apoptosis induced by high- and low LET radiations. *Radiat. Environ. Biophys.*, 1995; 34: 59-62.
- ICRP. Developmental effects of radiation on the brain of the embryo and fetus. In: *Annals of the ICRP*. ICRP Publication 49. Pergamon Press. 1986. New York. pp. 2-30.
- Ide H. Growth and differentiation of limb bud cells in vitro: implications for limb pattern formation. *Develop. Growth Differ.*, 1990; 32: 1-8.
- Kerr J. F. R., Wylie A. H., and A. R. Currie. Apoptosis: A basic biological phenomenon with wide ranging implications in tissue kinetics. *Br. J. Cancer*, 1972; 26, 239-257.
- Konermann G. Postimplantation defects in development following ionizing irradiation. *Adv. Radiat. Biol.*, 1987; 13: 91-167.
- Lee J. M., Abrahamson J. L. A., and A. Bernstein. DNA damage, oncogenesis and the p53 tumor-suppressor gene. *Mutat. Res.*, 1994; 307: 573-581.

- Levine A. J., Perry M. E., Chang A., Silver A., Dittmer D., Wu M., and D. Welsh. The 1993 Walter Hubert lecture: The role of the p53 tumor-suppressor gene in tumorigenesis. *Br. J. Cancer*, 1994; 69: 409-416.
- Lowe S. W., Ruley H. E., Jacks T., and D. E. Houseman. P53-dependent apoptosis modulates the cytotoxicity of anticancer agents. *Cell*, 1993a; 74: 957-967.
- Lowe S. W., Schmitt E. M., Smith S. W., Osborne B. A., and T. Jacks. P53 is required for radiation-induced apoptosis in mouse thymocytes. *Nature*, 1993b; 362: 847-849.
- Merritt A. J., Potten C. S., Kemp C. J., Hickman J. A., Balmain A., Lane D. P., and P. A. Hall. The role of p53 in spontaneous and radiation induced apoptosis in the gastrointestinal tract of normal and p53-deficient mice. *Cancer Res.*, 1994; 54: 614-617.
- Milaire J. and J. Mulnard. Histogenesis in 11-Day mouse embryo limb buds explanted in organ culture. *J. Exp. Zool.*, 1984; 232: 359-377.
- Milas L., Stephen L. C., and R. E. Meyn. Relation of apoptosis to cancer therapy. *In Vivo*, 1994; 8:665-674.
- Montenarch M. Marker genes for cytotoxic exposure: p53. *Stem Cell.*, 1995; 13 (suppl 1): 136 -141.
- NCRP. Considerations regarding the unintended radiation exposure of the embryo, fetus or nursing child. In: NCRP commentary No. 9. NCRP Publications Office. 1994. Bethesda. pp. 3-14.
- Norimura T. p53 suppresses teratogenesis. Proceedings of the Japan radiation research society 39th annual meeting. Kansai medical university Press. 1996. Osaka, Japan. pp 95.
- Norimura T., Nomoto S., Katsuki M., Gondo Y., and S. Kondo. P53-dependent apoptosis suppresses radiation-induced teratogenesis. *Nature Med.*, 1996; 2(5): 577-580.

- Potten C. S. The significance of spontaneous and induced apoptosis in the gastrointestinal tract of mice. *Cancer Metastasis Rev.*, 1992; 11: 179-195.
- Reed J. C. Regulation of apoptosis by bcl-2 family proteins and its role in cancer and chemoresistance. *Curr. Opin. Oncol.*, 1995; 7: 541-546.
- Sanders E. J. and M. A. Wride. Programmed cell death in development. *Int. Rev. Cytol.*, 1995; 163: 105-173.
- Schmid P., Lorenz A., Hameister H., and M. Montenarh. Expression of p53 during mouse embryogenesis. *Develop.*, 1991; 113(3): 857-65.
- Stewart B. W. Mechanisms of apoptosis: Integration of genetic, biochemical, and cellular indicators. *J. Natl. Cancer Inst.*, 1994; 86(17): 1286-1296.
- Tubiana M., Dutreix J., and A. Wambersic. Effects of irradiation on the human body: radiopathology. In: *Introduction to radiobiology*. Translated by D.K. Bewley. Taylor and Francis Press. 1990. New York. pp. 313-368.
- van der Hoeven F., Schimmang T., Volkmann A., Mattei M.-G., Kyewski B., and U. Ruther. Programmed cell death is affected in the novel mouse mutant Fused toes (Ft). *Develop.*, 1994; 120: 2601-2607.
- Walker N. I., Harmon B. V., Gobe G. C., and J. F. R. Kerr. Patterns of cell death. *Methods Achiev. Exp. Pathol.*, 1988; 13: 18-54.
- Wanek N., Muncoka K., Holler-Dinsmore G., Burton R., and S. V. Bryant. A staging system for mouse limb development. *J. Exp. Zool.*, 1989; 249: 41-49.
- Zakeri Z. F. and H. S. Ahuja. Apoptotic cell death in the limb and its relationship to pattern formation. *Biochem. Cell Biol.*, 1994; 72: 603-613.

Chapter I.

Effects of radiation on the cellular proliferation, differentiation and apoptosis in the mouse limb bud cell micromass culture system

Summary

Inhibitory effects from X-irradiation on cellular proliferation and differentiation, and radiation induced apoptosis were investigated in mouse embryonic limb bud cells cultured at a high cell density (micromass culture system). X-irradiation exhibited dose-dependent inhibitory effect on cellular proliferation and differentiation. The inhibitory effects from X-irradiation on cellular differentiation were greater than on cellular proliferation when compared at their ID50 values. In the present micromass culture system, cells irradiated died typically via apoptosis. Induction of apoptosis by X-irradiation of embryonic limb bud cells showed a dose-dependent dose-response relationship. Hoechst staining of apoptotic cells induced by X-rays showed typical chromatin DNA condensation. Time course and dose dependency for apoptotic cell counts were consistent with the appearance of DNA ladder pattern as revealed by electrophoresis. Limb bud cells from embryonic 11 and 11.5 day embryos underwent spontaneous apoptosis and radiation-induced apoptosis with different time courses. p53 protein level investigation by both Western blotting analysis of total cell lysates and immunohistochemical staining of the cultured cells showed a higher level of p53 protein after radiation, but there was no significant increase in amount of p53 protein in cells underwent spontaneous apoptosis.

These results indicated that (1) radiation-induced apoptosis may be an important factor on loss of cell interaction which causes a drastic inhibition on cell differentiation, or more directly by killing those cells that will undergo proliferation and differentiation, (2) there may be the presence of a radiosensitive cell population which undergo radiation-induced apoptosis

after X-irradiation, which would compose of probably those cells that will undergo differentiation in the subsequent stage, (3) radiation-induced apoptosis and spontaneous apoptosis may be caused by some different mechanisms.

Introduction

Micromass culture system

With the progress in methodology, technologically simple but biologically paralleled *in vitro* studies have been widely used due to their merits such as representing the very similar conditions of natural development, providing a large number of genetically homogenous samples, having a good quality control, being repeatable, and being easy for quantity and mechanism analysis of the results. Three years ago, Flint (1993) well described the micromass culture system using rat embryonic limb bud cell or mid brain cell. It is a *de novo* cell maturation system, which is paralleled *in vivo* and *in vitro*. In this micromass culture system, both cellular proliferation and differentiation could be examined. So, it has being widely used in the teratogenetic research. The merits of this system provided us no wander with a suitable candidate for investigating radiation effects on cellular proliferation and differentiation and the early established limb bud pattern formation model was also an effective tool which could further confirm the results from *in vitro* studies (Milaire and Mulnard 1984; Wanek *et al.* 1989).

With these backgrounds, my work first began with the establishment of the micromass system in our laboratory using mouse embryonic limb bud cells (Wang *et al.* 1996). Using this micromass culture system, I investigated the effects of X-irradiation on cellular proliferation, differentiation, and apoptosis induction in order to obtain some basic data for designing the limb bud in situ experiment. UVC-irradiation could cause many biological effects such as mutation due to resulting cellular DNA damage (Friedberg 1985;

Kiefer 1990). In this study, its effects on cellular proliferation and differentiation, as well as DNA damage were also investigated.

Apoptosis and necrosis

Apoptosis is a particular mode of cell death which can be distinguished by a characteristic pattern of morphological and molecular changes (Kerr *et al.* 1972; Wyllie *et al.* 1980). The morphological and biochemical changes were cell shrinkage, cell surface blebbing, degeneration of DNA into internucleosomal fragments and formation of apoptotic bodies. In tissue, the apoptotic cells were phagocytosed by macrophages or their neighboring cells (Walker *et al.* 1988, Arends *et al.* 1990; Bursch *et al.* 1990).

Necrosis is a passive and degenerative process. The early event of necrosis begins with the swelling of cell mitochondria, followed by the rupture of the plasma membrane and release of the cytoplasmic contents (many proteolytic enzymes), which triggers an inflammatory reaction in the tissue, often resulting in scar formation. DNA degradation is not so extensive as in the case of apoptosis, and the products of degradation are heterogeneous in size, and do not form any discrete bands during gel electrophoresis (Kerr and Harman 1991).

p53

Although some cells, such as some of the thymocytes, could undergo radiation induced apoptosis by a p53 independent way (Clarke *et al.* 1993), most cells showed the p53 dependent way when they underwent radiation induced apoptosis (Lowe *et al.* 1993a and 1993b; Merritt *et al.* 1994; Milas *et al.* 1994). As radiation could often induce a significant increase of p53

protein level in the embryonic tissues that underwent radiation-induced apoptosis (Norimura 1996; Norimura *et al.* 1996), in the present study I tried to detect changes of p53 protein content after X-irradiation in the embryonic limb bud cells. If there is an overproduction of the p53 protein in the radiation-induced apoptotic cells in limb buds, detection of the p53 positively stained cells could be used in the *in situ in vivo* study to localize the radiation-induced apoptosis in limb buds.

Significance of apoptosis study

The long-standing interest in apoptosis in variety of disciplines stems from its pivotal role in processes such as tissue development and organogenesis in embryology (Tomei and Cope 1991). Knowledge of apoptosis in developmental radiation biology will be helpful in understanding not only physiological embryogenesis and aging (Tomei *et al.* 1994) but also developmental pathogenesis such as radiation-induced teratogenesis. Apoptosis also plays an important role in such as the frequency of spontaneous apoptosis which is associated with progression of tumor malignancy (Potten 1992). The inherent capacity of tumor cells to respond by apoptosis correlates with expression of several oncogenes or tumor suppressor genes such as bcl-2, c-myc, ras, or p53, and may be prognostic of the treatment (Arends *et al.* 1990; Arends and Wyllie 1991; Tomei and Cope 1991; Wyllie 1992; Schwartzman and Cidowski 1993). Apoptosis may be triggered by tumor radiotherapy (Hickman 1992), so that research in apoptosis is also a great interest in oncology. The knowledge of apoptosis will be helpful in developing new radiotherapeutic strategies.

Materials and Methods

Micromass culture

Animals: ICR mice aged 8 - 10 weeks, weighing 22-26 g were used in this study. Females in estrus were mated with potent males overnight. The day when copulatory plug was found was designated day 1 of gestation (D1) or embryonic age day 1 for the embryo (E1).

Cultures and media: Details of the technique used for limb bud cell (LBC) cultures were essentially the same as described by Flint and Orton (1984) and Flint (1993) with some modifications. In brief, on day 11 of gestation, fore- and hind- limb buds were excised from the embryos in Ca^{2+} and Mg^{2+} -free Tyrode's solution, and treated with 0.25% trypsin-EDTA solution (Difco) at 37 °C for 20 min. Then after pipetting and filtration of the tissue dissociated cell suspension, the concentration of LBC was adjusted to 2×10^7 cells/ml. 24 well multi-well plates (16 mm in diameter, Falcon 3847) were used for culture at a volume of 10 μl cell suspension placed on the center of each well. After being incubated for 2 hr at 37 °C with 5% CO_2 and 95% air for cell attachment, radiation was performed in the experimental groups, then each well was fed with 1ml of culture medium, DMEM10 (Dulbecco's modified eagle medium, GIBCO, supplemented with 10% fetal calf serum, Flow Laboratories, penicillin 100 IU/ml and streptomycin 100mg/ml, GIBCO). The cells were incubated at 37 °C with 5% CO_2 and 95% air for 4 days.

X-ray irradiation

Irradiation of LBC cultures without medium was performed at room temperature with an X-ray machine (Pantak-320S, Shimadzu, Japan),

operated at 200 kVp and 19 mA, with a dose rate of 90R/min using a 0.5 mm Al + 0.5 mm Cu filter.

UVC-irradiation

UV light source was a germicidal lamp (Model UVG-54, Ultra-Violet Prod., INC., San Gabriel, Calif., USA), which emitted light mainly in the short wavelength range (UVC) with the peak at 254nm. The fluence rate was 0.5W/m² as determined by a UV digital radiometer (Model UVX Digital Radiometer, Ultra-Violet Prod., INC., San Gabriel, Calif., USA) with its Model UVX-25 sensor. Irradiation was performed 2 hr after seeding. The cells were irradiated with various doses of UVC without the medium.

Measurements of cellular proliferation and differentiation

Assay of cellular proliferation (total cell count)

Cell suspension was prepared in each group by the treatment of cultures with 0.25% trypsin-EDTA for 20 min at 37 °C. Cell number for each well after 4 day culture was measured by staining with Trypan Blue, and counting with a Fuch's Rosenthal haemocytometer.

Assay of cellular differentiation (chondrogenesis)

Cultures of the remaining wells in each group were used for both counting of the chondrogenic nodules stained with Alcian Blue and estimation of chondrogenic proteoglycan (PG). Cell layers were fixed with 10% formaldehyde containing 0.5% cetylpyridinium chloride (Nakarai tesque, Tokyo, Japan), pH 7.2, overnight, then washed thoroughly with 3% acetic acid adjusted to pH 1.0 with HCl, and stained with 0.5% Alcian Blue

3GX (Fluka) in 3% acetic acid solution overnight. After washing with 3% acetic acid, pH 1.0 to remove non-specific staining, the number of the nodules in each well was scored by scanning into a Power Macintosh computer (6100/60AV, Apple computer Inc, U. S. A.). Manipulation and analysis were performed by displaying the images on the monitor, digitizing the signal of darkness, and transferring the signal to the image processing software. Thus, the results were expressed digitally.

Assay of total protein content

Cell lysates of cultures were used to estimate the protein content per well using a Micro CBA Protein Assay Reagent Kit (PIERCE, Rockford, IL, U.S.A.). The procedure was that described in the Kit Instructions using the bovine serum albumin as a standard.

Assay of PG content

To measure PG quantitatively, Alcian Blue that bound specifically to PG was extracted overnight at room temperature with 0.3 ml of 10% sodium dodecyl sulfate (SDS) under gentle shaking. An aliquot of 0.2 ml extracts from each well was transferred to a 96-well microtiter plate and the absorbancies of the extracts at 620 nm were measured spectrophotometrically using an Immuno Reader NJ-2000 (Inter Med, U.S.A.). The absorbancy values of the extracts were used as a measure of PG production, and the value of per well in each dose group was used as the index.

Enzyme-linked immunosorbent assay (ELISA) of UV induced

damage in the genome overall

The extraction of DNA from cells was the same as described by Funayama *et al.* (1993). In brief, cells were lysed by the addition of lysis buffer (20 mM Tris-HCl (pH 8.0), 20 mM EDTA, 0.5% SDS, and 0.2mg/ml Range), and incubated at 37 °C for 3 hr. Following the addition of proteinase K (final conc. 0.2mg/ml), the lysates were incubated at 50 °C for 3 hr. They were extracted twice with phenol and once with chloroform. The DNA solutions thus obtained were concentrated by extraction with 2-butanol, and dialyzed 3 hr at 4 °C against UV endonuclease buffer (30 mM Tris-HCl, 40mM NaCl and 1 mM EDTA (pH 8.0)).

The procedure of ELISA was essentially the same as described by Mori *et al.* (1991). Polyvinylchloride flat-bottom microtiter plates (Nunc, DELTA SI B, Denmark) were incubated with genomic DNA of LBC cells (0.2 mg/ml for CPDs assay and 3mg/ml for (6-4)PPs assay, 50ml/well) in PBS at 37 °C for 16-20 hr. The monoclonal antibody TDM-2 against CPDs or 64M-2 against (6-4)PPs was added to wells (in quadruplicate) and incubated at 37 °C for 90 min. These monoclonal antibodies were gifts from Prof. O. Nikaido of Kanazawa University. The plates were incubated with affinity-purified goat anti-mouse immunoglobulin G (IgG) conjugated with peroxidase (Zymed, San Francisco, CA) at 37 °C for 90 min. Finally the substrate solution, consisting of 0.04% o-phenylene diamine and 0.007% H₂O₂ in citrate-phosphate buffer, was added to each well. Two molar H₂SO₄ was added to stop the reaction and the absorbancy at 490 nm was measured using a Microplate Reader Model 450 (Bio-Rad).

Identification and quantification of apoptosis

Fluorescence microscopy (FM)

For morphological examination by fluorescence microscopy, limb bud cells were washed with PBS and fixed with 1% glutaraldehyde in 0.1 M phosphate buffer. The samples were stained with Hoechst 33342 (Sigma), and the number of chromatin-condensed cells were counted.

Electrophoresis

Free-DNA (low molecular weight DNA) was isolated by a modification of the method of Ohyama and Shimokawa (1995) and Selins and Cohen (1987). Limb bud cells in pellet was washed with PBS, re-suspended in lysis buffer, centrifugated at 16000 rpm to remove high molecular weight DNA and other undissolved materials. An aliquot of the supernatant containing low molecular weight DNA was incubated with DNA-free RNase A and proteinase K (Boehringer Mannheim Biochemica, Mannheim, Germany) in sequence. Then free-DNA was precipitated with NaCl and isopropanol solution overnight at -20 °C. After centrifugation, they were dried and re-suspended in Tris-HCl and EDTA buffer. 123 base pairs DNA ladder (GIBCO BRL, Life technologies, INC) was used as the ladder DNA marker. DNA fragmentation was investigated with 1.3% agarose (Bio-Rad Laboratories, Richmond, CA, USA) and 0.65% synergel (Diversified Biotech, Boston, MA, USA) gel electrophoresis performed at 10 V/cm for 2 hr. DNA was visualized under UV light and photographed.

Assay of p53 protein

Western blotting analysis.

Western blot analysis was performed by conventional conditions as described (Koike *et al.* 1995; Takahashi and Ohnishi 1995). Cell lysates were boiled, cleared by centrifugation, and the supernatant was quantitated using Bio-Rad Protein Assay Kit (Bio-Rad Laboratories, Life Science Group, New York, USA) and a DU-65 spectrophotometer (Beckman Instruments, INC. Fullerton, CA, USA). Proteins were separated by 7.5% SDS-polyacrylamide gel (SDS-PAGE). After electrophoretic transfer onto a nitrocellulose membrane (0.45 μ m, NT-31 Finetrap, Eido INC, Tokyo, Japan) and blocking non-specific binding sites with 1% bovine serum albumin, the membrane was incubated with 1 μ g/ml anti-p53 antibody (clone AB565, Chemicon International INC, USA). The corresponding protein was visualized using an Immun-Blot Assay Kit (Bio-Rad Laboratories, Life Science Group, New York, USA) and the procedures were done according to its instruction manual. The resulting bands were quantitated using a computer with a NIH image analyzer (Version 1.54, National Institutes of Health, USA).

p53 immunohistochemical staining of cultures

Cultures were fixed with 3% buffered formalin and subsequently processed with 100% methanol. Endogenous peroxidase activity was blocked by incubation with 1% hydrogen peroxide. Samples were exposed to a 10% solution of normal non-immune goat serum, then exposed to 1 μ g/ml anti-p53 antibody (clone AB565, Chemicon International INC, USA). The correspondingly stained cells were visualized using an Immun-Blot Assay Kit (Bio-Rad Laboratories, Life Science Group, New York, USA) and the

procedures were done according to its instruction manual. Cultures were photographed using a color CCD TV camera (ELMO Co., LTD, Japan) and the resulting intensity was quantitated using a computer (Power Macintosh 6100/60AV, Apple Computer Inc, USA) with a NIH image analyzer (Version 1.54, National Institutes of Health, USA).

Statistical analysis

Paired *t*-tests, the chi-squared or Student's *t* tests were performed to detect differences of index percentages between the irradiated and sham operated control. Data are presented as mean value \pm SD. All *P* values tested were two-sided. A *P* value <0.05 was considered significant.

Results

Inhibition of cellular proliferation and differentiation

The total cell number of the un-irradiated limb bud cell cultures after 4 day culture became about 4 times of the initial number, the doubling time being about 48.8 hr. Immediately after cell dissociation from tissues, there was no Alcian Blue-stainable cells, and the appearance of nodule producing PG occurred between 1 and 3 days after plating. The cultures on the 4th day showed 252 ± 35 chondrogenic nodules in each well which could be stained by the Alcian Blue and was surrounded by the non-PG-producing cells (Fig. I-1). When the freshly isolated limb bud cells were irradiated with X-rays at 2 hours after incubation, both number and size of PG-producing nodules on the 4th day were decreased (Fig. I-2). X-irradiation effects on limb bud cell proliferation and chondrogenesis were shown in Fig. I-3. X-rays induced a dose-dependent inhibitory effect on cellular proliferation and chondrogenesis (numbers of total cells and that of PG-producing nodules at 4th day). The formation of PG-producing nodules was more sensitive to radiation than the cellular proliferation with ID50 (their inhibitory doses that reduced the value by 50% of the control) of about 5.2 and 6.1 Gy, respectively (Fig. I-3).

In the case of UVC-irradiation, similar results were found regarding the inhibitory effects. Fig. I-4 showed UVC effects on LBC proliferation and differentiation. UVC induced a dose-dependent inhibitory effect on the LBC proliferation and differentiation. The formation of PG-producing nodules was more sensitive to UVC-irradiation than the cellular proliferation when compared at their ID50 values.

Induction of DNA Damage by UVC

Cyclobutane pyrimidine dimers (CPDs) and (6-4) photoproducts ((6-4)PPs) were two kinds of major DNA damage caused by UV-irradiation (Kiefer 1990). Fig. I-5 (a) showed the results of UVC on induction of CPDs and (6-4) 6-4)PPs. The dose-dependent induction of CPDs and (6-4)PPs was observed. For the DNA repair kinetics, data were illustrated in Fig. I-5 (b). Results indicate that LBC removed both CPDs and (6-4)PPs through the excision repair. The repair for (6-4)PPs was faster than that for CPDs among these cells.

Inhibition of total protein content and PG content

X-rays decreased the total protein and PG contents per well. The effect of X-rays on inhibition of PG production per well was greater than on the total protein content per well when compared at their ID 50 values (Fig. I-3). The ID50 values for total protein and PG content were 5.8 Gy and 3.6 Gy, respectively.

The ID50 of UVC for PG production per well was 6.3J/m². Comparing to its ID50 value on proliferation, this result showed that PG production was a more sensitive index for evaluation of UVC effects on inhibition of differentiation.

Induction of apoptosis

Fig. I-6 was the morphological observation by fluorescence microscopy. Radiation increased the number of cells with typical chromatin condensation (Fig. I-6). Gel electrophoresis for free-DNA extracted from irradiated cells

visualized a typical "DNA ladder" pattern. Fig. I-7 showed the photos of gel electrophoresis of DNA extracts of cells from both E11 and E 11.5 embryos after 5 Gy irradiation. The degree of DNA fragmentation reflected the trends of apoptosis time course. By counting the number of cells with condensed chromatin, I found the different apoptosis time courses for the cells from E11 and E11.5 embryos (Fig. I-8 and Fig. I-9). I also found that the induction of apoptosis was dose-associated, and this was true for both cells from E11 and E11.5 embryos (Fig. I-9).

Increase of p53 protein in both cell lysates and cultures

Typical stainings for p53 protein were demonstrated in Fig. I-11 and Fig. I-12 by Western blot analysis and immunohistochemical staining of cultures, respectively. Results by Western blot analysis showed that after 5 Gy irradiation, there was a detectable increase of p53 protein at 30 min with a peak at 3 hr after radiation followed by decline. The increase of p53 protein was dose-associated. Cultures irradiated showed mild to strong positive staining for p53 protein with radiation dose increased (Fig. I-12). Fig. I-13 and Fig. I-14 were results quantitated from the graphic data presented in Fig. I-11 and Fig. I-12, respectively, using graphic processing methods.

Discussion

The micromass culture is a system highly sensitivity to teratogens such as chemicals (Renault *et al.* 1989) and radiation (Garrison and Uyeki 1988). Limb bud cell micromass cultures exhibit extensive histotypic cellular reorganization and maturation and undergo proliferation and differentiation within 4 days, and their quantification could be done by a relatively simple procedure. Investigation of radiation induced apoptosis in such an *in vitro* system provided us a model of both cellular proliferation and differentiation of normal cells interrupted by radiation. In addition, as the present system is a *de novo* system, these data obtained from *in vitro* study may also reflect an *in vivo* situation.

In the micromass culture system, cell could repair UVC-induced DNA damage. Both X-irradiation and UVC-irradiation inhibited cellular differentiation more effectively than cellular proliferation in the present micromass culture system. Though the interruption of adhesion and interaction may play an important role in the present system (Moscona 1975; Solursh and Reiter 1980), when taking the *in vivo* situation of limb bud morphogenesis into account, I believe that these data indicated the difference of cell characters in response to radiation. Regarding the commitment to spontaneous apoptosis, the limb bud cell micromass culture seemed to include roughly two kind of cells: the cells which will continue to undergo proliferation and differentiation, and the cells that will undergo spontaneous apoptosis. The current knowledge status from studies on the genetic pathways that control apoptosis in the vertebrate limb formation leaves many questions rather than answers to us. It is not clear, for example,

whether any of the events in the apoptosis are common to all cell types. Can some cell types be killed more easily than others? How is about the genetic status of such cells? I found that radiation induced cell death via typical apoptosis with the p53 protein overproduction. As there is usually a relation between p53 gene overexpression and occurrence of apoptosis, investigation of p53 overexpression would be used in the limb bud in situ *in vivo* study. As one of the interesting points I found during these experiments, that cells from different embryonic days responded to radiation with different radiosensitivities regarding apoptosis. This indicated that some of embryonic cells of different developing stages may be already differently committed. These *in vitro* results may reflect the developmental condition of limb bud mesenchymal cells *in vivo* regarding to their radiosensitivities.

The micromass culture was a partial model of the events taking place in the whole embryo (Flint *et al.* 1984). Data presented in this chapter provided us a clue to understand the events happened after radiation in the limb buds. Taking the documented information relating to the normal development of limb buds into account, the present data led us some hypotheses that (1) radiation may exert its deleterious effects on development of limb buds via apoptosis *in vivo*, (2) the mesenchymal cells composed of different populations of radiosensitivity, (3) spontaneous apoptosis and radiation-induced apoptosis may have different molecular mechanisms, and (4) radiation induced apoptosis may have a relation to radiation induced teratogenesis on the morphogenesis during embryogenesis *in vivo*.

As one of the classic triad of radiation embryologic syndromes, the congenital malformations could be induced with greatest effectiveness

during the period of organogenesis. The organogenesis period of the mouse was from E6.5 to E12. The incidence of gross congenital malformations peaks at the early stage and falls off rapidly as organogenesis diminishes (Brent 1977). According to the data from micromass culture investigation and taking the development time of mouse limbs (from E9) into account, an X-ray dose of 5.0 Gy was finally chosen to be used in the following experiments.

In the following two chapters, efforts were made to prove those hypotheses using limb bud in situ *in vivo* and whole limb bud and limb bud tissue cultures *in vitro* studies, respectively.

a	b
c	d

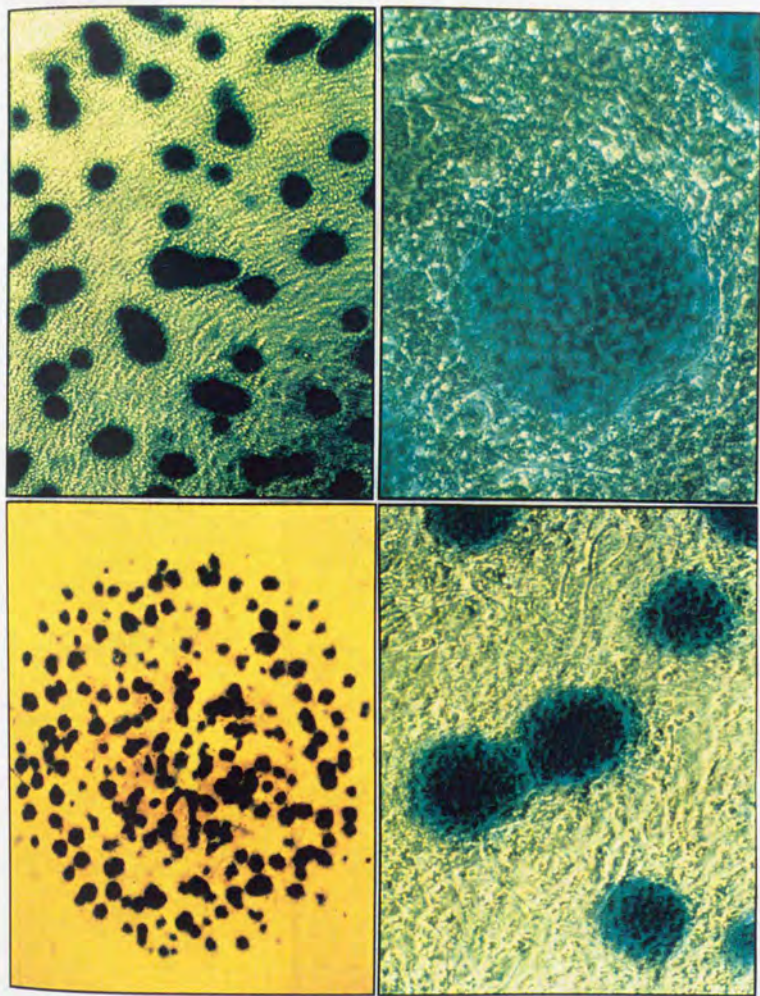
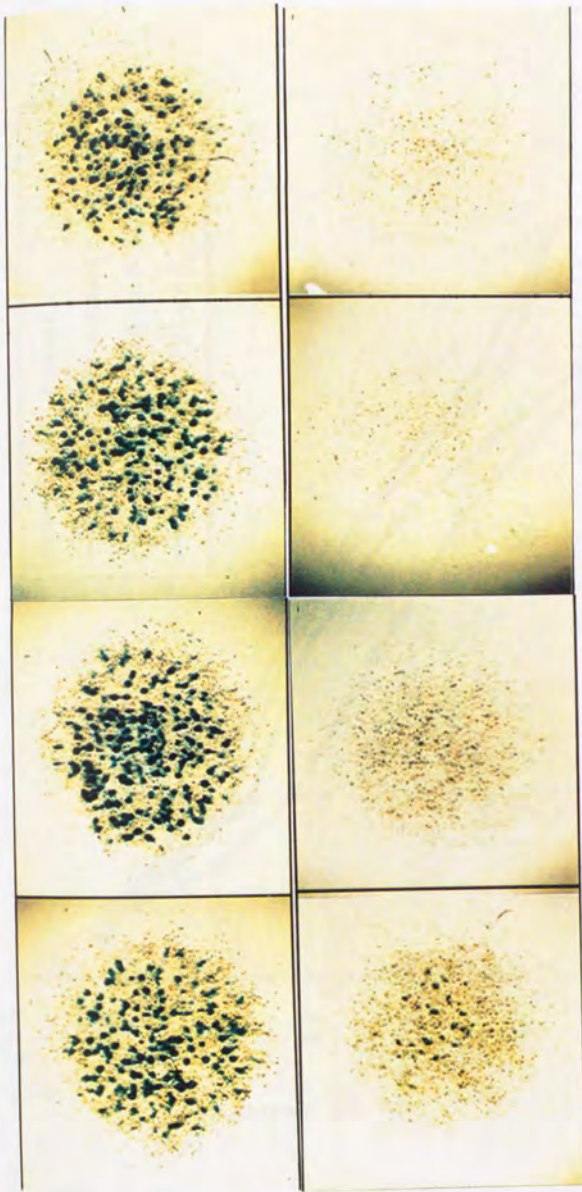


Fig. I-1. Appearance of a mouse embryonic limb bud cell culture of control stained with Alcian Blue on the 4th day after incubation.



a	b	c	d
e	f	g	h

Fig. 1-2. Appearance of mouse embryonic limb bud cell cultures of the control and the irradiated groups stained with Alcian Blue on the 4th day after X-irradiation.

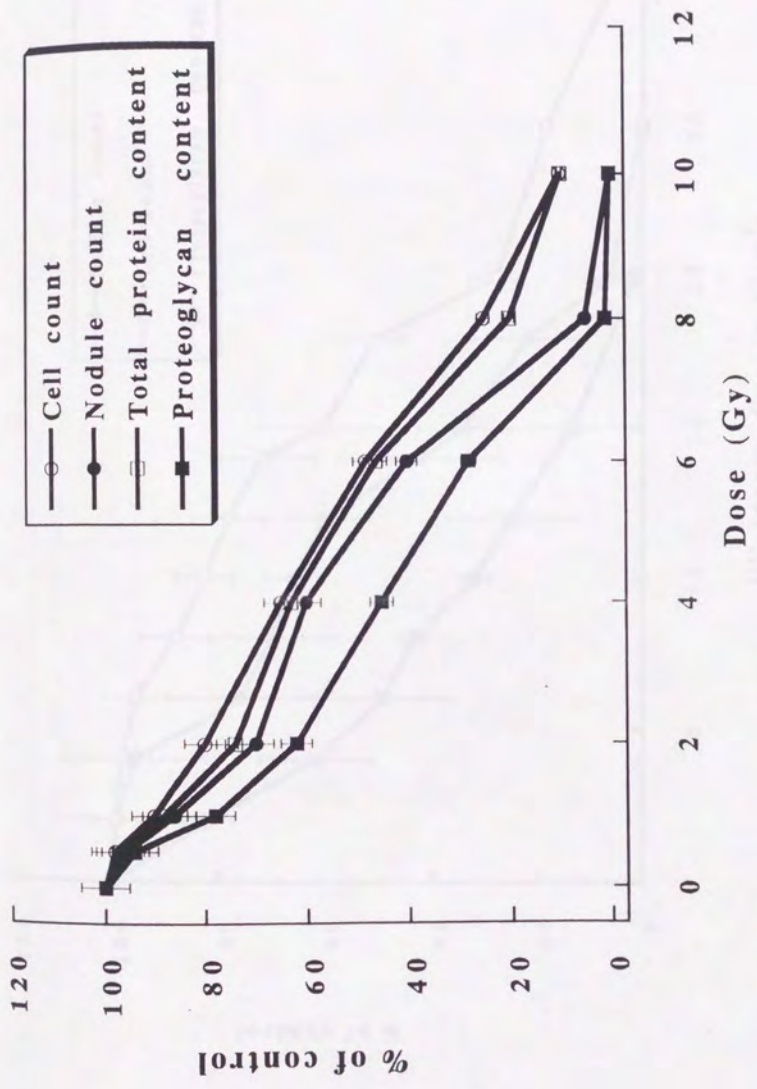


Fig. 1-3. Inhibitory effects of X-irradiation on cellular proliferation and differentiation in the limb bud cell culture.

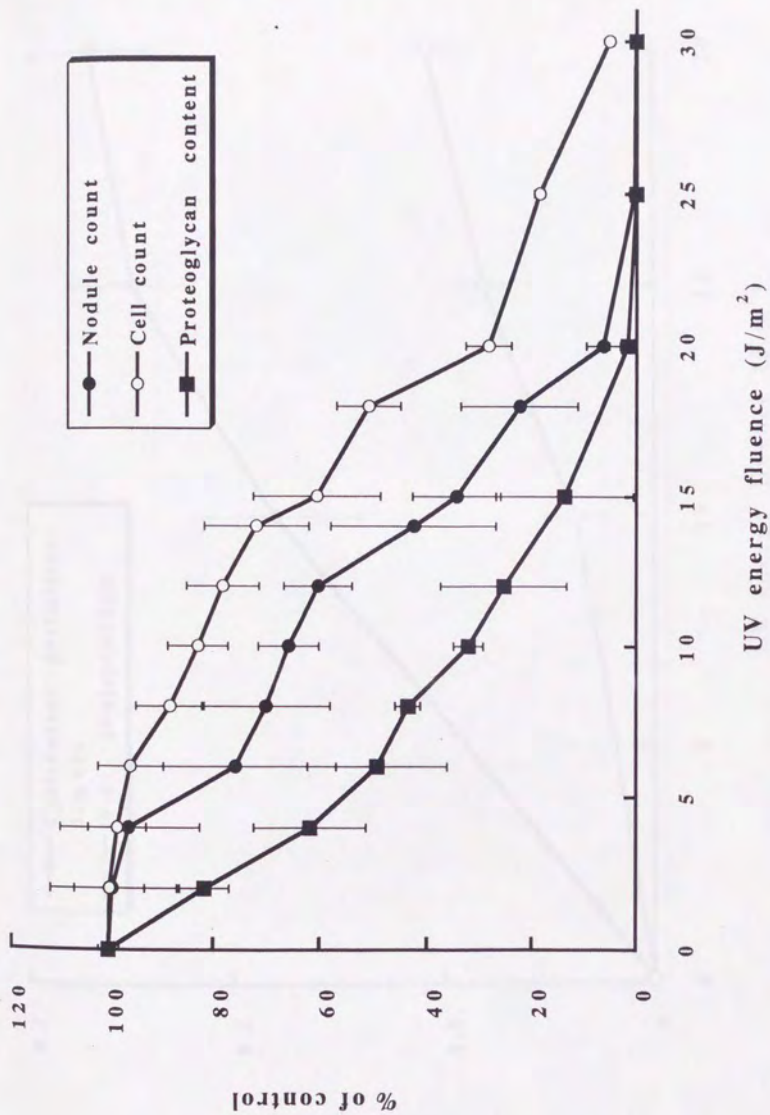


Fig. 1-4. Inhibitory effects of UVC-irradiation on cellular proliferation and differentiation of cultured mouse embryonic cells.

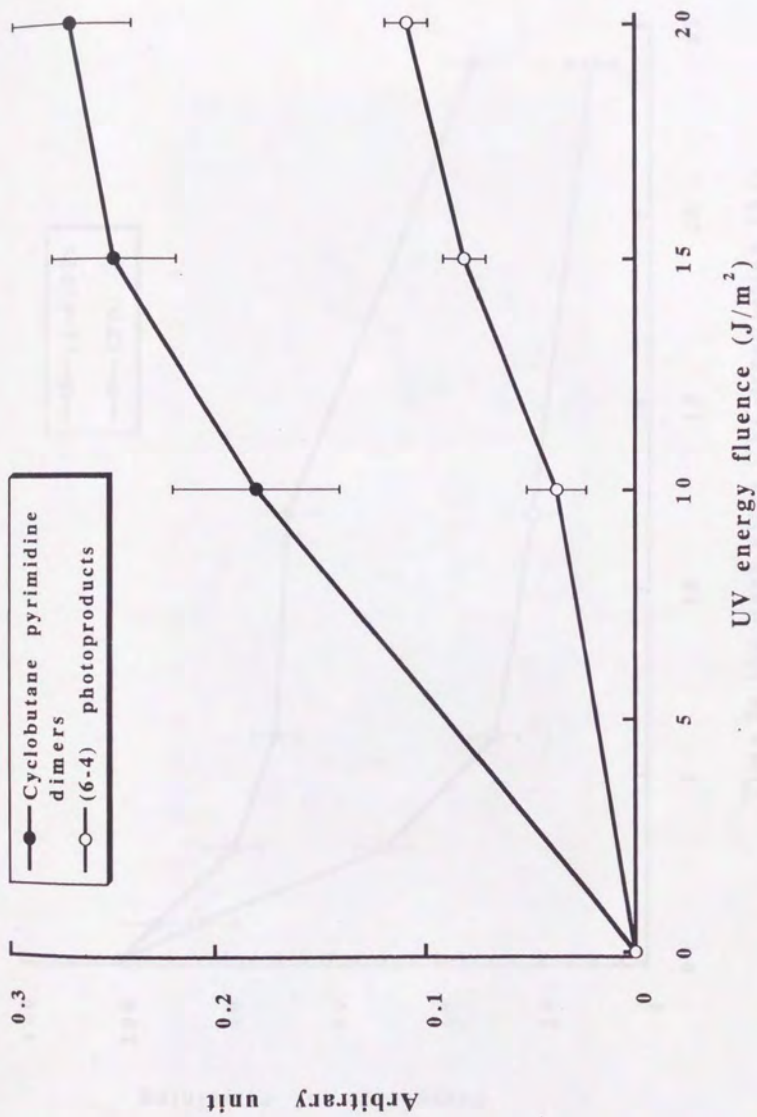


Fig. I-5(a). Induction by UVC-irradiation of DNA damage in cultured mouse embryonic cells.

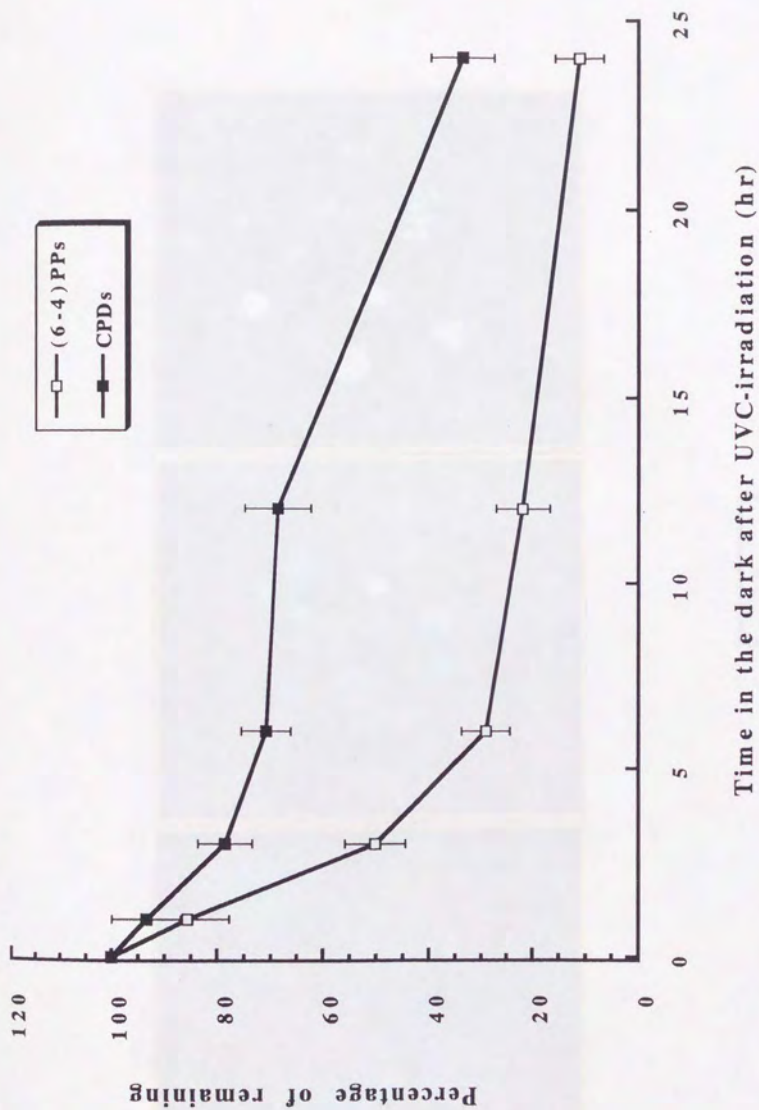
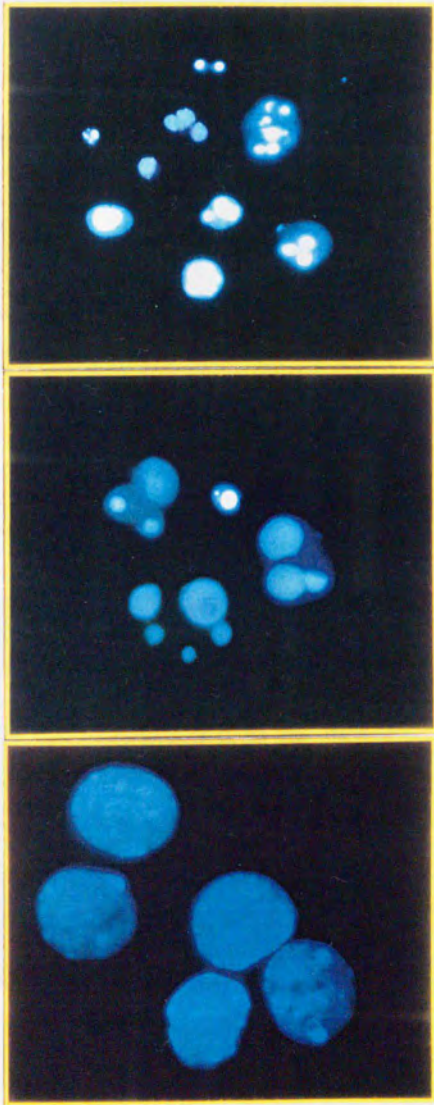


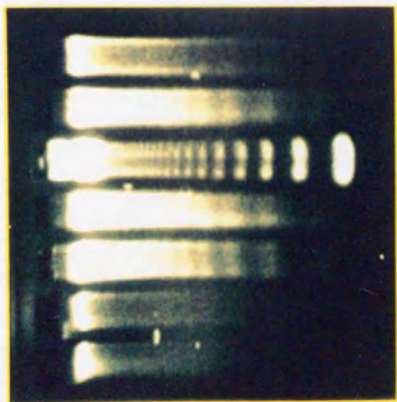
Fig. I-5(b). DNA repair kinetics in cultured mouse embryonic cells.



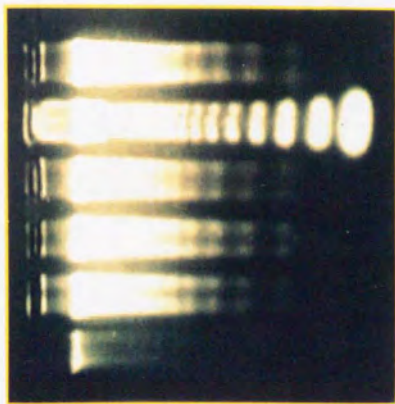
a	b	c
---	---	---

Fig. I-6. Images of cell nuclei by fluorescent dye staining.

1 2 3 4 5 6 7



1 2 3 4 5 6



a b

Fig. 1-7. Analysis by gel electrophoresis of the free DNA extracted from cultured cells.

after irradiation to $\frac{1}{2}$ % of apoptotic cells

Fig. 18

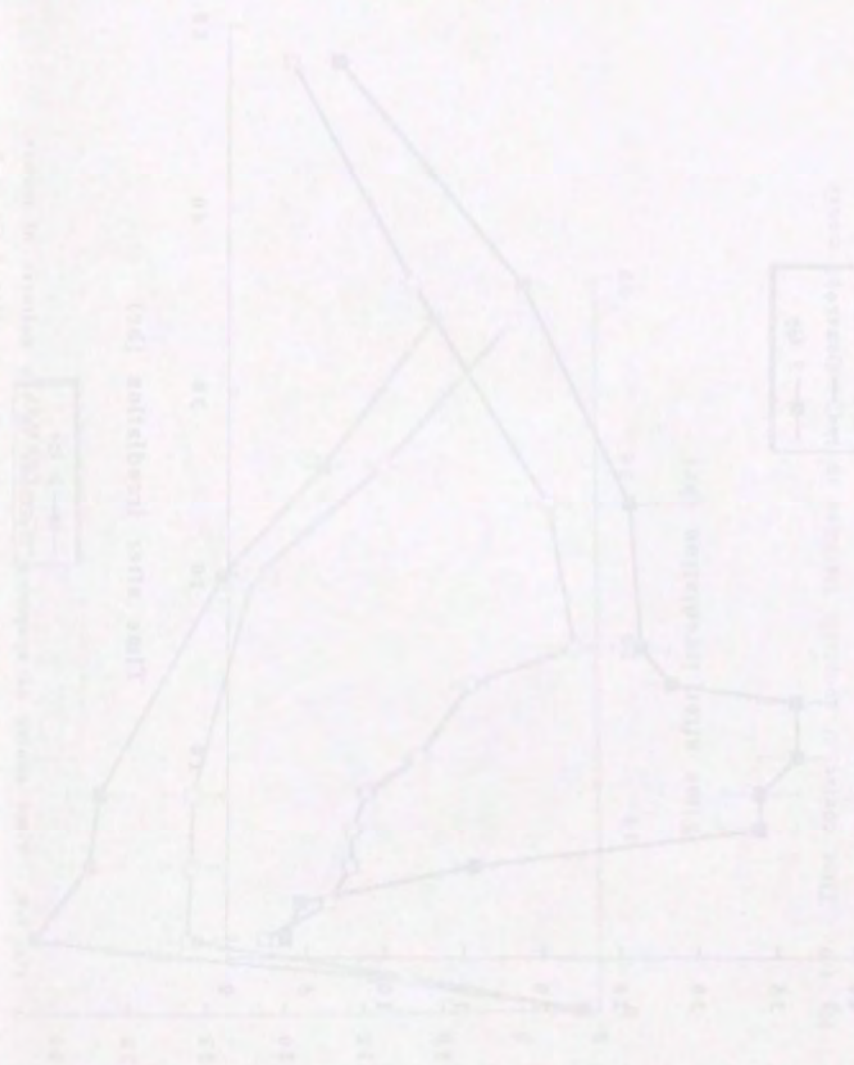


Fig. 18. The survival of lymphatic lymphoma cells in MacLeod's medium after irradiation with ^{60}Co gamma rays. The cells were irradiated with 1000 rads and then cultured in MacLeod's medium. The percentage of apoptotic cells was determined at the times indicated. The results are shown in the graph.

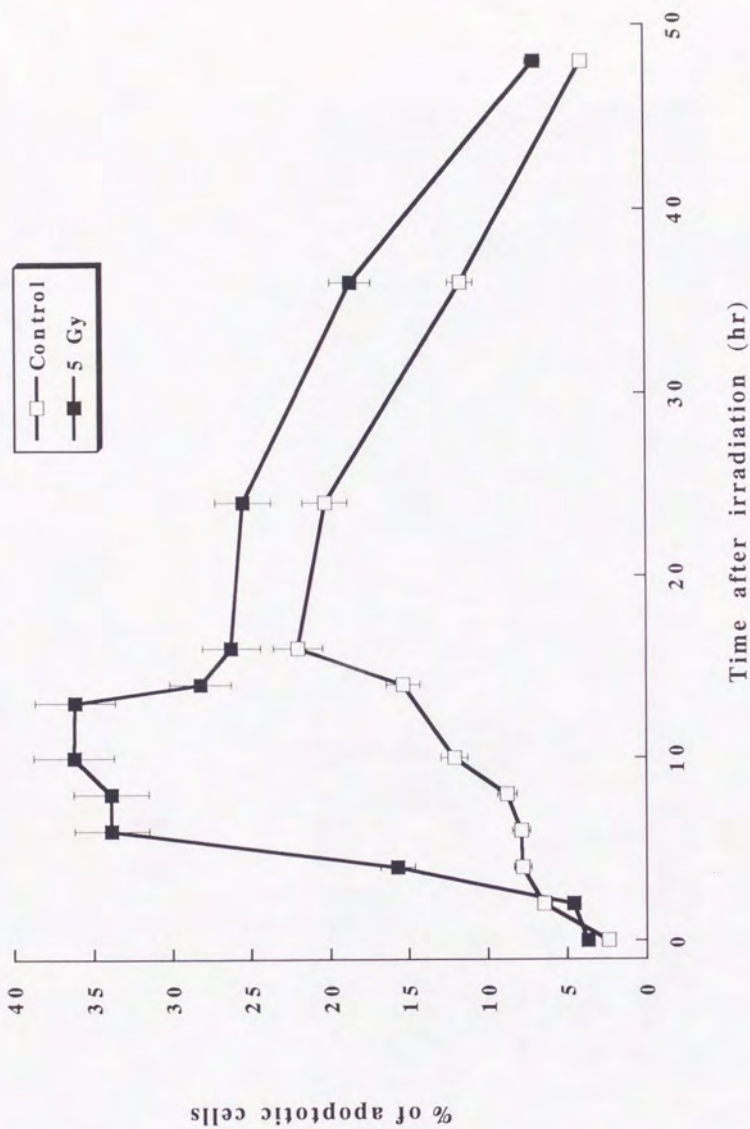


Fig. 1-8. Time course of apoptotic fractions in the cultures of mouse embryonic limb bud cells from E11 embryos after 5 Gy of X-

Fig. 1-8. Time course of apoptotic fractions in the cultures of mouse

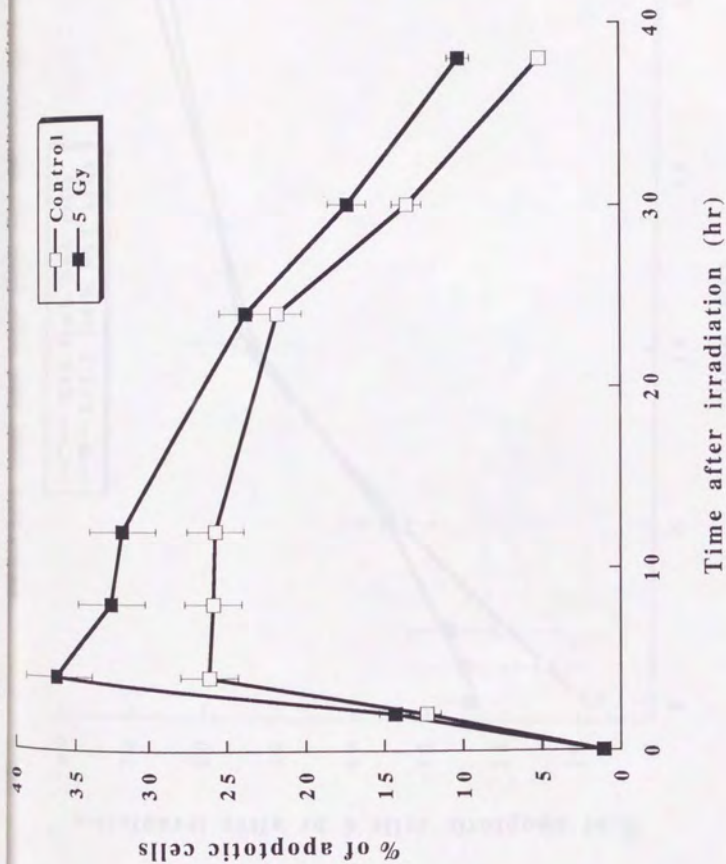


Fig. 1-9. Time course of apoptotic fractions in the cultures of mouse embryonic limb bud cells from E11.5 embryos after 5 Gy of X-irradiation.

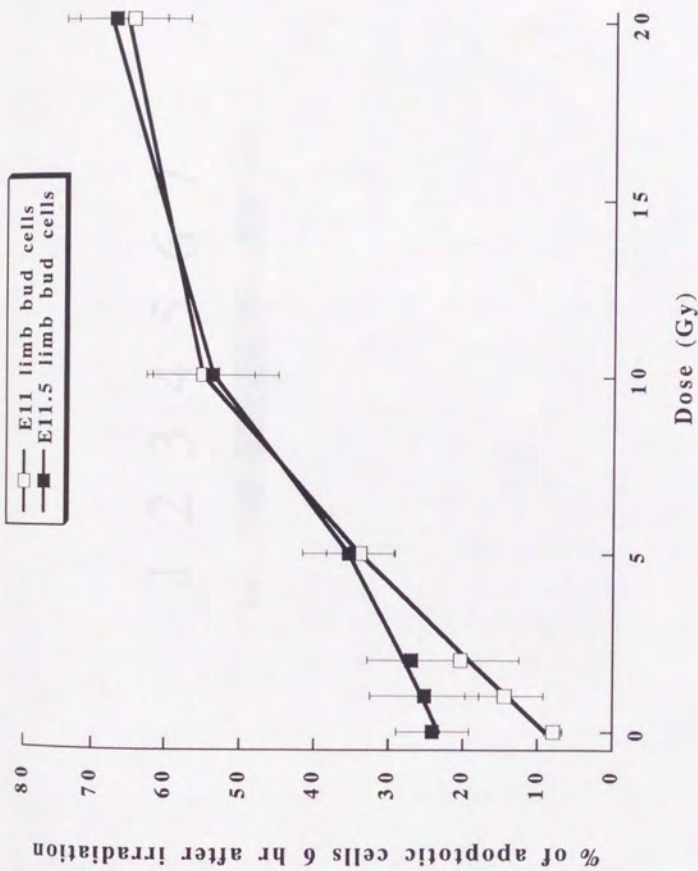
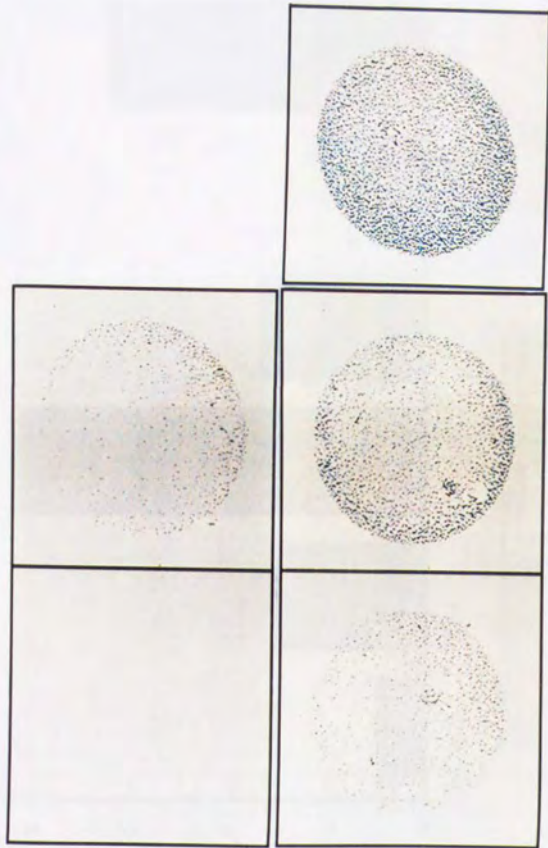


Fig. I-10. Radiation dose-response curves of apoptotic fractions in limb bud cells from different embryonic ages (E11 and E11.5).

1 2 3 4 5 6 7



Fig. I-11. Western blotting analysis of p53 protein in cell lysates.



a	b	
c	d	e

Fig. I-12. Immunohistochemical staining of p53 protein in limb bud cell cultures.

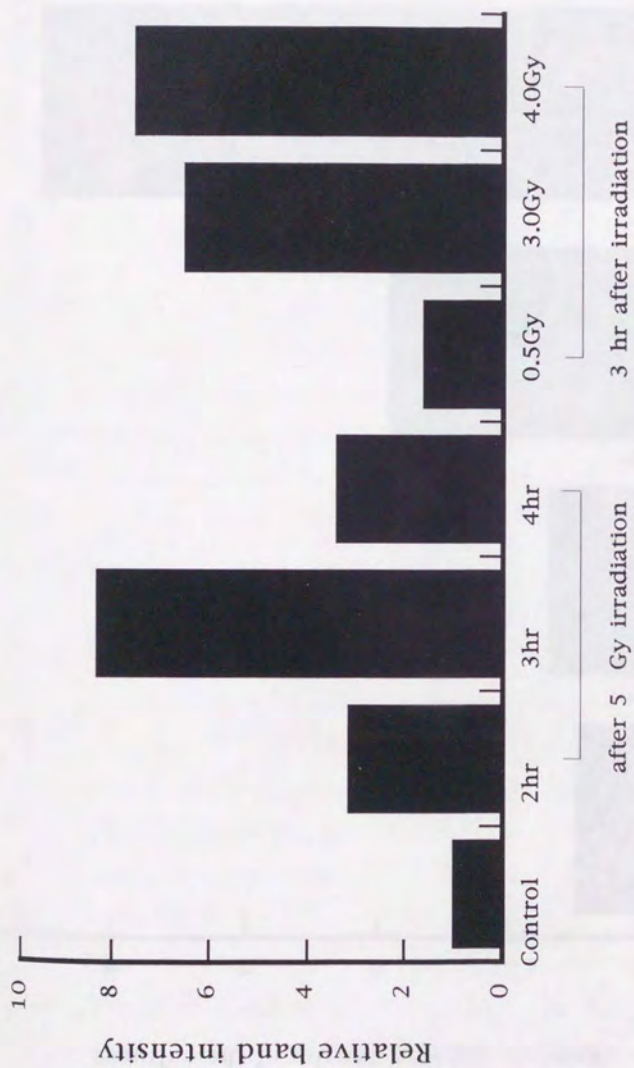


Fig. I-13. Quantitative analysis of p53 protein levels in cell lysate of cultured cells after irradiation.

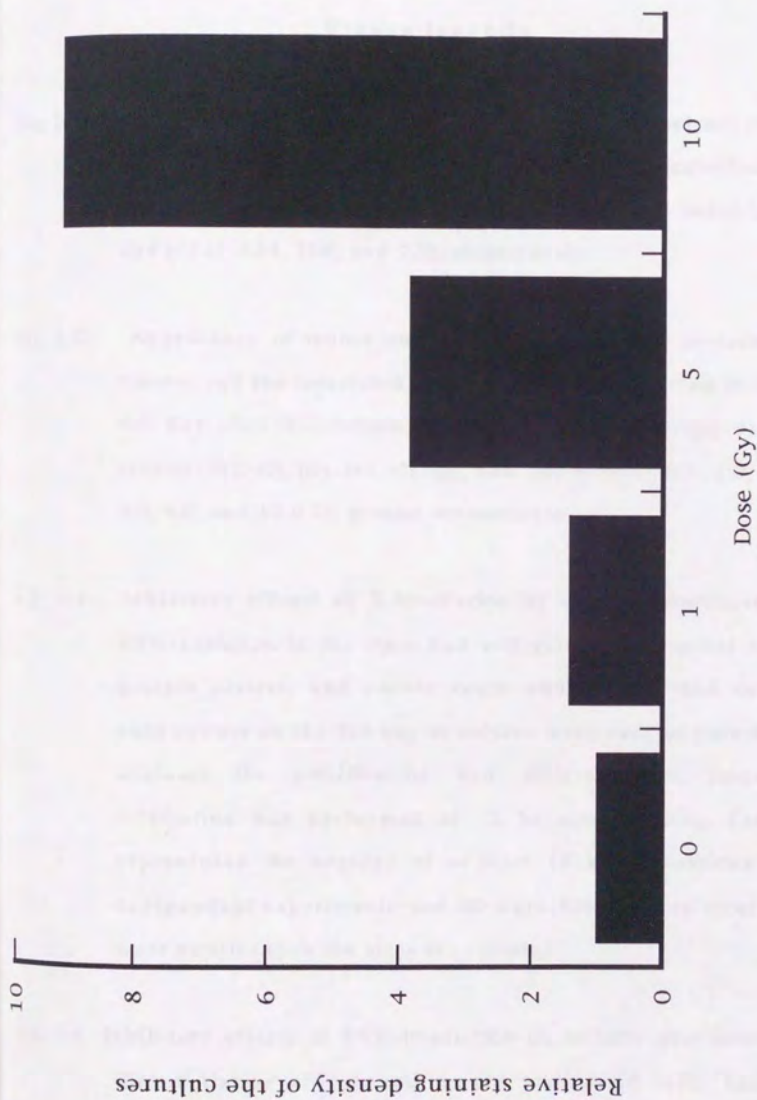


Fig. I-14. Quantitative analysis of p53 protein levels in cultured cells 3hr after irradiation.

Figure legends

Fig. I-1. Appearance of a mouse embryonic limb bud cell culture of control stained with Alcian Blue on the 4th day after incubation. Photos showed a whole culture (a) at $\times 22$ and cartilage nodules (b), (c), and (d) at $\times 44$, 110, and 220, respectively.

Fig. I-2. Appearance of mouse embryonic limb bud cell cultures of the control and the irradiated groups stained with Alcian Blue on the 4th day after X-irradiation. Photos were at $\times 11$: (a) was of the control; (b), (c), (d), (e), (f), (g), and (h) were of 0.5, 1.0, 2.0, 4.0, 6.0, 8.0, and 10.0 Gy groups, respectively.

Fig. I-3. Inhibitory effects of X-irradiation on cellular proliferation and differentiation in the limb bud cell culture. Cell count and total protein content, and nodule count and proteoglycan content in each culture on the 4th day of culture were used as parameters to evaluate the proliferation and differentiation, respectively. Irradiation was performed at 2 hr after seeding. Each point represented the average of at least 18 determinations from 3 independent experiments and SD were indicated as error bars or were smaller than the sizes of symbols.

Fig. I-4. Inhibitory effects of UVC-irradiation on cellular proliferation and differentiation of cultured mouse embryonic cells. Each point represented the average of at least 12 determinations from 5

independent experiments and SD were indicated as error bars or were smaller than the sizes of symbols.

Fig. 1-5(a). Induction by UVC-irradiation of DNA damage in cultured mouse embryonic cells. Each point represented the average of at least 12 determinations from 5 independent experiments and SD were indicated as error bars or were smaller than the sizes of symbols.

Fig. 1-5(b). DNA repair kinetics in cultured mouse embryonic cells. Each point represented the average of at least 12 determinations from 5 independent experiments and SD were indicated as error bars or were smaller than the sizes of symbols.

Fig. 1-6. Images of cell nuclei by fluorescent dye staining. Photos were at $\times 1000$. Images of normal (a) and apoptotic cells (b) and (c) as visualized by Hoechst 33342 fluorescent dye staining indicated by arrows. Apoptotic cells were defined morphologically as those with densely condensed chromatin.

Fig. 1-7. Analysis by gel electrophoresis of the free DNA extracted from cultured cells. Radiation dose was 5 Gy in the exposed group. (a) cells from E11 embryos, and (b) cells from E11.5 embryos. In (a) and (b), lane 1 was just after radiation (= control, 0 hr), lane 5 was DNA marker (123bp); Lane 6 was 24 hr after radiation; in (a) lanes 2, 3, and 4 were respectively 4, 8, and 12 hr after radiation; in (b) lanes 2, 3, and 4 were 2, 4, and 10 hr after radiation.

Fig. I-8. Time course of apoptotic fractions in the cultures of mouse embryonic limb bud cells from E11 embryos after 5 Gy of X-irradiation. Each point represented the average of at least 4 determinations from 3 independent experiments and SD were indicated as error bars or were smaller than the sizes of symbols.

Fig. I-9. Time course of apoptotic fractions in the cultures of mouse embryonic limb bud cells from E11.5 embryos after 5 Gy of X-irradiation. Each point represented the average of at least 4 sample determinations from 3 independent experiments and SD were indicated as error bars or were smaller than the sizes of symbols.

Fig. I-10. Radiation dose-response curves of apoptotic fractions in limb bud cells from different embryonic ages (E11 and E11.5). Each point represented the average of at least 4 sample determinations from 3 independent experiments and SD were indicated as error bars or were smaller than the sizes of symbols.

Fig. I-11. Western blotting analysis of p53 protein in cell lysates. Total cell lysates were separated on 7.5% SDS-PAGE and analyzed by Western blotting using anti-p53 polyclonal antibody (AB565). Lane 4 was nontreated control; Lanes 1, 2 and 3 were sampled 3 hr after irradiation with 0.5, 3.0 and 4.0 Gy respectively; lanes 5, 6, and 7 were 2, 3, and 4 hr after irradiation with 5.0 Gy.

Fig. I-12. Immunohistochemical staining of p53 protein in limb bud cell cultures. Cultures were fixed and stained with anti-p53 antibody (AB565), the stained cells were visualized using an Immun-Blot Assay Kit. Photos were at $\times 11$: (a) was a negative control (control cultures without AB565 addition); (b) was control; (c), (d), and (e) were cultures 3 hr after irradiation with 1, 5, and 10 Gy, respectively.

Fig. I-13. Quantitative analysis of p53 protein levels in cell lysates of cultured cells after irradiation. Each band density in Fig. I-9. was quantitated using an image analyzer taking the control lane as 100%.

Fig. I-14. Quantitative analysis of p53 protein levels in cultured cells 3 hr after radiation. Staining density of each culture in Fig. I-10. was quantitated using an image analyzer taking control as 100%.

References

- Arends M. J. and A. H. Wyllie. Apoptosis: mechanisms and roles in pathology. *Int. Rev. Exp. Pathol.*, 1991; 32: 223-54.
- Arends M. J., Morris R. G., and A. H. Wyllie. Apoptosis. The role of endonuclease. *Am. J. Pathol.*, 1990; 136, 593-608.
- Brent R. L. Radiations and other physical agents. In: *Handbook of teratology*. Ed. Wilson J. G. And F. C. Fraser. 1977, Plenum Press, New York, pp 153-223.
- Bursch W., Lleine L., and M. P. Tenniswood. The biochemistry of cell death by apoptosis. *Biochem. Cell Biol.*, 1990; 68(9): 1071-1074.
- Clarke A. R., Purdie C. A., Harrison D. J., Morris R. G., Bird C. C., Hooper M. L., and A. H. Wyllie. Thymocyte apoptosis induced by p53-dependent and independent pathways. *Nature*, 1993; 362: 849-852.
- Flint O. P., Orton T. C., and R. A. Ferguson. Differentiation of rat embryo cells in culture: response following acute maternal exposure to teratogens and non-teratogens. *J. Appl. Toxicol.*, 1984; 4(2): 109-116.
- Flint O. P. and T. C. Orton. An in vitro assay for teratogens with cultures of rat embryo midbrain and limb bud cells. *Toxicol. Appl. Pharmacol.*, 1984; 76: 383-395.
- Flint O. P. In vitro tests for teratogens: Desirable endpoints, test batteries and current status of the micromass teratogen test. *Reproduct. Toxicol.*, 1993; 7: 103-111.
- Friedberg E. C. DNA damage and human disease. In "DNA repair", Ed. E.C. Friedberg, W. H. Freeman and Company, 1985. New York, pp. 505-542.
- Funayama T., Mitani H., and A. Shima. Ultraviolet-induced DNA damage and

- its photorepair in tail fin cells of the Medaka, *Oryzias latipes*, *Photochem. Photobiol.*, 1993; 58, 380-385.
- Garrison C. J. and E. U. Uyeki. The effects of gamma-radiation on chondrogenic development in vitro. *Radiat. Res.*, 1988; 116, 356-363.
- Hickman J. A. Apoptosis induced by anticancer drugs. *Cancer Metastasis Rev.*, 1992;11(2):121-139.
- Kerr J. F. R., Wyllie A. H., and A. R. Currie. Apoptosis: a basic biological phenomenon with wide-ranging implications in tissue kinetics. *Br. J. Cancer*, 1972; 26(4): 239-257.
- Kerr J. F. R. and B. V. Harman. Definition and incidence of apoptosis: an historical perspective. In: *Apoptosis: the molecular basis of cell death*. Tomei L. D. and Cope F. O. (Ed.) Cold Spring Harbor Laboratory Press, Plainview, 1991, New York, pp 1 - 29.
- Kiefer J. Repair and recovery. In "Biological Radiation Effects", Ed. J. Kiefer, Springer-Verlag, 1990. Berlin, Heidelberg, Germany, pp 212-239.
- Koike M., Ishino K., Ikuta T., Huh N., and T. Kuroki. Growth enhancement of normal human keratinocytes by the antisense oligonucleotide of retinoblastoma susceptibility gene. *Oncogene* 1995; 10: 117-122.
- Lowe S. W., Ruley H. E., Jacks T., and D. E. Houseman. P53-dependent apoptosis modulates the cytotoxicity of anticancer agents. *Cell*, 1993a; 74: 957-967.
- Lowe S. W., Schmitt E. M., Smith S. W., Osborne B. A., and T. Jacks. P53 is required for radiation-induced apoptosis in mouse thymocytes. *Nature*, 1993b; 362: 847-849.
- Merritt A. J., Potten C. S., Kemp C. J., Hickman J. A., Balmain A., Lane D. P., and P. A. Hall. The role of p53 in spontaneous and radiation induced

- apoptosis in the gastrointestinal tract of normal and p53-deficient mice. *Cancer Res.*, 1994; 54: 614-617.
- Milaire J. and J. Mulnard. Histogenesis in 11-Day mouse embryo limb buds explanted in organ culture. *J. Exp. Zool.*, 1984; 232: 359-377.
- Milas L., Stephen L. C., and R. E. Meyn. Relation of apoptosis to cancer therapy. *In Vivo*, 1994; 8:665-674.
- Mori T., Nakane M., Hattori T., Matsunaga T., Ihara M., and O. Nikaido. Simultaneous establishment of monoclonal antibodies specific for cyclobutane pyrimidine dimer or (6-4) photoproduct from the same mouse immunized with the ultraviolet-irradiated DNA, *Photochem. Photobiol.*, 1991; 54, 225-232.
- Moscona A. Cell recognition, histotypic adhesion and enzyme induction in embryonic cells. In: Slavkin, H.C.; Greulich, R.C. eds. *Extracellular matrix influences on gene expression*. New York: Academic Press; 1975: 52-67.
- Norimura T. p53 suppresses teratogenesis. *Proceedings of the Japan radiation research society 39th annual meeting*. Kansai medical university Press. 1996. Osaka, Japan. pp 95.
- Norimura T., Nomoto S., Katsuki M., Gondo Y., and S. Kondo. P53-dependent apoptosis suppresses radiation-induced teratogenesis. *Nature Med.*, 1996; 2(5): 577-580.
- Ohyama H. and T. Shimokawa. DNA electrophoresis. In: *The latest experimental methods for apoptosis research*. Ed. Tsujimoto Y., Tone S., and T. Yamada. Youdosya Press. Tokyo, 1995. pp 61-67.
- Potten C. P. The significance of spontaneous and induced apoptosis in the gastrointestinal tract of mice. *Cancer Metastasis Rev.*, 1992; 11(2): 179-195.

- Renault J. Y., Melcion C., and A. Cordier. Limb bud cell culture for in vitro teratogen screening: Validation of an improved assessment method using 51 compounds, *Teratogenesis Carcinog. Mutagen.*, 1989; 9: 83-96.
- Schwartzman R. A. and J. A. Cidlowski. Apoptosis: the biochemistry and molecular biology of programmed cell death. *Endocr. Rev.*, 1993; 14: 133-151.
- Selins K. S. and J. J. Cohen. Gene induction by gamma-irradiation leads to DNA fragmentation in lymphocytes. *J. Immunol.*, 1987; 139: 3199-3206.
- Solursh M. and R. S. Reiter. Evidence for histogenic interactions during in vitro limb chondrogenesis, *Dev. Biol.*, 1980; 78, 141-150.
- Takahashi A. and T. Ohnishi. Method for detection of apoptosis related protein. In: *The latest experimental methods for apoptosis research*. Ed. Tsujimoto Y., Tone S., and T. Yamada. Youdosha Press. Tokyo, 1995. pp 194-204.
- Tomei L. D. and F. O. Cope. In: *Apoptosis: the molecular basis of cell death*. Ed. Tomei L. D. and F. O. Cope. Cold Spring Harbor Laboratory Press, Plainview, 1991, New York, pp 1-29.
- Tomei L. D., Cope F. O., and P. J. Barr. Apoptosis: Aging and phenotypic Fidelity. In: *Apoptosis II: the molecular basis of apoptosis in disease*. Ed. Tomei L. D. and F. O. Cope. Cold Spring Harbor Laboratory Press, Plainview, Cold Spring Harbor Laboratory Press, Plainview, 1994, New York, pp 377-421.
- Walker N. I., Harmon B. V., Gobe G. C., and J. F. R. Kerr. Patterns of cell death. *Methods Achiev. Exp. Pathol.*, 1988; 13: 18-54.
- Wanck N., Muncoka K., Holler-Dinsmore G., Burton R., and S. V. Bryant. A staging system for mouse limb development. *J. Exp. Zool.*, 1989; 249: 41-

49.

Wang B., Fujita K., Uchida N., Mitani H., Yamada T., and A. Shima. Effects of UVC-irradiation on the mouse embryonic cell culture with or without fluorescent light treatment. *Mutation Research DNA Repair*. 362: 175-180, 1996.

Wyllie A. H., Kerr J. F. R., and A. R. Currie. Cell death: the significance of apoptosis. *Int. Rev. Cytol.* 1980; 68: 251-306.

Wyllie A. H. Apoptosis and the regulation of cell numbers in normal and neoplastic tissues: an overview. *Cancer Metastasis Rev.*, 1992; 11: 95-103.

Chapter II.

Localization of apoptosis in the limb buds irradiated *in utero*

Summary

Radiation-induced apoptosis was identified and localized in mouse embryonic limb buds in situ *in vivo*. D11 and D11.5 pregnant mice were irradiated with 5 Gy of X-rays. Pathological section observation showed that morphologically different cells were located in the pre-digital and pre-interdigital regions of limb buds. There was a significant increase in apoptotic cells in the pre-digital mesenchymal tissues in the both fore- and hindlimb buds 4 hr after radiation, while cells located in the pre-interdigital regions of the forelimb buds did not show a significant increase of apoptotic cells after radiation. The hindlimb buds lag behind the forelimbs developmentally. There was also an increase in apoptotic cells in the pre-interdigital mesenchymal tissues after radiation. There was a higher p53 protein level as measured by counting p53 positively stained cells in the pre-digital areas after radiation. The distribution of p53 positively stained cells in the limb buds was the same as that of radiation induced apoptotic cells. A dose of 0.3 Gy caused an increase in apoptotic cells mainly in the pre-digital region of E11 forelimb buds. Radiation induced a significantly higher fetus death and malformations of limb buds. The teratogenesis severity by radiation on hindlimb buds was higher than that on forelimb buds.

These results indicated that (1) radiation-induced apoptosis mainly occurred in cells that located in the pre-digital regions, which would otherwise undergo proliferation and differentiation in the subsequent developmental stage(s), (2) radiation-induced apoptosis was associated with a dose-dependent expression of p53 protein, and (3) radiation-induced

apoptosis was responsible for radiation teratogenesis.

Introduction

Apoptosis and morphogenesis

It is well known that apoptosis plays an important role in the normal course of development (Kerr *et al.* 1972). During embryogenesis and organ morphogenesis, certain cells are programmed to fall in death at a specific location and a predictable time. During the development of limbs, the occurrence of cell death at predictable regions has been described in many species, such death of mesenchymal cells appears to be one of the events indispensable for morphogenesis of the normal form of a limb.

Pattern formation and apoptosis during morphogenesis of limb

The limb buds have been widely used for the study of pattern formation. By removal or grafting experiments and comparison of the incidence of cell death in the mouse and chick limbs, (1) the pattern formation has been understood by the concepts of interactions among various regions of the limb bud, including the zone of polarizing activity (ZPA), apical ectodermal ridge (AER), non-ridge ectoderm and distal mesoderm (progress zone); and (2) the role that apoptosis played in shaping and pattern formation during morphogenesis in the course of development is provided (Councovanis *et al.* 1995).

In the case of the chick limb, the AER induces outgrowth in the underlying mesoderm progress zone (PZ), and determines the width of the subsequent digit field. The anterior necrotic zone (ANZ) and the posterior necrotic zone (PNZ) appear to limit the length of the AER. (Usage of the term

necrotic is misleading, however, since the dying cells display the features of apoptosis.) After the death of the underlying ANZ and PNZ, the overlying region of the AER regresses (morphologically displaying apoptosis). In the case of the mouse, the normal limbs lack a PNZ and contain a smaller ANZ than chick limbs. This results in mouse limb buds that are wider than the chick and the formation of five digits rather than the three formed in a normal chick wing. Some mutants are helpful in understanding the morphogenesis: In chicks, the *talpid3* mutant lacks both ANZ and PNZ; an abnormally long AER results in the formation of supernumerary digits. In mice, those carrying the mutation Dominant hemimelia (*Dh*) lack an ANZ altogether, and commonly display 7-8 digits per paw, with the extra digits always located anteriorly (Randy *et al.* 1994; Councouvanis *et al.* 1995).

Apoptosis also occurs in the interdigital tissues, where it functions to separate the digits. Mutations that cause a reduction of cell deaths result in digits that remain joined by webs of mesenchymal tissue, as in the cases of Polysyndactyly (*Ps*) mutant mice, *talpid3* mutant chicks (Johnson 1969; Hinchliffe and Thorogood 1974), and the experimental model of webbed chick (Tone *et al.* 1983). Excessive cell death can also produce limb defects, such as those caused by the wingless (*ws*) mutation of the chick. In the case of early and excessive cell death in the ANZ, the wing bud is eliminated entirely (Hinchliffe and Ede 1973).

Radiation, apoptosis, p53 expression and teratogenesis

There is usually an unusually higher expression of p53 gene in radiation-induced apoptosis. In the micromass culture system a higher production of p53 protein in the cell lysates and cultures of the irradiated

groups were found (Chapter I). In this Chapter, detection of p53 protein positive cells and the localization of these cells were made in the limb bud in situ *in vivo* study.

With the establishment of the staging system for developing mouse limbs (Wanek *et al.* 1989) and the construction of mouse limb bud fate maps using *ex utero* surgical techniques and carbon particle injections (Muneoka *et al.* 1989), the fate maps enable us to correlate initial morphological changes in the irradiated early limb buds to their final defects. The present study is aimed at revealing the initial pathological changes induced by radiation, investigating and confirming the *in vitro* work (chapter I) on apoptosis induction and its relation to cell proliferation and differentiation, which may correlate to the final limb bud teratogenesis.

Materials and Methods

Animals

ICR mice aged 8 - 10 weeks, weighing 22-26 g were used in this study. Females in estrus were mated with potent males overnight. The day when copulatory plug was found was designated day 1 of gestation (D1) or embryonic age day 1 for the embryo (E1).

X-ray irradiation

The pregnant mice were irradiated on D11 or D11.5 at room temperature with an X-ray machine (Pantak-320S, Shimadzu, Japan), operated at 200 kVp and 19 mA, with a dose rate of 90 R/min measured by an exposure ratemeter (Applied Engineering INC, Japan) using a 0.5 mm Al + 0.5 mm Cu filter.

Identification and localization of apoptosis in limb bud sections

Light microscopy (LM)

Heamatoxylin and Eosin staining (HE staining)

Briefly, the limb buds were fixed in 10% buffered formalin, subsequently processed using routine techniques and paraffin embedded. 3 μ m serial sections in a plane parallel to the volar aspects of the limbs were prepared, deparaffinized, and rehydrated. The slides were finally washed three times in distilled water, stained with heamatoxylin and eosin, dehydrated, cleared in xylene and mounted with xylene-based coverslipping

medium.

The staining was photographed at 100 X and quantified on an Olympus microscope at 400 X using a square graticule. Cells with nucleus condensation or containing apoptotic bodies were referred to as apoptotic cells (Li *et al.* 1995). About 200 nuclei were counted in each limb bud in both the pre-digital regions of digit IV (but not in the regions of presumptive joints on the digital ray) and the pre-interdigital regions between digit III and digit IV. At least 6 limb buds were examined in each group. The percentage of condensed nuclei was used as the apoptotic cell index (%).

Terminal deoxynucleotidyl transferase mediated dUTP nick end labeling (TUNEL)

Limb buds were fixed by perfusion and immersion in 10% buffered formalin phosphate. After dehydration overnight, samples were paraffin embedded and sections (3 μ m) were prepared.

The method is based on the specific binding of terminal deoxynucleotidyl transferase (TDT) to 3'-OH ends of DNA, ensuing a synthesis of a polydeoxynucleotide polymer. After the exposure of nuclear DNA on histological sections to proteolytic treatment, TDT was used to incorporate biotinylated deoxyuridine at sites of DNA breaks. The protocol was a modification of what previously described (Gavrieli *et al.* 1992; Tone and Tanaka 1995). Briefly, after deparaffinizing, digesting protein with proteinase K and quenching endogenous peroxidase activity with 1% H₂O₂ in phosphate buffered saline, slides were placed in equilibration buffer and then in TDT, biotin-16-2'-deoxyuridine-5'-triphosphate (biotin-dUTP) followed by stop and wash buffer, and the peroxidase - conjugated avidin.

Peroxidase was detected with diaminobenzidine. The sections were counterstained with methyl green. Positive controls were treated with DNase I (1 U/ml) before DNA labeling. For negative controls, TDT was omitted from the reaction mixture. Reagents were purchased from Boehringer Mannheim GmbH, Mannheim, Germany.

The TUNEL staining was used to confirm the observation by HE staining. At the early stage of limb bud development, the mesoderm areas are composed of strongly basophilic cells which cause a high background staining, and this causes difficulty in distinguishing the TUNEL positive cells from those cells with a higher staining background. Staining sections were therefore not used for quantitative analysis.

Electrophoresis

Free-DNA (low molecular weight DNA) was isolated by a modification of the method of Selins and Cohen (1987) and Ohyama and Shimokawa (1995). Limb buds were dissected and cell suspension was prepared. After centrifugation, cells in the pellet were washed with PBS, re-suspended in lysis buffer, centrifuged at 16000 rpm to remove high molecular weight DNA and other undissolved materials. An aliquot of the supernatant containing low molecular weight DNA was incubated with DNA-free RNase A followed by proteinase K (Boehringer Mannheim Biochemica, Mannheim, Germany) in sequence. Then free-DNA was precipitated with NaCl and isopropanol solution overnight at -20 °C. After centrifugation, it was dried and re-suspended in Tris-HCl and EDTA buffer. 123 base pairs DNA ladder (GIBCO BRL, Life technologies, INC) was used as a ladder DNA marker. DNA fragmentation was investigated with 1.3% agarose (Bio-Rad Laboratories,

Richmond, CA, USA) and 0.65% synergel (Diversified Biotech, Boston, MA, USA) gel electrophoresis performed at 10 V/cm for 2 hr. DNA was visualized under UV light and photographed.

p53 immunohistochemical staining

p53 immunoreactivity was evaluated with the polyclonal antibody (clone AB565, Chemicon International INC, Temecula, CA, USA) derived from rabbits immunized with recombinant p53 protein. The antibody recognizes p53 protein of both wild and mutant forms. The protocol was a modification of Cattoretti *et al.* (1988), Iuzzolino *et al.* (1994) and Rennison *et al.* (1994). Briefly, the limb buds were fixed in 10% buffered formalin and subsequently processed with routine techniques and paraffin embedded. 3 μ m sections were prepared, deparaffinized, and rehydrated. Endogenous peroxidase activity was blocked by incubation with 1% hydrogen peroxide. Samples were exposed to a 10% solution of normal non-immune goat serum, then exposed to AB565 at 1:800 dilution, incubated at 4 °C overnight. On the following day, sections were exposed to biotinylated goat anti-rabbit IgG at 1:100 dilution, and followed by peroxidase conjugated avidin at 1:100 dilution in sequence. Peroxidase was detected using 3,3'-diaminobenzidine (DAB) and hydrogen peroxide buffered solution. All reagents were purchased from Boehringer Mannheim Biochemica, Germany.

The slides were finally washed three times in distilled water, counterstained with methyl green, dehydrated, cleared in xylene and mounted with xylene-based coverslipping medium. Negative controls were the sham control sections exposed to 1:1000 normal rabbit serum in place of the primary antibody AB565. The staining was photographed at 100 X and

quantified on an Olympus microscope at 400 X using a square graticule. 4 to 5 graticules were counted in each limb bud in both the pre-digital regions of digit IV and the pre-interdigital regions between digit III and digit IV. At least 6 limb buds in each group were examined. The mean number of p53-positive nuclei per graticule was used as the p53 labelling index (p53LI).

Transmission electron microscopy (TEM)

The protocol was similar to those described by Li *et al.* (1995) with some modifications. In brief, limb buds were fixed by perfusion with 3% glutaraldehyde in sodium cacodylate buffer and by immersion in this fixative for 2 hr, then they were postfixed in 1% osmium tetroxide phosphate buffer for 3 hr, dehydrated through graded ethanol, and embedded in Epon 812. Semi-thin sections (0.5-1.0 μm) of areas of interest were stained with toluidine blue. Ultrathin sections (90 nm) were stained with uranyl acetate and lead citrate (Reynolds' method), attached onto 150-mesh copper grids pre-treated with Formvar, and examined with a Hitachi 7000 transmission electron microscope.

Identification of congenital malformation of limbs

Malformation observation

The glossary of digital defects was the same as described by Kurishita and Ihara (1989).

Aphalangy (Aph): missing digit, but metacarpal or metatarsal is present;

Atelephalangy: absence of distal phalanx;

Amesophalangy: absence of middle phalanx;

Abasophalangy: absence of proximal phalanx;

Ectrodactyly (Ect): missing digit or metacarpal or metatarsal;

Syndactyly: cutaneous or osseous fusion of adjacent digits;

Lateral metacarpal or metatarsal fusion: fusion of adjacent metacarpals or metatarsals;

Closely apposed metacarpals or metatarsals: narrowed intervening cavity of adjacent metacarpals or metatarsals;

Brachydactyly (Bra): general classification for shortness of finger or toe.

On D19, the pregnant animals were killed by cervical dislocation and only the limb bud malformations of living fetuses were examined. External direct examination and observation of skeletal preparation were performed. The protocol for skeletal preparation was as described (Inouye 1976; Zhou *et al.* 1989). In brief, fetuses were fixed in 95% ethanol, treated with 1% KOH, stained with alizarin red S. The examination for possible skeletal abnormalities was performed under a microscope (Olympus, BH-2, Tokyo, Japan).

As the soft tissue defects could not be distinguished from skeletal defects by external observation, the analysis of the radiation-induced digital defects performed was only on the basis of skeletal findings in resultant animals of prenatal 5 Gy irradiation. Meanwhile, for the defects observed are mainly of Aph and Ect that the data were presented in the glossary of Aph, Ect, and other else defects (others).

Results

Induction of apoptosis in limb buds *in situ in vivo*

Heamatoxylin and Eosin staining

Fig. II-1 showed photos of whole organ HE staining sections of both forelimb and hindlimb from E11 and E11.5 embryos. The typical staining of both pre-digital and pre-interdigital regions were demonstrated in Fig. II-2 to Fig. II-5. In the sections of controls of the forelimb buds, the cells located in the pre-digital regions had a tight intercellular connection with their neighboring cells. They had a larger volume of cytoplasm compared to the cells located in the pre-interdigital regions which had more intercellular space and with many dendrite-like structures on the cell surface. The cells located in the pre-digital regions were bigger in size than the cells located in the pre-interdigital regions. Many cells at mitosis in the pre-digital regions could be observed. In the sections of pre-digital regions of the hindlimb buds, similar morphology was observed, while those morphologically different two kinds of cells were found in the pre-interdigital regions. 4 hr after radiation, many cells located in the pre-digital regions with condensed cell nuclei and separated from their neighboring cells were observed. 8 hr after radiation, phagocytosis of the apoptotic cells could be also observed. The data obtained from graphic observations were shown in Fig. II-6 and Fig. II-7, respectively. In the pre-digital regions of limb buds, 5 Gy of X-irradiation induced a significant increase in number of apoptotic cells in both forelimb bud and hindlimb bud of E11 and E11.5 embryos. The apoptotic index of hindlimb bud was significantly higher than that of forelimb bud. The apoptotic index became lower when checked 8 hr after radiation

compared to that at 4 hr after radiation. In the pre-interdigital regions of limb buds, 5 Gy of X-irradiation induced a significant increase in apoptotic cells only in hindlimb bud of E11 and E11.5 embryos 4 hr after radiation, the maximum apoptotic index being about 10%. On the other hand, the apoptotic index was about 48% in the cells located in the pre-digital regions after the same dose and checked at the same time point.

TUNEL staining

Fig. II-8 showed the photos of TUNEL staining sections. Similar to the HE staining data, results of TUNEL staining showed that there was a significant increase of the positively stained cells after irradiation in the pre-digital regions than that of in the pre-interdigital regions. In the pre-interdigital regions of hindlimb buds, there was also an increase in the apoptotic index after radiation, but its absolute value was much lower than that obtained in the cells located in the pre-digital regions. These data were well consistent with the apoptosis induction data obtained by HE staining criteria.

Electrophoresis

Fig. II-9 composed of gel electrophoresis results. Without radiation, the presence of fragmented DNA extracted from the limb buds is revealed as a ladder-like pattern with smear showing discrete peaks corresponding to about 360 base pairs. Preparations from E13 and E14 limb buds showed a DNA ladder. When 5 Gy was given on D11, a DNA ladder appeared 4 hr later, and more clearly but with smear pattern 8 hr later; 1 day later, a DNA ladder with more smear pattern was found. When the same dose was given on D11.5, though a DNA ladder could be detected from 2 hr later, the DNA

ladder was always accompanied by the smear pattern.

Increase of p53 protein-positive staining cells

Typical stainings for p53 protein were demonstrated in Fig. II-10 for whole limb bud and section areas of interest, respectively. In the sections of control limb buds, very few p53 protein positively stained cells were found scattered in pre-digital regions and in pre-interdigital regions. 4 hr after irradiation, a significant increase in the number of p53 protein positively stained cells in the limb buds was detected. The p53 index of pre-digital regions were much higher compared to the pre-interdigital regions with the values of about 12.4 and 2.2 in the forelimb bud of E11 embryos. 8 hr after radiation, the p53 index decreased (Fig. II-11 and Fig. II-12). Regarding the pre-digital regions to the induction of p53 protein-positive staining cells, the hindlimb bud also showed more sensitive than that of the forelimb bud, and similar result was found for the pre-interdigital region observation.

Transmission electron microscopy (TEM)

Fig. II-13 showed the image of normal forelimb bud of E11 embryos. Cells located in the pre-digital regions and pre-interdigital regions were of different morphology. The differences between these two kinds of cells were clearly observable. The former were bigger in size with less dendrites and the later smaller and with many dendrites. Few spontaneous apoptotic cells and their phagocytosis were observed in the pre-interdigital regions of the forelimb buds. After a dose of 0.3 Gy, cells with apoptotic morphological changes could be easily observed in the pre-digital regions but not in pre-interdigital regions (Fig. II-14). The TEM data were consistent with the data

by HE and TUNEL.

Identification of congenital limb bud malformation

External gross observation

Table II-1 showed the incidence of death and anomalies in fetuses irradiated on E11 and examined on E19. Radiation induced a dose-associated increase of fetuses death and an increase of limb bud malformation in the living fetus. Fig.II-15 and Fig. II-16 were photos of major types of limb malformations induced by radiation in the present study. Results showed that the teratogenetic sensitivity of limb buds to the radiation was different as the resulting limb malformation was more severe in the hindlimb buds than that in the forelimb buds from the same embryo.

Skeleton preparation

Fig. II-17 and Fig. II-18 presented photos of the typical staining of limb bud skeleton prepared from both the control and those 5 Gy irradiated on D11 and D11.5. The severity of hindlimb bud malformation was greater than that of the forelimb bud. When the fetuses were irradiated with a low dose, the malformation was mainly of brachydactyly (data not shown). A dose of 5 Gy resulted in mainly aphyalangy and ectrodactyly.

The whole organ limb bud sections by HE staining also histologically confirmed the malformation results (Fig. II-19).

All malformation data in the 5 Gy irradiated group were summarized in Table II-2. These results showed a significant difference of radiation teratogenetic sensitivity between forelimb buds and hindlimb buds.

Discussion

Results of the morphological investigation in the present study confirmed the assumption based on the *in vitro* results. Results obtained by the HE staining together with TUNEL method indicated that cells located in the pre-digital and pre-interdigital regions were with different morphology. Under electron microscopic observation, most of the cells located in the pre-digital regions showed less dendrites and more cytoplasm than the cells located in the pre-interdigital regions. 4 hr after radiation with 5 Gy, many cells located in the pre-digital regions underwent typical apoptotic morphological changes, while most of the cells that located in the pre-interdigital areas had no significant morphological changes. Radiation-induced apoptosis mainly occurred among cells located in the pre-digital areas where cells were undergoing proliferation and differentiation. In the forelimb buds, radiation-induced apoptosis hardly occurred in the cells located in pre-interdigital mesenchymal tissue regions where cells stopped DNA synthesis and scheduled to go spontaneous apoptosis shown by Mori *et al.* (1995) in a BrdU/anti-BrdU immunohistochemical study.

As a positive regulator of cell death, particularly of apoptosis, it was found in the present study that after radiation cells located at the pre-digital regions showed a higher level of p53 protein where a higher frequency of apoptosis was also found. Most of the cells located in the pre-digital tissues of limb bud are some kind of stem-like cells as they could undergo both proliferation and differentiation in the subsequent developmental stage(s) (Mori *et al.* 1995). The results about immunohistochemical staining of p53 protein in the present study were very similar to the studies by Hendry *et*

al. (1995). The p53 index of the pre-digital regions was significantly higher compared to that of the pre-interdigital regions after irradiation. For the forelimb bud, the increase of p53 index of the pre-interdigital regions was not significant compared with the control. All these results showed the same distribution situation of the p53 positively stained cells and the radiation-induced apoptotic cells in the limb buds after radiation. These results indicated that radiation-induced apoptosis was p53-dependent in the limb buds.

As 0.2 Gy is believed to be the threshold dose for radiation-induced morphological teratogenesis during embryogenesis, in the present experiment a dose of 0.3 Gy was used in the electron microscopical study. Under such a dosage, almost all the apoptotic cells were found in the pre-digital areas. This results also supported the hypothesis posed.

The digital defects induced by irradiation occurred in all digits. However, there was an order of susceptibility which is contrary to the order of digital development in both forelimb and hindlimb. Similar to the research work on the malformation pattern and the digital teratogenic susceptibility about the chemicals induced digital defects (Ritter *et al.* 1973; Scott *et al.* 1977; Kochhar *et al.* 1978), the digital developmental stage was one of the important factors that affect the susceptibility. In the present study, the difference in radiosensitivities among digits is also thought to be due to the time of major teratogenic events. Most of the cells that rapidly undergo proliferation and differentiation were easily to be killed by radiation via radiation-induced apoptosis. Some of the survived cells may activate the cell repair mechanism to help the organ develop normally but the final results also depend on the damage the cell type and location. The cells that already

committed to undergo spontaneous apoptosis finally eliminated themselves. Some of the cells that were relatively highly differentiated could survive. The pattern of digital defects was specific for each developmental stage at which the radiation was performed. So the cell death play a main role in determining the degree and pattern of digital defects of the surviving fetuses.

The differences between the forelimb and the hindlimb, and among the digits of the same limb is considered to be due to a difference in developmental stage because the progress of development of the forelimb precedes that of the hindlimb, and the progress of development of some digits also precedes that of the others in the same limb, for an example, the digit IV develops first and followed by others. Radiation induced cell death presumably reduced the number of mesodermal cells that undergo proliferation and differentiation in the pre-digital areas. When the dose given is small, a reduction of limb bud size - brachydactyly (Bra) could be expected. The high dose could share a similar pathological event with the attribution to the server degree of damage which could cause aphyllangy (Aph) and ectrodactyly (Ect). In the present study, the digit IV was the only digit which could be often identified finally in the radiation-induced aphyllangy (Aph) in the forelimb buds and there was higher percentage of ectrodactyly (Ect) in the hindlimb buds on E19.

Study by Norimura *et al.* (1996) using both p53^{+/+}, p53^{+/-}, and p53^{-/-} mice showed that in both the pre-implantation period (E3.5) and the early stage of organogenesis (E9.5), p53-dependent radiation-induced apoptosis led to a wide range of cell death in embryos and fetuses which resulted in a higher rate of prenatal death. P53-dependent radiation-induced apoptosis

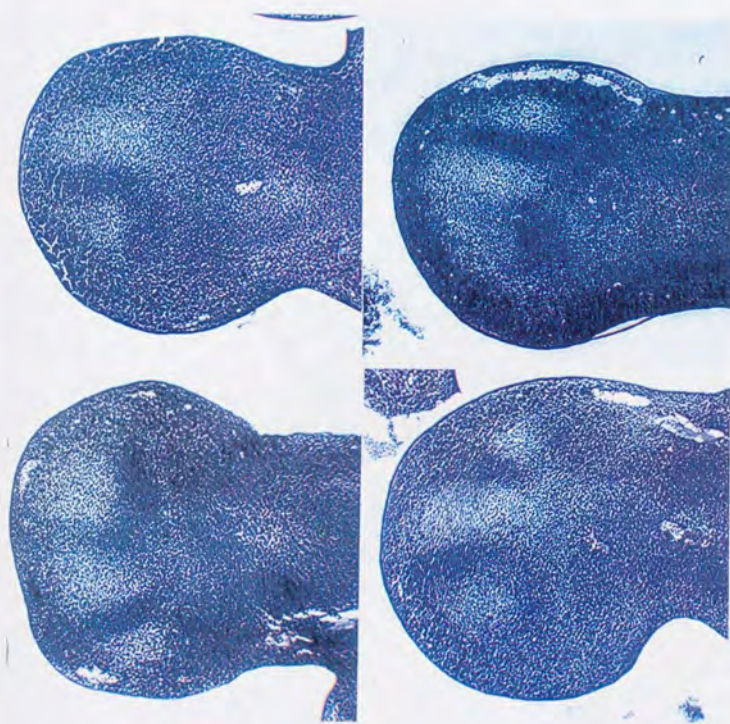
"protected" fetuses from continuing development with congenital malformations in both the pre-implantation period and the early time of organogenesis. As the early fetuses have a tissue repair capacity that cells with radiation induced un-repairable injuries will commit "altruistic suicide" for the survival of the whole body (Kondo 1988).

In the whole period of organogenesis, the prenatal death rate decreased with time while the malformation rate maintained a high level (Russell and Russell 1957). In the present study, I irradiated the fetuses at the late stage of organogenesis (E11 and E11.5). Results showed that there was a higher rate of prenatal death and in the mean time digital defects occurred in all living fetuses. These results indicated that radiation-induced apoptosis resulted in not only prenatal death, but also congenital malformations. These results together with the documented data indicated that embryos and fetuses of early organogenesis were very sensitive to radiation killing effects due to occurrence of radiation-induced apoptosis. The badly damaged embryos and fetuses were selected to die while the repairable embryos and fetuses could develop almost morphological normally. Fetuses of late organogenesis period were relatively resistant to radiation induced killing effects. Some fetuses with radiation-induced apoptosis in organs could further develop with malformations.

The normal development of limb buds requires an ordered process of cell divisions, differentiation and cell death. The cell death processes were tightly controlled both spatially and temporally. The breakdown of the control of apoptosis seemed to be a key step in the morphogenesis of limb buds after irradiation.

The embryo was a part of the pregnant animal, and radiation-induced

teratogenesis is defined as the specific somatic effect. Limb buds were also the organs of the embryo, so certain factors from both the pregnant animal and the embryo itself may affect the response of limb buds to the radiation damage. Modern technology provided us a relatively idealistic *in vitro* organ culture system, to prove the hypothesis and exclude the factors that could confound with the experiment results from outside of the limbs. In the Chapter III, I will try to establish a short term culture system for mouse limb bud, and introduce radiation into such a system to investigate radiation effects on apoptosis induction with emphasis on radiation-induced apoptosis location in the limb buds *in vitro*.



a	b
c	d

Fig. II-1. Light micrographs of mouse E11 and E11.5 limb bud sections parallel to the plane.

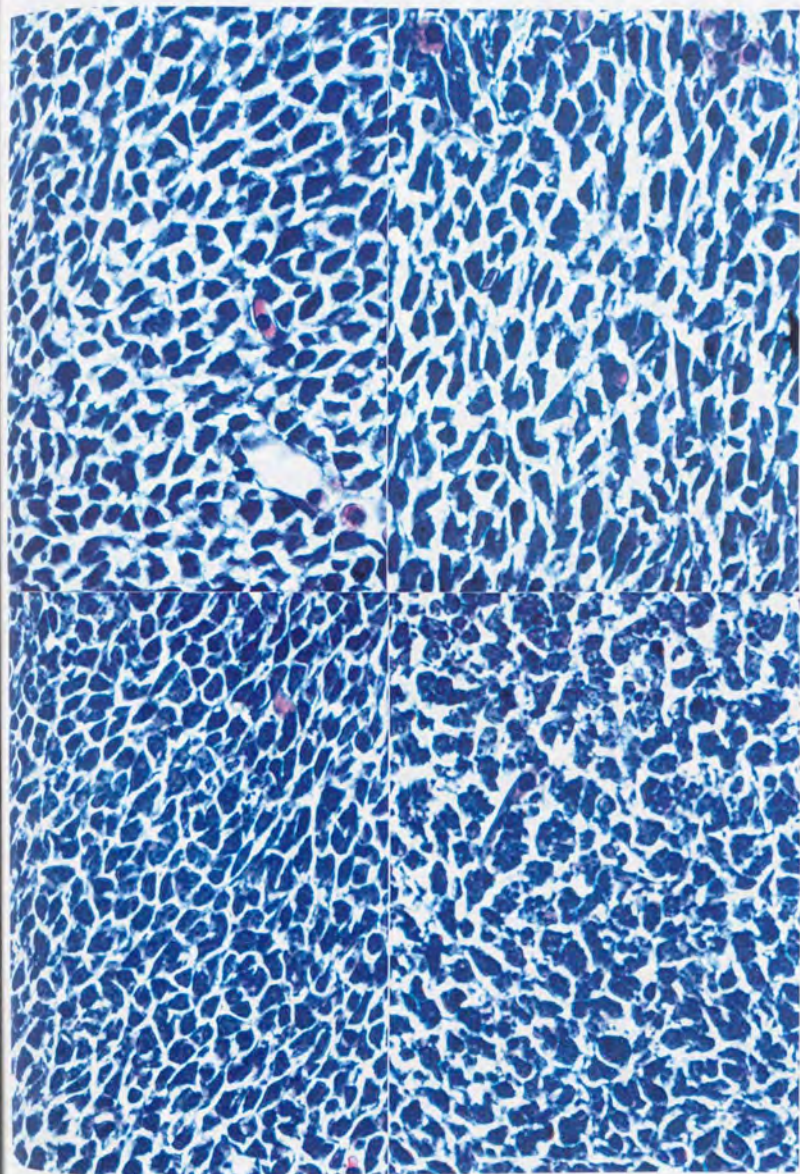
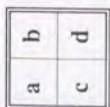


Fig. II-2. Higher magnification light micrographs of mouse E11 forelimb bud sections parallel to the plane.

a	b
c	d

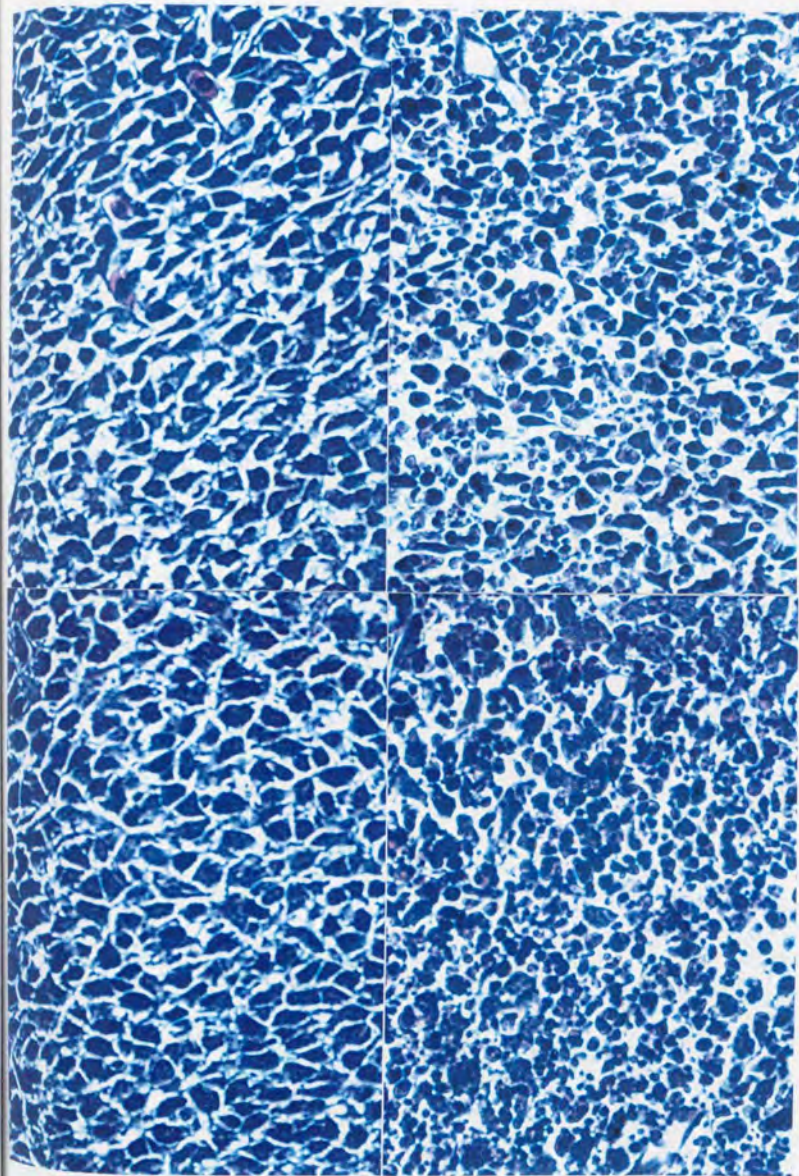


Fig. 11-3. Higher magnification light micrographs of mouse E11 hindlimb bud sections parallel to the plane.

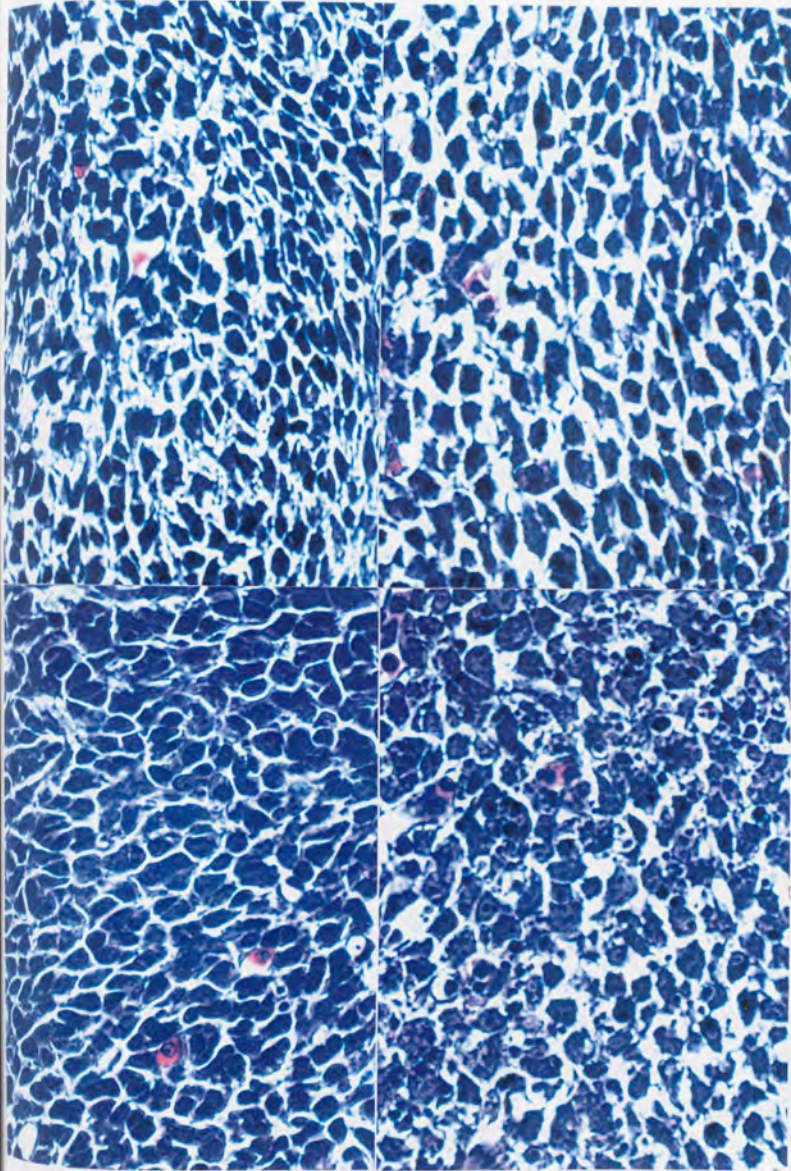
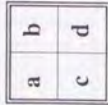
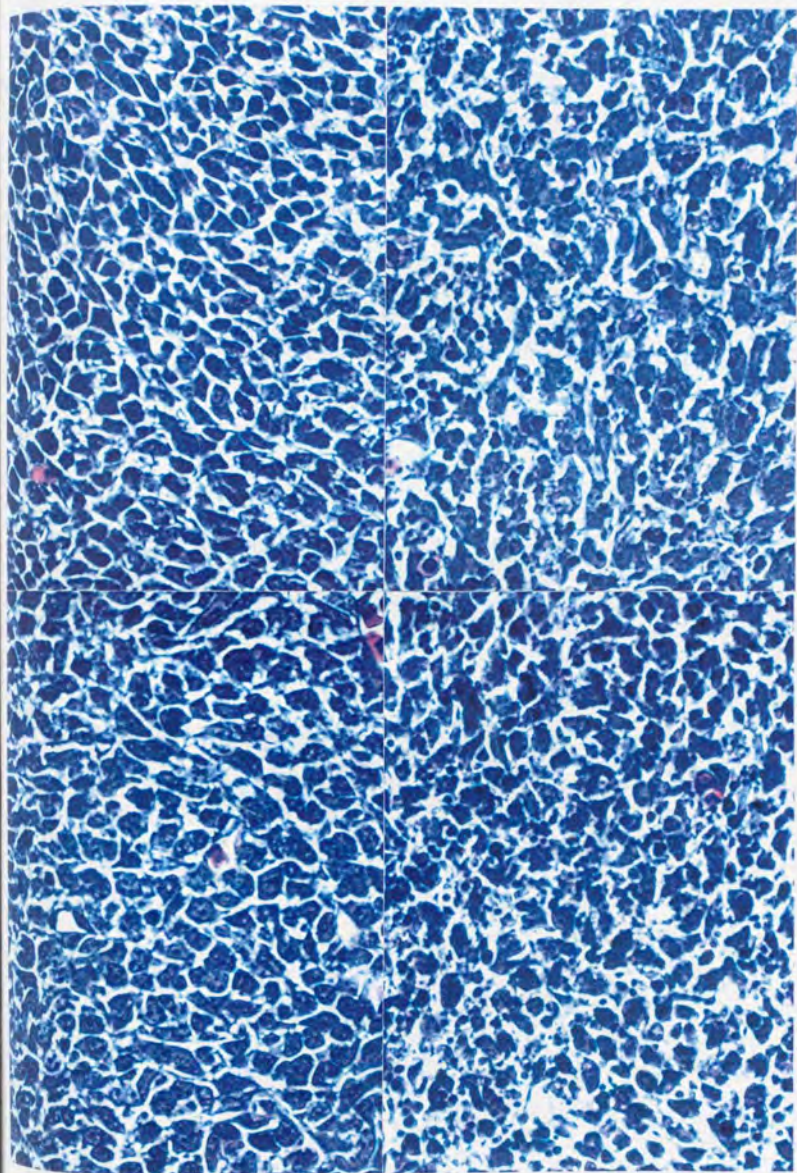
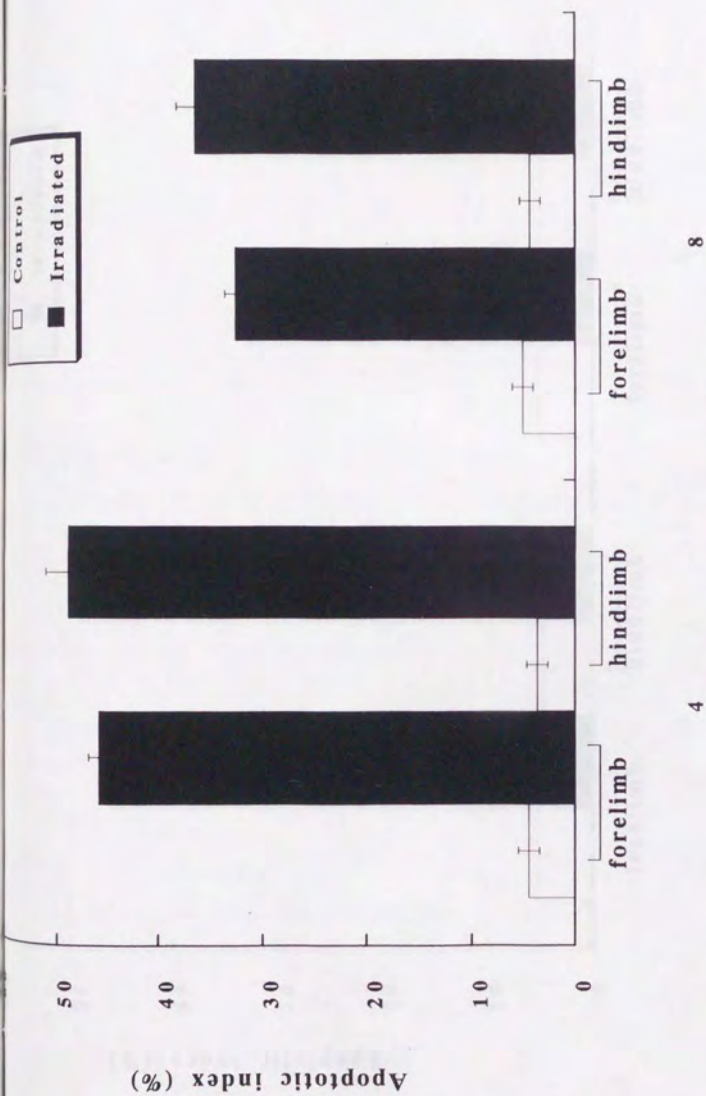


Fig. II-4. Higher magnification light micrographs of mouse E11.5 forelimb bud sections parallel to the plane.



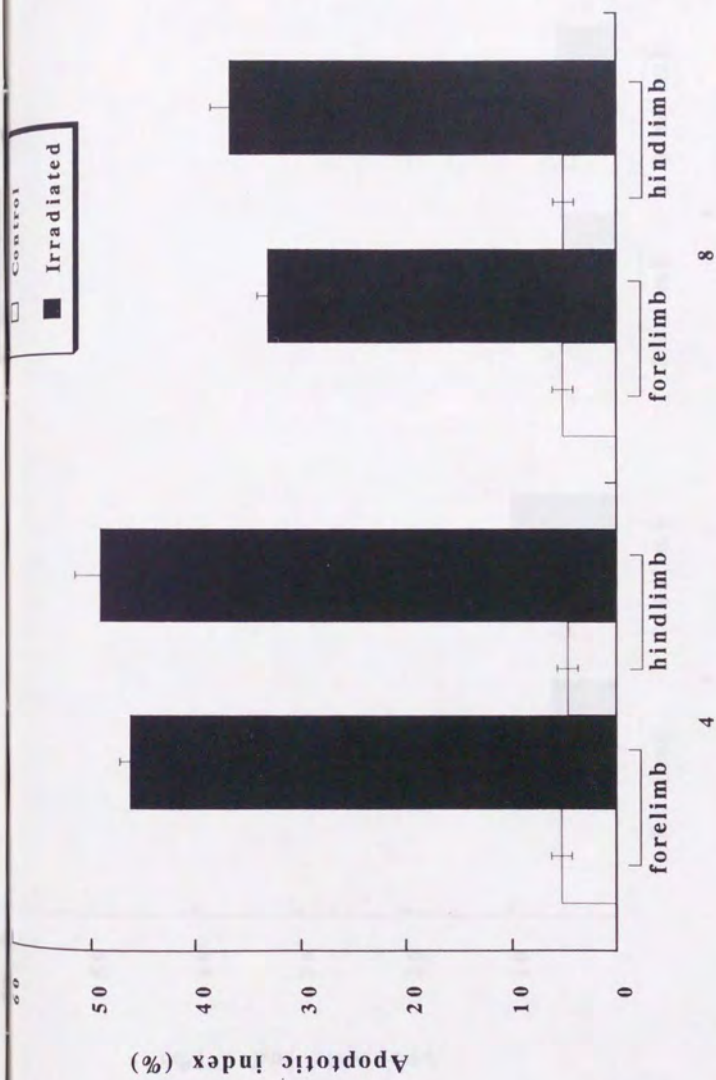
a	b
c	d

Fig. II-5. Higher magnification light micrographs of mouse E11.5 hindlimb bud sections parallel to the plane.



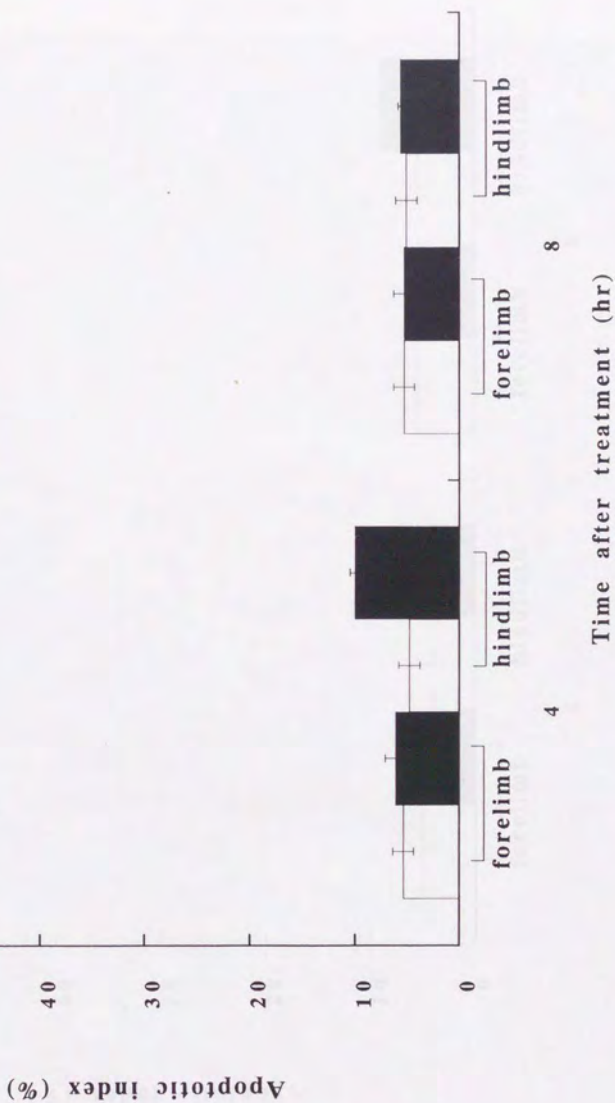
a. Pre-digital mesenchymal tissues of E11 limb buds

Fig. II-6. Induction of apoptosis by 5 Gy of X-rays in the pre-digital regions of mouse E11 and E11.5 limb buds.



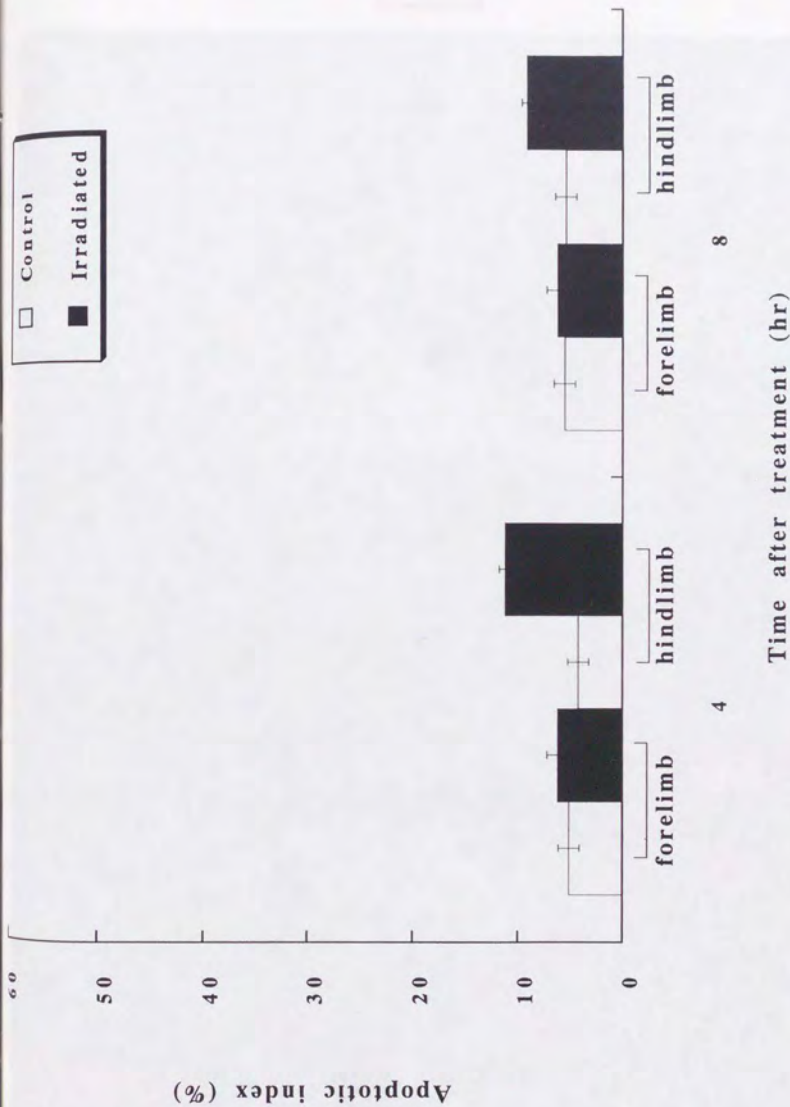
b. Pre-digital mesenchymal tissues of E11.5 limb buds

Fig. II-6. Induction of apoptosis by 5 Gy of X-rays in the pre-digital regions of mouse E11 and E11.5 limb buds.



a. Pre-interdigital mesenchymal tissues of E11 limb buds

Fig. II-7. Induction of apoptosis by 5 Gy of X-rays in the pre-interdigital regions of mouse E11 and E11.5 limb buds.



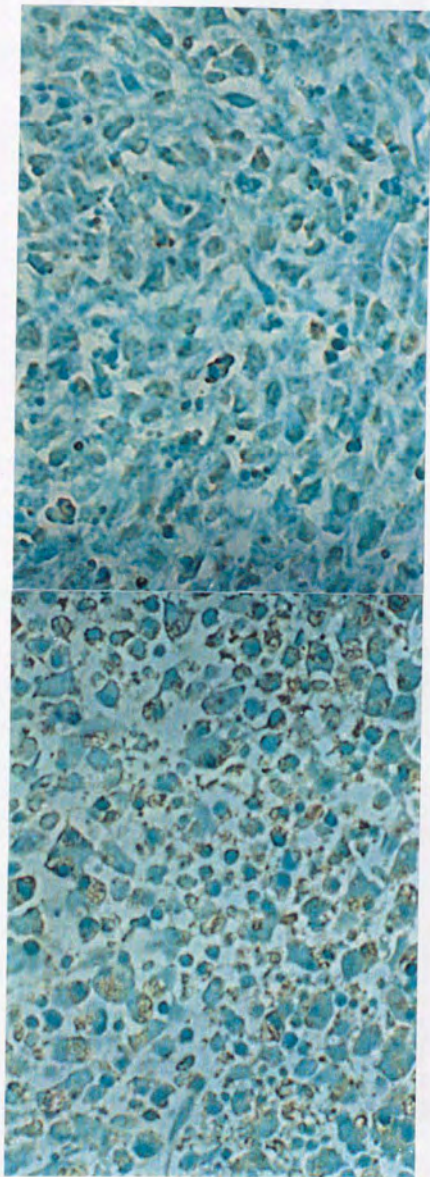
b. Pre-interdigital mesenchymal tissues of E11.5 limb buds

Fig. II-7. Induction of apoptosis by 5 Gy of X-rays in the pre-interdigital regions of mouse E11 and E11.5 limb buds.

a	b
c	d



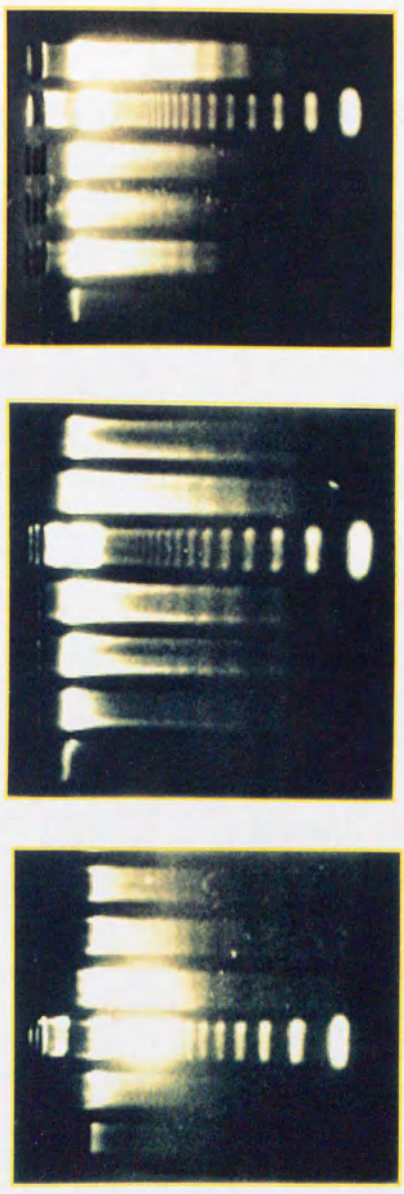
Fig. II-8. TUNEL staining of limb bud sections.



e f

Fig. II-8. TUNEL staining of limb bud sections.

1 2 3 4 5 6 1 2 3 4 5 6 7 1 2 3 4 5 6



a	b	c
---	---	---

Fig. II-9. Analysis of free DNA extracted from limb buds by electrophoresis.

a	b
c	d

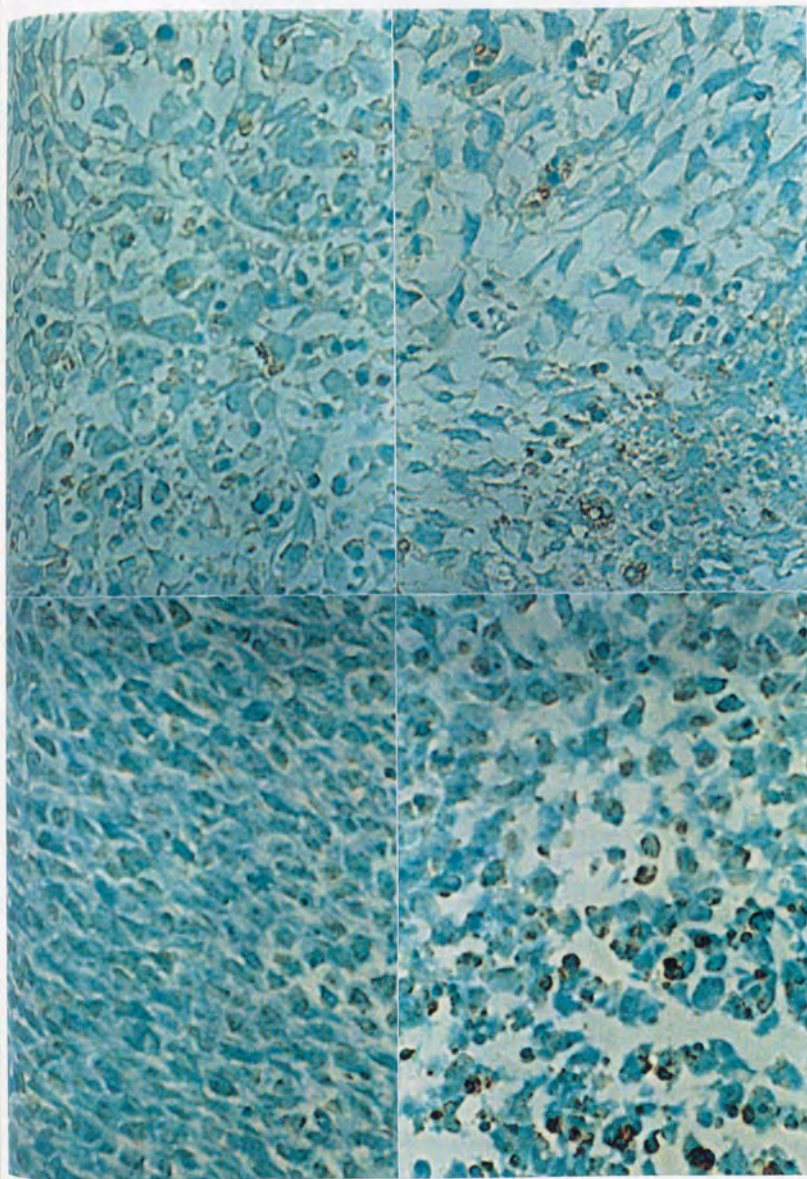
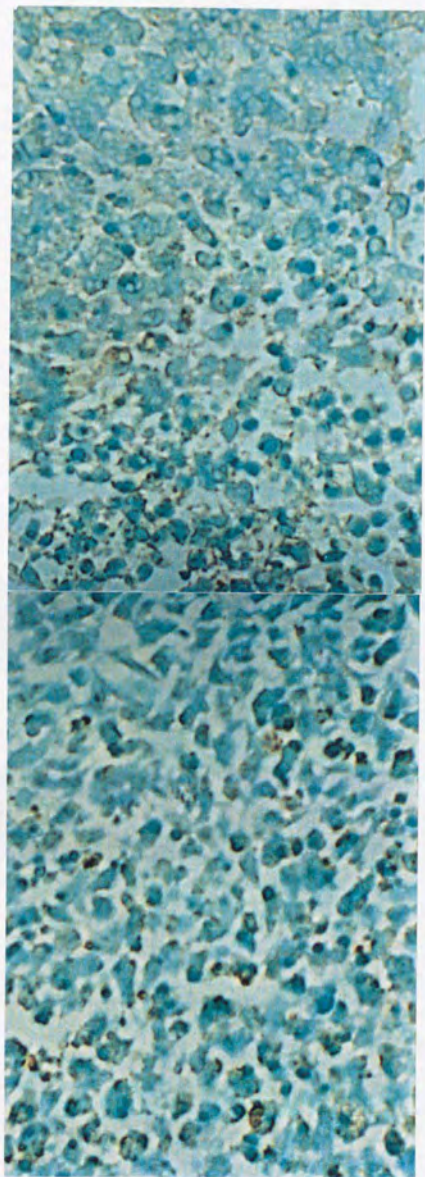
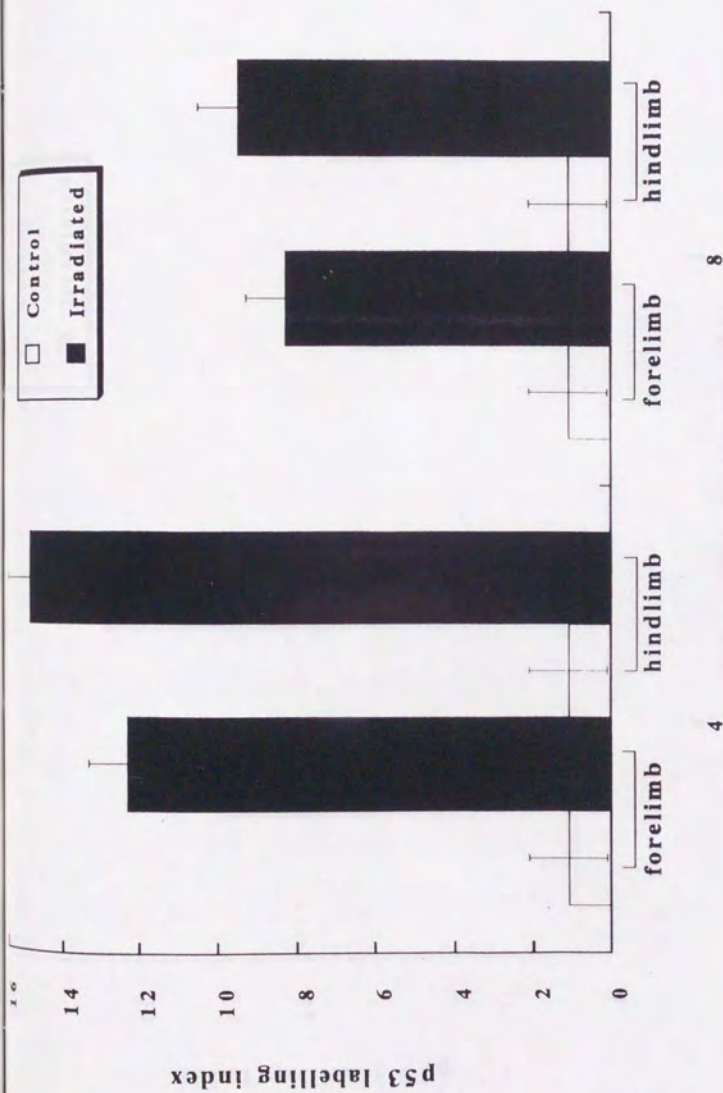


Fig. II-10. Immunohistochemical stainings of mouse limb bud sections parallel to the plane.



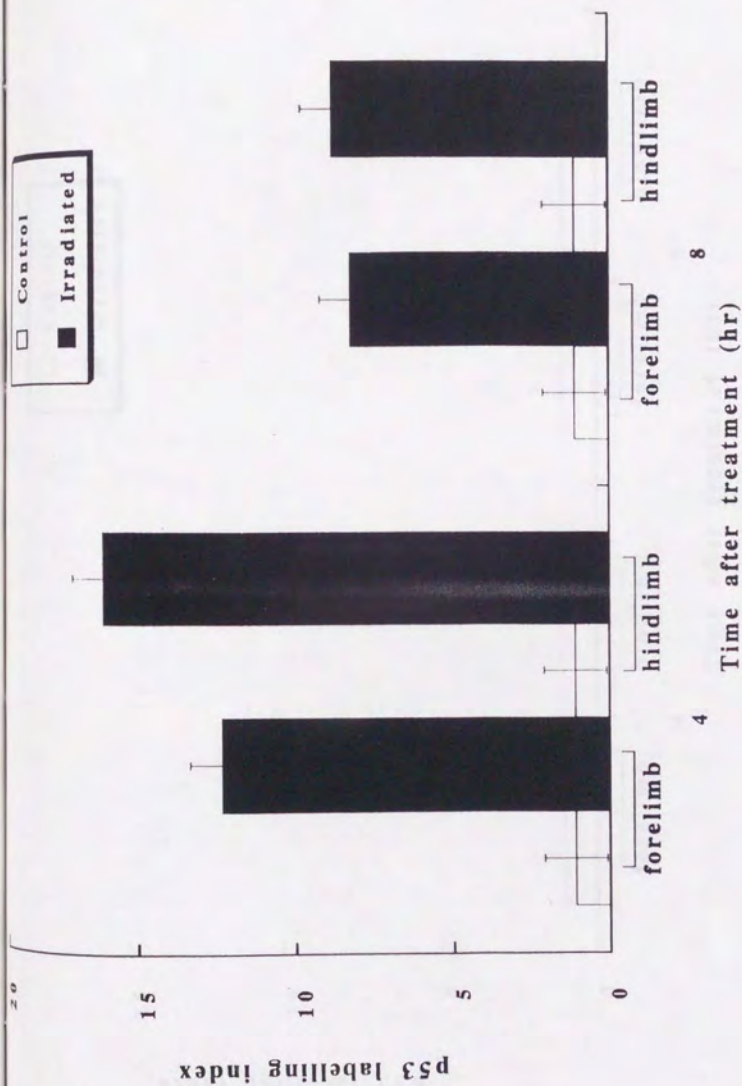
c	f
---	---

Fig. II-10. Immunohistochemical stainings of mouse limb bud sections parallel to the plane.



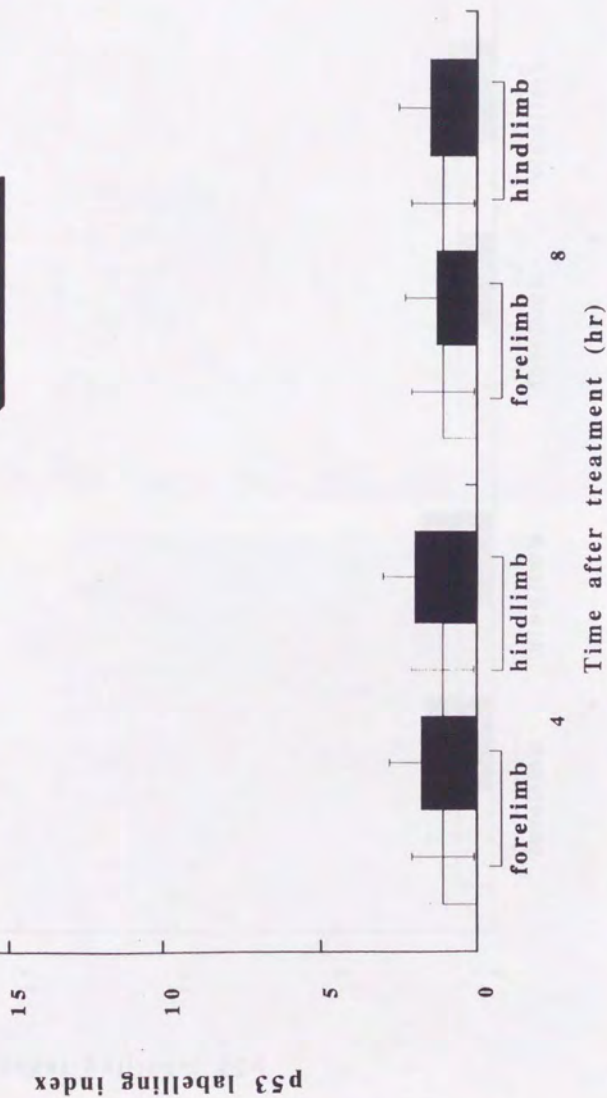
a. Pre-digital mesenchymal tissues of E11 limb buds

Fig. II-11. Increase of p53 protein level in the pre-digital region of limb buds after X-irradiation *in situ in vivo*.



b. Pre-digital mesenchymal tissues of E11.5 limb buds

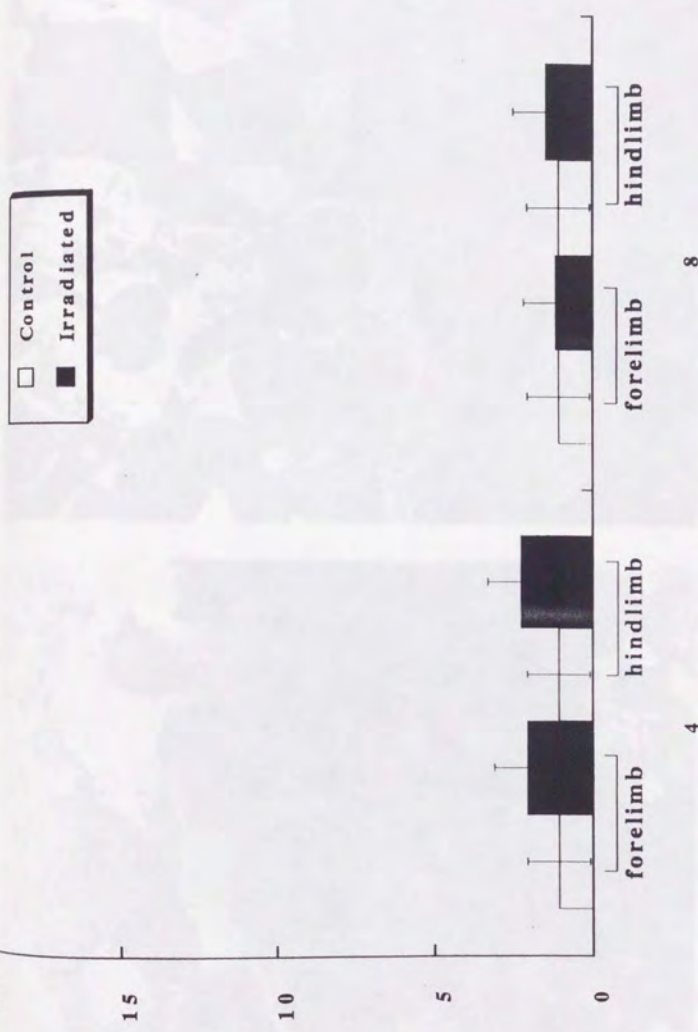
Fig. II-11. Increase of p53 protein level in the pre-digital region of limb buds after X-irradiation *in situ in vivo*.



a. Pre-interdigital mesenchymal tissues of E11 limb buds

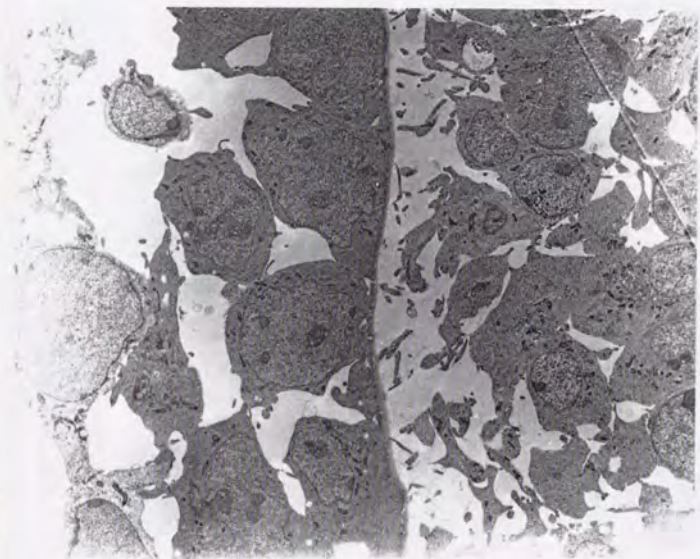
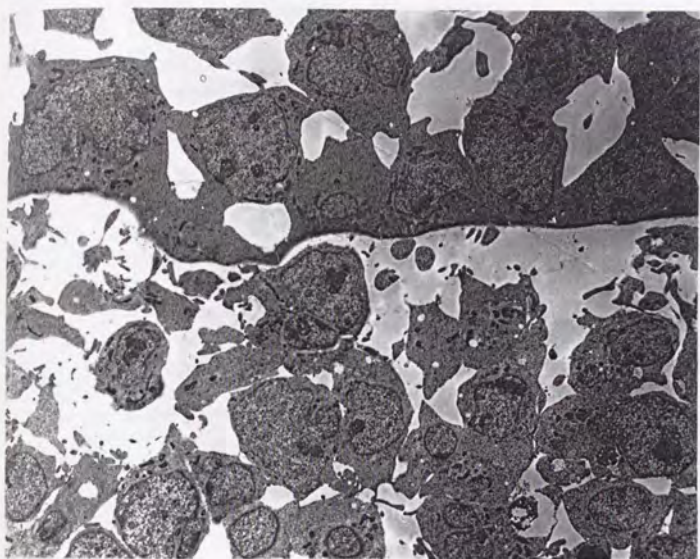
Fig. II-12. Increase of p53 protein level in the pre-interdigital region of limb buds after X-irradiation *in situ in vivo*.

p53 labelling index



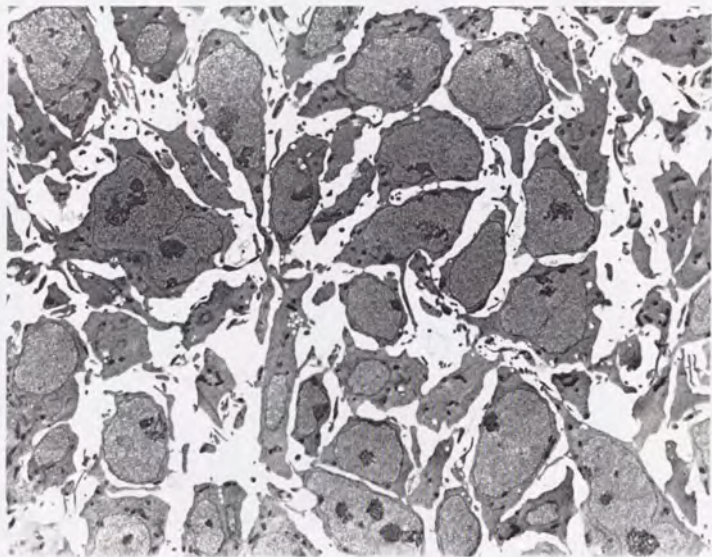
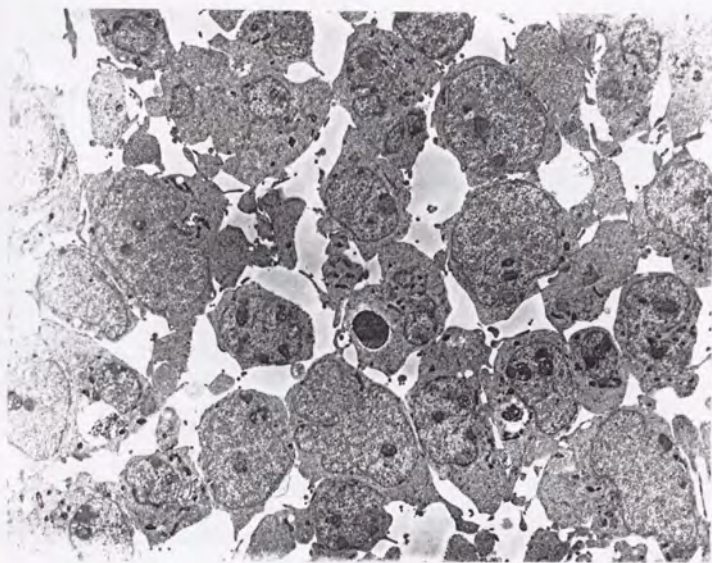
b. Pre-interdigital mesenchymal tissues of E11.5 limb buds

Fig. II-12. Increase of p53 protein level in the pre-interdigital region of limb buds after X-irradiation *in situ in vivo*.



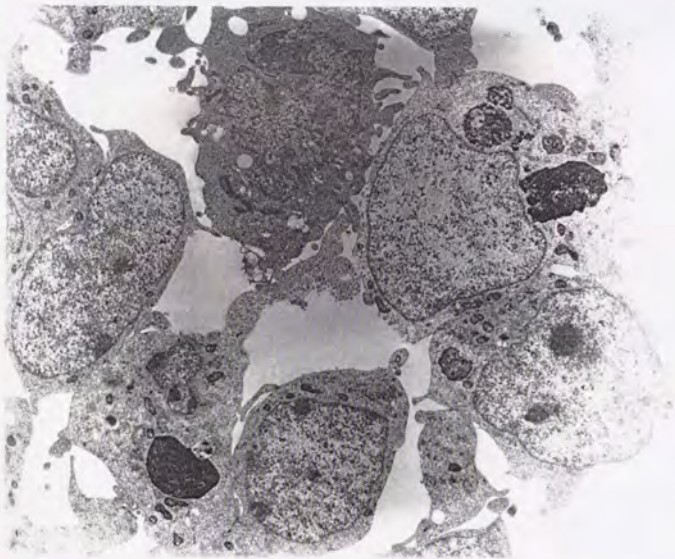
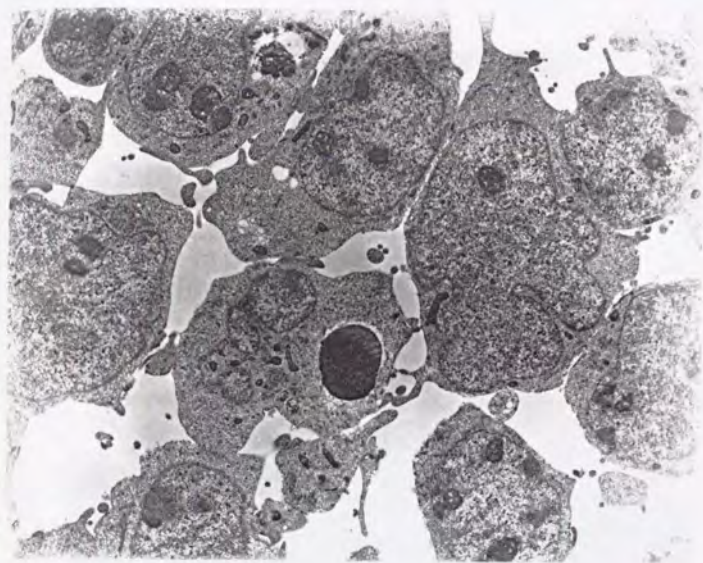
a b

Fig. II-13. Transmission electron micrographs of forelimb bud sections of control.



a	b
---	---

Fig. II-14. Transmission electron micrographs of E11 forelimb bud sections.



c	d
---	---

Fig. II-14. Transmission electron micrographs of E11 forelimb bud sections.

a	b
c	d

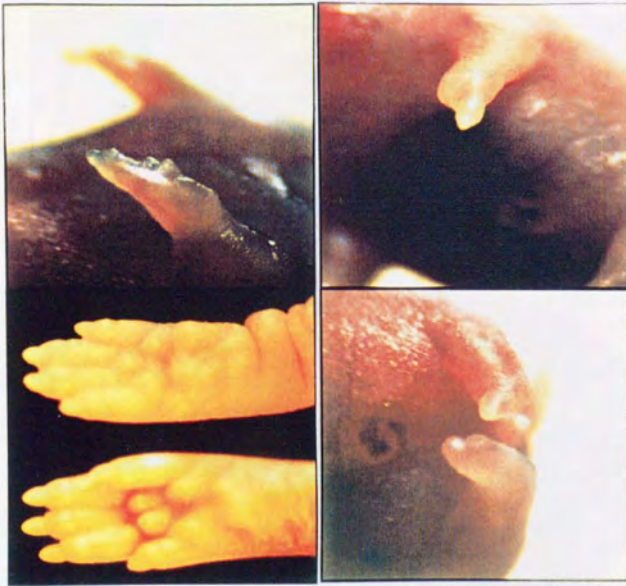
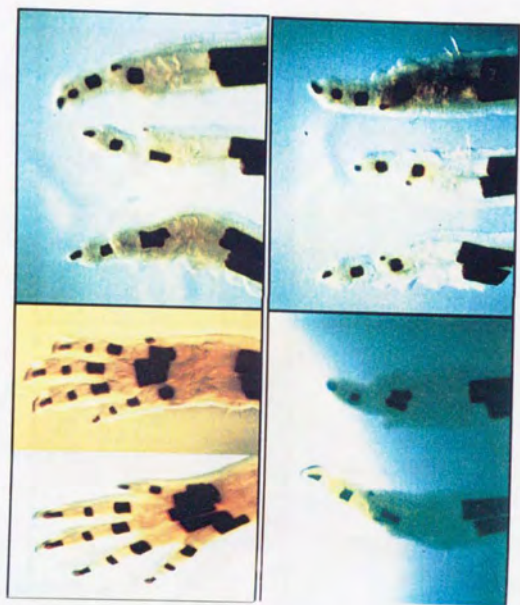


Fig. II-15. Limb bud teratogenesis by prenatal X-irradiation.

a	b
c	d



Fig. II-16. Limb bud teratogenesis by prenatal X-irradiation.



a	b
c	d

Fig. II-17. Whole mount skeleton preparations of E19 limbs.

a	b
c	d

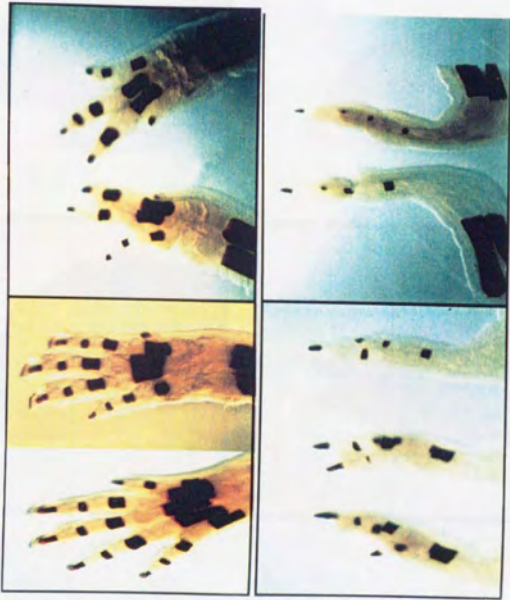
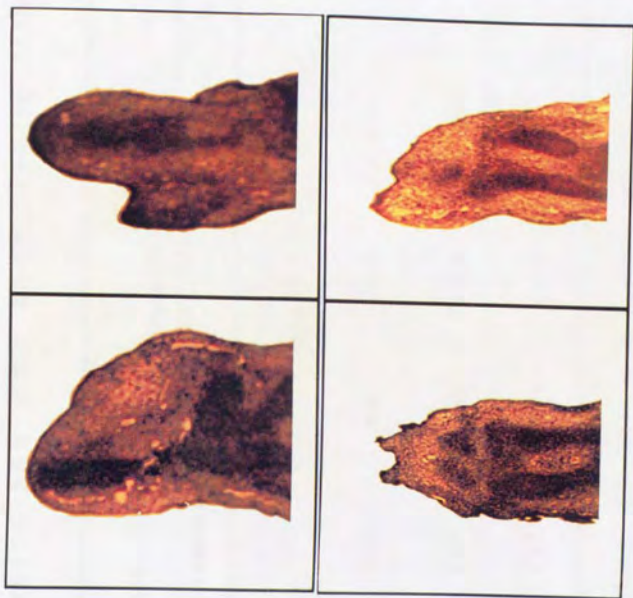


Fig. II-18. Whole mount skeleton preparations of E19 limbs.



a	b
c	d

Fig. II-19. Light micrographs of prenatal 5 Gy irradiated mouse E19 limb sections parallel to the plane stained with Hematoxylin and Eosin.

Table II-1

Incidences of deaths and limb anomalies in fetuses on E19

Radiation dose (Gy)	Pregnant mice examined	Placentas examined	Dead fetuses all fetuses	Death (%) in fetuses	Number of alive fetuses	% of fetuses with malformed limb in living fetuses
0	16	237	53	22.4	184	0
1	16	241	64	26.6	177	6.2** ^a
2	16	242	131	54.1	111	19.8** ^a
5	16	247	201	81.4	36	100** ^a

^a Significant difference in comparison with control;

* mainly of brachydactyly;

** mainly of aplangy and ectrodactyly.

Table II-2

Incidences of limb anomalies examined on E19 in
fetuses irradiated with 5 Gy on E11 and E11.5

Radiation Time (day)	Pregnant mice examined	Placentas alive fetuses examined	forelimb			hindlimb			
			aplangy	ectrodactyly	others	aplangy	ectrodactyly	others	
11	16	247	36	21	14	1*	5	31	-
11.5	16	249	38	25	13	-	4	34	-

* brachydactyly

Figure legends

- Fig. II-1. Light micrographs of mouse E11 and E11.5 limb bud sections parallel to the plane. Limb bud sections were stained with Heamatoxylin and Eosin. (a) E11 forelimb bud, (b) E11 hindlimb bud, (c) E11.5 forelimb bud, and (d) E11.5 hindlimb bud. Magnification was at $\times 80$.
- Fig. II-2. Higher magnification ($\times 800$) light micrographs of mouse E11 forelimb bud sections parallel to the plane. Sections were stained with Heamatoxylin and Eosin. (c) pre-digital region, and (d) pre-interdigital sections 4 hr after irradiation with 5 Gy, and (a) and (b) were their controls, respectively.
- Fig. II-3. Higher magnification ($\times 800$) light micrographs of mouse E11 hindlimb bud sections parallel to the plane. Sections were stained with Heamatoxylin and Eosin. (c) pre-digital region, and (d) pre-interdigital sections 4 hr after irradiation with 5 Gy, and (a) and (b) were their controls, respectively.
- Fig. II-4. Higher magnification ($\times 800$) light micrographs of mouse E11.5 forelimb bud sections parallel to the plane. Sections were stained with Heamatoxylin and Eosin. (c) pre-digital region, and (d) pre-interdigital sections 4 hr after irradiation with 5 Gy, and (a) and (b) were their controls, respectively.

Fig. II-5. Higher magnification ($\times 800$) light micrographs of mouse E11.5 hindlimb bud sections parallel to the plane. Sections were stained with Heamatoxylin and Eosin. (c) pre-digital region, and (d) pre-interdigital sections 4 hr after irradiation with 5 Gy, and (a) and (b) were their controls, respectively.

Fig. II-6. Induction of apoptosis by 5 Gy of X-rays in the pre-digital regions of mouse E11 (a) and E11.5 (b) limb buds.

Fig. II-7. Induction of apoptosis by 5 Gy of X-rays in the pre-interdigital regions of mouse E11 (a) and E11.5 (b) limb buds.

Fig. II-8. TUNEL staining of limb bud sections. Almost no positive stained cells in the pre-digital (a) and pre-interdigital (b) regions of E11 limb sections. More limb bud cells were stained positive 4 hr after irradiation with 5 Gy. Sections from irradiated E11 embryo: (c) pre-digital regions (d) pre-interdigital regions. Sections from irradiated E 11.5 embryos: (e) pre-digital regions (f) pre-interdigital regions. Magnification: $\times 800$.

Fig. II-9. Analysis of free DNA extracted from limb buds by electrophoresis. In (a), lane 3 was DNA ladder marker (123bp). Lanes 1, 2, 4, 5, and 6 were free DNA extracted from E11.5, E12, E13, E14, and E15 limb buds in situ *in vivo*, respectively. (b), lane 5 was DNA ladder marker (123 bp). Lanes 1, 2, 3, 4, and 6 were free DNA extracted from E11 limb buds in situ *in vivo* at 0, 4, 8, 12, and 24 hr after

irradiation with 5 Gy. Lane 7 was control from E12 limb buds in situ *in vivo*. (c), lane 5 was DNA ladder marker (123 bp). Lanes 1, 2, 3, 4, and 6 were free DNA extracted from E11.5 limb buds in situ *in vivo* 0, 2, 4, 10, and 24 hr after irradiation with 5 Gy. The presence of fragmented DNA was revealed as a ladder and smear pattern showing discrete peak corresponding to fragments 360 base pairs.

Fig. II-10. Immunohistochemical stainings of mouse limb bud sections parallel to the plane. Limb bud sections were stained with anti-p53 polyclonal antibody (AB565) and counterstained with Methyl Green. Cells with p53 protein levels higher than usual were positively stained as dark brown color in sections. Few positive staining in the control sections of forelimb bud pre-digital (a) and pre-interdigital (b) regions. Many cells were strongly positive stained in the pre-digital region (c) but in pre-interdigital region (d) after irradiation in the E11 forelimb buds, while in case of irradiated E11 hindlimbs, there were many strongly positive stained cells in the pre-digital regions (e), and there were also certain positive stained cells in the pre-interdigital regions (f). Magnification: $\times 800$.

Fig. II-11. Increase of p53 protein level in the pre-digital region of limb buds after X-irradiation in situ *in vivo*. (a) E11 and (b) E11.5.

Fig. II-12. Increase of p53 protein level in the pre-interdigital region of limb

buds after X-irradiation in situ *in vivo*. (a) E11 and (b) E11.5.

Fig. II-13. Transmission electron micrographs of forelimb bud sections of control. (a) E11 and (b) E11.25. Cells in pre-digital regions (marked with **) showed bigger in size and less dendrite-like structure. Note spontaneous apoptotic cell showing condensed nucleus in (b). Magnification was $\times 3000$.

Fig. II-14. Transmission electron micrographs of E11 forelimb bud sections at magnification of $\times 6000$. (a) and (b) were 6 hr after irradiation with 0.3 Gy. Cells with higher electron density and condensed nuclei were apoptotic cells. Note the apoptotic cells phagocyted by the neighboring cells.

Fig. II-15. Limb bud teratogenesis by prenatal X-irradiation. Pregnant mice were irradiated with 5 Gy on D11, E19 fetuses were examined at the time of cesarean section. Photographs showed the external appearance of the E19 fore- and hindlimbs. (a), fore- and hind limbs of control; (b) to (d) irradiated. Note the defect pattern of hindlimbs showed higher severity (mainly ectrodactyly) than that of the forelimbs (mainly aplangy). Magnification at $\times 10$ for (a), and at $\times 8$ for (b) to (d).

Fig. II-16. Limb bud teratogenesis by prenatal X-irradiation. Pregnant mice were irradiated with 5 Gy on D11.5, E19 fetuses were examined at the time of cesarean section. Photographs showed the external

appearance of the E19 fore- and hindlimbs. (a) to (d) were all of the irradiated. Note the defect pattern of hindlimbs showed higher severity (aphlangy and ectrodactyly) than that of the forelimbs (mainly aphlangy and few brachydactyly). Magnification at $\times 10$ for (a), and at $\times 8$ for (b) to (d).

Fig. II-17. Whole mount skeleton preparations of E19 limbs. Pregnant mice were irradiated with 5 Gy on D11, E19 fetuses obtained by cesarean section and limbs were stained with Alizarin red S. Photographs showed the skeletal appearance of the E19 fore- and hindlimbs. (a), fore- and hind limbs of control; (b) to (d) irradiated. Note the defect pattern of hindlimbs showed higher severity (mainly ectrodactyly) than that of the forelimbs (mainly aphlangy). Magnification at $\times 8$.

Fig. II-18. Whole mount skeleton preparations of E19 limbs. Pregnant mice were irradiated with 5 Gy on D11.5, E19 fetuses obtained by cesarean section and limbs were stained with Alizarin red S. Photographs showed the skeletal appearance of the E19 fore- and hindlimbs. (a) to (d) were all of the irradiated. Note the defect pattern of hindlimbs showed higher severity (aphlangy and ectrodactyly) than that of the forelimbs (mainly aphlangy and few brachydactyly). Magnification at $\times 8$.

Fig. II-19. Light micrographs of prenatal 5 Gy irradiated mouse E19 limb sections parallel to the plane stained with Heamatoxylin and Eosin.

(a) and (b) were forelimb and hindlimb ectrodactyly, respectively. Sympus apus with both calcaneum and talus of a left hindlimb (c) and only calcaneum of a right limb (d) fetuses irradiated on E11. Magnification at $\times 30$ for (a) and (b), and at $\times 22$ for (c) and (d).

References

- Cattoretti G., Rilke F., Andreola S., D'Amato L., and D. Delia. p53 expression in breast cancer. *Int. J. Cancer*. 1988; 41: 178-183.
- Councouvanis E. C., Martin G. R., and J. H. Nadeau. Genetic approaches for studying programmed cell death during development of laboratory mouse. *Method. Cell Biol.*, 1995; 46: 387 - 440.
- Gavrieli Y., Sherman Y., and S. A., Ben-Sasson. Identification of programmed cell death in situ via specific labeling of nuclear DNA fragmentation. *J. Cell Biol.*, 1992; 119(3): 493-501.
- Hendry J. H., Potten C. S., and A. Merritt. Apoptosis induced by high- and low LET radiations. *Radiat. Environ. Biophys.*, 1995; 34: 59-62.
- Hinchliffe J. R. and D. A. Ede. Cell death and the development of form and skeletal pattern in the limbs of talpid3 (ta3) mutant chick embryos. *J. Embryol. Exp. Morphol.*, 1973; 30: 753-772.
- Hinchliffe J. R. and P. V. Thorogood. Genetic inhibition of mesenchymal cell death and the development of form and skeletal pattern in the normal and wingless (ws) chick embryos. *J. Embryol. Exp. Morphol.*, 1974; 31: 747-760.
- Inouye M. Differential staining of cartilage and bone in fetal mouse skeleton by alcian blue and alizarin red S. *Cong. Anom.*, 1976; 171-173.
- Iuzzolino P., Ghimenton C., Nicolato A., Giorgiutti F., Fina P., Doglioni C., and M. Barbareschi. p53 protein in low-grade astrocytomas: a study with long-term follow up. *Br. J. Cancer*, 1994; 69: 586-591.
- Johnson D. R. Polysyndactyly, a new mutant gene in the mouse. *J. Embryol. Exp. Morphol.*, 1969; 21: 285 -294.
- Kerr J. F. R., Wyllie A. H., and A. R. Currie. Apoptosis: a basic biological

- phenomenon with wide-ranging implications in tissue kinetics. *Br. J. Cancer*, 1972; 26(4): 239-257.
- Kochhar D., Penner J., and J. MacDay. Limb development in mouse embryos. Reduction defects, cytotoxicity and inhibition of DNA synthesis produced by cytosine arabinoside. *Teratology*, 1978; 18: 71-92.
- Kondo S. Altruistic cell suicide in relation to radiation hormesis. *Int. J. Radiat. Biol.*, 1988; 53: 95-102.
- Kurishita A. and T. Ihara. Dose-related induction of digital malformation in rats by 5-azacytidine: description of the defects. *Cong. Anom.*, 1989; 29: 59-71.
- Li Y., Sharov V. G., Jiang N., Zaloga C., Sabbah H. N., and M. Chopp. Ultrastructural and light microscopic evidence of apoptosis after middle cerebral artery occlusion in the rat. *Am. J. Pathol.*, 1995; 146(5): 1045-1051.
- Mori C., Nakamura N., Kimura S., Irie H., Takigawa T., and K. Shiota. Programmed cell death in the interdigital tissue of the fetal mouse limb is apoptosis with DNA fragmentation. *Ana. Record*, 1995; 242: 103-110.
- Muneoka K., Wanek N., and S. V. Bryant. Mammalian limb bud development: In situ fate maps of early hindlimb buds. *J. Exp. Zool.*, 1989; 249: 50-54.
- Norimura T., Nomoto S., Katsuki M., Gondo Y., and S. Kondo. p53-dependent apoptosis suppresses radiation-induced teratogenesis. *Nature Med.*, 1996; 2(5): 577-580.
- Ohyama H. and T. Shimokawa. DNA electrophoresis. In: *The latest experimental methods for apoptosis research*. Ed. Tsujimoto Y., Tone S., and T. Yamada. Youdosya Press. Tokyo, 1995. pp 61-67.
- Randy T. O. C., Johnson L., Riddle R. D., and C. J. Tabin. Mechanisms of limb patterning. *Curr. Opin. Genet. Develop.* 1994; 4: 535 - 542.
- Renninson J., Baker B. W., WmcGown A. T., Murphy D., Norton J. D., Fox B. W.,

- and D. Crowther. Immunohistochemical detection of mutant p53 protein in epithelial ovarian cancer using polyclonal antibody CMI: correlation with histopathology and clinical features. *Br. J. Cancer*, 1994; 69: 609-61.
- Ritter E. J., Scott, W. J., and J. G. Wilson. Relationship of temporal patterns of the cell death and development to malformations in the rat limb. Possible mechanisms of teratogenesis with inhibitors of DNA synthesis. *Teratology*, 1973; 7: 219-226.
- Russell L. B. and W. L. Russell. An analysis of the changing radiation response of the developing mouse embryo. *J. Cell Physiol.*, 1957; 43(suppl 1): 1030-1049.
- Scott W. J. , Ritter, E. J., and J. G. Wilson. Delayed appearance of ectodermal cell death as a mechanism of polydactyly induction. *J. Embryol. Exp. Morphol.*, 1977; 42: 93-104.
- Selins K. S. and J. J. Cohen. Gene induction by gamma-irradiation leads to DNA fragmentation in lymphocytes. *J. Immunol.*, 1987; 139: 3199-3206.
- Tone S. and S. Tanaka. In situ labelling (TUNEL method). In: *The latest experimental methods for apoptosis research*. Ed. Tsujimoto Y., Tone S., and T., Yamada. Youdosya Press. Tokyo, 1995. pp 41-48.
- Tone S., Tanaka S., and Y. Kato. The inhibitory effect of 5-bromodeoxyuridine of the programmed cell death in the chick limb. *Develop. Growth and Differ.*, 1983; 25(4): 381-391.
- Wanek N., Muneoka K., Holler-Dinsmore G., Burton R., and S. V. Bryant. A staging system for mouse limb development. *J. Exp. Zool.*, 1989; 249: 41-49.
- Zhou X. Y., Dong J. C., Zhou S. Y., Chen J. D., and F. R. Guo. Experimental study on relative biological effectiveness of tritium and risk estimates of genetic damage. *Chn. Med. J.*, 1989; 102(11): 872-878.

Chapter III.

Further analysis of the localization of apoptosis in the mouse limb buds in the organ culture system

Summary

Radiation-induced apoptosis was identified and localized in cultured mouse embryonic limb buds, and was investigated in the cultured mouse limb bud tissues *in vitro*. E11 and E11.5 mouse limb buds were irradiated with 5 Gy of X-rays and cultured for half a day *in vitro*. Observation of pathological sections by HE staining under a microscope showed that in the forelimb buds there were two kinds of morphologically different cells that located in the pre-digital and pre-interdigital regions, respectively. Radiation-induced cell death was identified both morphologically and biochemically with regard to apoptosis. In the case of the forelimb buds, there was a significant increase in the number of apoptotic cells in the pre-digital regions 4 hr after irradiation, while there were only few apoptotic cells that were found in the pre-interdigital regions. On the other hand, for the hindlimb buds, there were a mixed cell population of these two kinds of cells located in the pre-interdigital regions. A slight increase in the apoptotic cell number was also found in the pre-interdigital regions of the hindlimbs after radiation.

Cells from pre-digital and pre-interdigital regions of E12 forelimb buds underwent apoptosis with different time courses. Cells from the pre-digital regions had a higher radiosensitivity and underwent radiation-induced apoptosis several hours after irradiation, while cells from the pre-interdigital regions underwent spontaneous apoptosis and radiation was hardly affecting the increase of apoptotic fractions in the cultures.

Results were consistent with those obtained from the limb bud *in situ in vivo* study. Results indicated that limbs as organs of embryos *in situ* or as

individual organs *in vitro* responded to radiation damage similarly at least in the early time after irradiation. These results also confirmed the previous work presented in Chapter II, as well as the hypotheses regarding cell radiosensitivity and the way that radiation affects morphogenesis during development.

Introduction

Prenatal development, characterized by intensive cell proliferation, cell differentiation and cell migration during organogenesis, shows a high sensitivity to many teratogens. As one of the teratogens, irradiation induces malformations of various organs (UNSCEAR 1977). Therefore, radiation exposure of embryos and fetuses is of great concern for understanding of teratogenic mechanism of environmental teratogens. Irradiation effects on embryogenesis are strongly dependent on the developmental stage at exposure and on the radiation dose. In the mean time, the irradiated embryos provided us an idealistic model to study the mechanism of radiation teratogenesis, especially regarding to cell proliferation, differentiation and cell death during organogenesis (Michel 1989).

The mouse limb development is an exquisitely regulated complex of cell movement, division, differentiation, and death. The orchestration of this process has been under investigation for many years (Zakeri and Ahuja 1994). The mouse limbs, with their combination of repetitive patterns (the digits) and variation in pattern (each digit being different from the others), have been major experimental tools.

In the Chapter II, I studied the radiation effects on limb bud morphogenesis during embryogenesis *in situ in vivo* and found that radiation induced teratogenesis via induction of apoptosis. Radiation-induced apoptosis occurred mainly in the pre-digital tissues where cells will otherwise undergo proliferation and differentiation in the subsequent developmental stage. Results of the prenatal radiation-induced malformation pattern and severity of the limb buds of the living fetuses prenatally

irradiated indicated the important role played by radiation-induced apoptosis in the radiation teratogenesis.

The developing mouse limb buds in culture undergo growth, cellular differentiation and tissue organization processes similar to those occurring *in vivo*. Large numbers of limb buds with their corresponding controls from carefully staged embryos could be cultured for a short period of time and grown in a chemically defined medium. Because of this ability, the assay has the potential as a biological test system for the elucidation of mechanisms responsible for the teratogenic activity of radiation (Friedman 1987). As one of a battery of test systems, it provides a suitable methodology to investigate the radiation effects and to confirm the *in vivo* work using limb bud *in situ*. The limb bud culture system and its deriving tissue culture system will no doubt provide us more data to understand the radiation effects on the development. Because of the exclusion of maternal, nutritional, hormonal and other confounding factors such as tissue interactions, results obtained in the organ culture system also make it easy to analyze causality.

In the present study, I hoped to use the limb bud organ and tissue culture systems as model systems to study radiation effect on the cellular proliferation, differentiation, and induction of cell death during morphogenesis and confirm the *in vivo* results presented in Chapter II.

Materials and Methods

Organ and tissue culture procedures

Animals: ICR mice aged 8 - 10 weeks, weighing 22-26 g were used in this study. Females in estrus were mated with potent males overnight. The day when copulatory plug was found was designated day 1 of gestation (D1) or embryonic age day 1 for the embryo (E1).

The protocols were as described previously (Lessmollmann 1976; Tone *et al.* 1983; Milaire and Mulnard 1984; Friedman 1987; Desbiens *et al.* 1987; Tone 1995) with some modifications. In brief, the isolated limb buds of E11 or E11.5 embryos, or tissues from the digital and interdigital areas of forelimb buds of E12 embryos were transferred to pieces of cellulose nitrate filtration membranes (pore size 0.45 μm , Tokyo Roshi Kaisha, Ltd., Japan) carried by grids of stainless steel (Ikeda Rika, Tokyo, Japan) placed in 35 mm Petri dishes. In the limb bud culture, limb buds from the same embryo were always used half in the control and half in the irradiated group. In the tissue culture, the decision of tissue location in the forelimb buds to be sampled was according to a previous Nile Blue staining of their corresponding opposite forelimb buds.

The culture medium was DMEM10L (Dulbecco's Modified Eagle Medium, GIBCO), supplemented with 10% fetal calf serum (Flow Laboratories), ascorbic acid (150 ng/ml), L-glutamine (200 ng/ml), penicillin 100 IU/ml and streptomycin 100mg/ml (GIBCO).

The medium was adjusted to wet the explants through the membrane without submerging them. The buds were always placed with their volar aspects lying on the filter. The assembly was kept at 37 °C with 5% CO₂ and

95% air in a water-saturated incubator.

X-ray irradiation

X-irradiation was performed at room temperature with an X-ray machine (Pantak-320S, Shimadzu, Japan), operated at 200 kVp and 19 mA, with a dose rate of 90 R/min measured by an exposure ratemeter (Applied Engineering INC, Japan) using a 0.5 mm Al + 0.5 mm Cu filter.

The assembly was irradiated under the same conditions as those used in the *in vivo* study (Materials and Methods in Chapter II).

It takes about 6 days to let the explants develop into a higher stage which corresponds to limbs of E13-14 embryos *in vivo*. After such a long period of incubation the tetradactylous pattern resulting from the oligosyndactylous digits and the modification of apical ectoderm often occurs. In the present study, the limb buds were collected for histological examination at 4 and 8 hr after irradiation, respectively. As the degree of limb development (size and shape) is largely dependent on the age - more exactly, stage of the embryo from which the limb bud is removed (Barrach and Neubert 1980), the staging work was done under quality control.

The tissue culture was incubated for a period as long as 10 hr.

Identification, localization and qualification of apoptosis

The histological procedures were the same as those used in the *in vivo* study. The cell preparation for morphological examination by fluorescence microscopy was performed by trypsinizing the tissue, fixing the cells with 1% glutaraldehyde in 0.1 M phosphate buffer, and staining the cells with Hoechst 33342 (Sigma). The chromatin-condensed cells were counted as

apoptotic cells.

Identification and localization of apoptosis in the whole limb buds

Nile Blue sulphate staining

4 hr after irradiation, some limb buds were stained with Nile Blue sulphate, a lysosomotropic vital dye, to identify areas of cell death. Limb buds were stained in a 1:5000 solution of Nile Blue sulphate dissolved in PBS for 30 to 40 minutes at 37 °C in an incubator. After that, the limb buds were rinsed in Tyrode solution and photographed.

Identification and localization of apoptosis in limb bud sections

Light microscopy (LM)

Heamatoxylin and eosin staining (HE staining) was used. Briefly, the limb buds were fixed in 10% buffered formalin and subsequently processed using routine techniques and paraffin embedded. 3 μ m serial sections in a plane parallel to the volar aspect of the limbs were prepared, deparaffinized, and rehydrated. The sections were finally washed three times in distilled water, stained with heamatoxylin and eosin, dehydrated, cleared in xylene and mounted with xylene-based coverslipping medium.

The staining was photographed at 100 X and quantified on an Olympus microscope at 400 X using a square graticule. Cells with nuclear condensation or containing apoptotic bodies were referred to as apoptotic cells (Li *et al.* 1995). About 200 nuclei were counted in each limb bud in both the pre-digital regions of digit IV (but not in the regions of presumptive joints on the digital ray) and the pre-interdigital regions between digit III and digit IV. At least 6 limb buds were examined in each group. The percentage of

condensed nuclei was used as the apoptotic cell index (%).

Fluorescence microscopy (FM)

To determine the fraction of apoptotic cells in tissue cultures, cell suspensions of the pre-interdigital and pre-digital tissues cultured were prepared separately by trypsinizing the tissues. Then, cells were washed with PBS and fixed with 1% glutaraldehyde in 0.1 M phosphate buffer. The samples were stained with Hoechst 33342 (Sigma) for morphological examination. The cells with chromatin condensation were counted under a fluorescent microscope.

Results

Induction of apoptosis in cultured limb buds

Nile Blue sulphate staining (NB)

Fig. III-1 displayed the typical photos of whole organ NB staining. For the forelimb buds, in the control buds dye uptake was observed only in the distal part of pre-interdigital regions. Documented data showed that in the NB positively stained areas phagocytosis of the spontaneous apoptotic cells occurred (Mori *et al.* 1995). 4 hr after 5 Gy of X-rays, in the pre-interdigital regions the dye uptake was almost the same as in the control for the corresponding regions, while the excessive dye uptake was observed in the pre-digital regions. Distribution of the dye uptake in the pre-digital regions was found mainly in the distal part. For the hind limb buds, no clearly positively stained regions were found in the control buds, and a relatively uniform distribution of the dye uptake was found in the distal part of the buds 4 hr after irradiation. To confirm the distribution pattern of dye uptake in the limb buds, NB staining was also applied to the cultured forelimb buds of E12 embryos as they showed distinctly the pre-digital and pre-interdigital regions. Fig. III-2 displayed clearly the difference between control and the irradiated E12 forelimb buds on dye uptake distribution. The photos showed clearly that radiation-induced increase of dye uptake preferably distributed in the distal parts of the pre-digital regions.

Heamatoxylin and Eosin staining of cultured limb bud sections

Fig. III-3 displayed sections of both forelimb and hindlimb from E11 and E11.5 embryos. Some of the typical stainings of both pre-digital and pre-

interdigital regions were demonstrated in Fig. III-4 to Fig. III-7. In the sections of controls of the forelimb buds, the cells located in the pre-digital regions had a tight intercellular connection with their neighboring cells, they had a larger volume of cytoplasm compared to the cells located in the pre-interdigital regions which had more intercellular space and with many dendrite-like structures on the cell surface. The cells that located in the pre-digital regions were bigger in size than the cells that located in the pre-interdigital regions. Many cells that underwent mitosis in the pre-digital regions could be observed. In the sections of pre-digital region of the hindlimb buds, similar morphology was observed, while those two kinds of morphologically different cells were found in the pre-interdigital regions. 4 hr after radiation, many cells located in the pre-digital regions with condensed cell nuclei and separated from their neighboring cells were observed. 8 hr after radiation, phagocytosis of the apoptotic cells could be also observed. These graphic data showed no specific morphological differences compared to those obtained from the *in situ in vivo* study (Chapter II).

The statistical data based on the graphic observations were shown in Fig. III-8 and Fig. III-9, respectively. In the pre-digital regions of limb buds, 5 Gy of X-irradiation induced a significant increase in numbers of apoptotic cells in both fore- and hindlimb bud of E11 and E11.5 embryos. The apoptotic index of hindlimb buds was significantly higher than that of forelimb buds. The apoptotic index became lower when checked 8 hr after radiation compare to that at 4 hr after radiation. In the pre-interdigital regions of limb buds, 5 Gy of X-rays induced a significant increase in the numbers of apoptotic cells only in hindlimb buds of E11 and E11.5 embryos

4 hr after radiation, the maximum apoptotic index obtained being about 12%. The apoptotic index was about 50% in the cells located in the pre-digital regions after the same dose and checked at the same time point. These results were similar to those obtained from the limb bud in situ *in vivo* study (Chapter II). Some sections were also stained with TUNEL method, and the results were consistent to the HE methods, and they were also similar to the limb bud in situ *in vivo* studies (data not shown).

Induction of apoptosis in cultured E12 forelimb bud tissues

Fig. III-10 was the photos showing visualized nuclei of cells from cultured limb bud tissues using fluorescent dye staining. Cells with chromatin condensation were found. Analysis by gel electrophoresis of free DNA extracted from the cultured tissues also showed a DNA ladder pattern which appeared obviously 4 hr after irradiation and remained at the similar level during the later period of observation (data not shown). By counting the apoptotic cells and calculating the apoptotic cell percentage, the time course for radiation induced apoptosis was investigated at a dose of 5 Gy. These results were shown in Fig. III-11 and Fig. III-12. An increase in number of apoptotic cells identified by nuclear chromatin condensation was found 2 hr after radiation in the cells from the cultured pre-digital tissues. They reached a peak at 8 hr after radiation, and then decreased (Fig. III-11). The apoptotic percentage in the control showed a slow increase trend in the control (Fig. III-12). For the pre-digital tissue culture (Fig. III-12), an increase in number of apoptotic cells was found from 2 hr after radiation. The apoptotic fractions (%) reached a maximum about 6 hr after radiation and remained at 22%; in the control, the apoptotic fractions showed slightly

lower values parallel to those of the irradiated.

Discussion

Programmed cell death is recognized as an essential event in morphogenesis as well as in the normal turnover of cells in adult tissues (Wyllie *et al.* 1980, Hurlle 1988, Clarke 1990, Ellis *et al.* 1991). For the formation of limbs during development, cell death plays a key role by eliminating unnecessary cells to achieve complicated histogenesis and organogenesis (Zakeri and Ahuja 1994). Study of radiation induced apoptosis now possesses an important position in the field of radiation biology to understand the mechanism of radiation effects (Fritz-Niggli 1995).

Techniques of organ culture *in vitro* represent a sensitive model system for radiobiological studies. They are also a very useful support for the data obtained *in vivo*, especially regarding the mechanism of radiation damage. Numerous biological endpoints of both morphology and biochemistry have been available in this *in vitro* system. The apoptotic cell death was used as the endpoint and examined morphologically and pathologically.

Results obtained in the present study were consistent with those obtained from the limb buds *in situ in vivo* study (Chapter II). These results confirmed the localization work on radiation induced apoptosis in the limb buds *in vitro*. Under the *in vitro* conditions of the present study, possible effects from the embryo itself and the pregnant animal could be excluded. Results indicated that during the short period of time after irradiation, the mouse embryonic limb buds responded to the radiation damage *in vivo* the same as *in vitro* regarding induction of apoptosis by radiation and the distribution of radiation-induced apoptosis. These results also supported data presented in Chapter II that radiation induced teratogenesis were

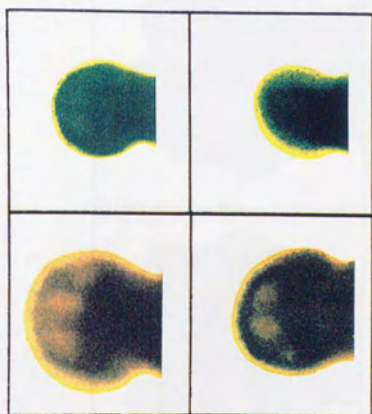
mainly of aplangy in the forelimb, and of aplangy and ectrodactyly in the hindlimbs.

In the tissue culture study, cells from pre-interdigital regions of E12 forelimb buds died via apoptosis *in vitro* without any treatment. This apoptotic cell death is thought to be spontaneous. This result was very similar to those of the early work on avian limb buds (Saunders and Fallon 1967, Fallon and Saunders 1968) which showed that the cells of the posterior necrotic zone undergo cell death on schedule after being excised and cultured *in vitro*. This result suggested that these cell were already committed to undergo spontaneous apoptosis at the time when they were excised. Radiation exerted almost no effect on induction of an increase in number of apoptotic cells in the pre-interdigital tissue cultures. It is suggested that once the cells were committed to the spontaneous apoptosis, they were hardly affected by radiation to undergo radiation-induced apoptosis. From this point of view, these cells showed a lower radiosensitivity before they started their spontaneous apoptosis program.

Together with the results from *in vitro* micromass and limb buds in situ *in vivo* studies, it is indicated that (1) radiation exerts its deleterious effects on development during limb bud morphogenesis via induction of apoptosis, (2) radiation induced apoptosis mainly occurred among cells that otherwise undergo proliferation and differentiation in the subsequent developing stages, (3) forelimb bud and hindlimb bud of the same embryo had different radiosensitivities due to their developmental status, (4) cells already committed to undergo spontaneous apoptosis showed a lower radiosensitivity before they start the spontaneous apoptosis program, and (5) radiation induced apoptosis in the late period of organogenesis could

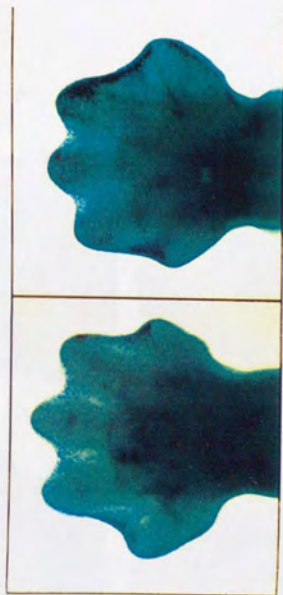
result in teratogenesis.

To reveal the mechanism is most important to understand the radiation effects on development. Many clues were obtained by utilization of the modern technology so far, but many more questions are remaining to be answered in the future. There are many works to be done using new assays and especially using the gene engineering method to analyze the role that apoptosis plays in limb bud morphogenesis with or without exposure to teratogens. Many mouse mutants are to be characterized with respect to apoptosis, and a large number of apoptosis-related genes still remain to be identified, mapped, and characterized (Counouvanis *et al.* 1995). Utilization of these rich resources is likely to produce considerable progress in understanding the genetic control of apoptosis and its function in normal and abnormal development in the future.



a	b
c	d

Fig. III-1. Observations of mouse limb buds by Nile Blue Sulphate staining.



a	b
---	---

Fig. III-2. Observations of mouse E12 forelimb buds by Nile Blue Sulphate staining.

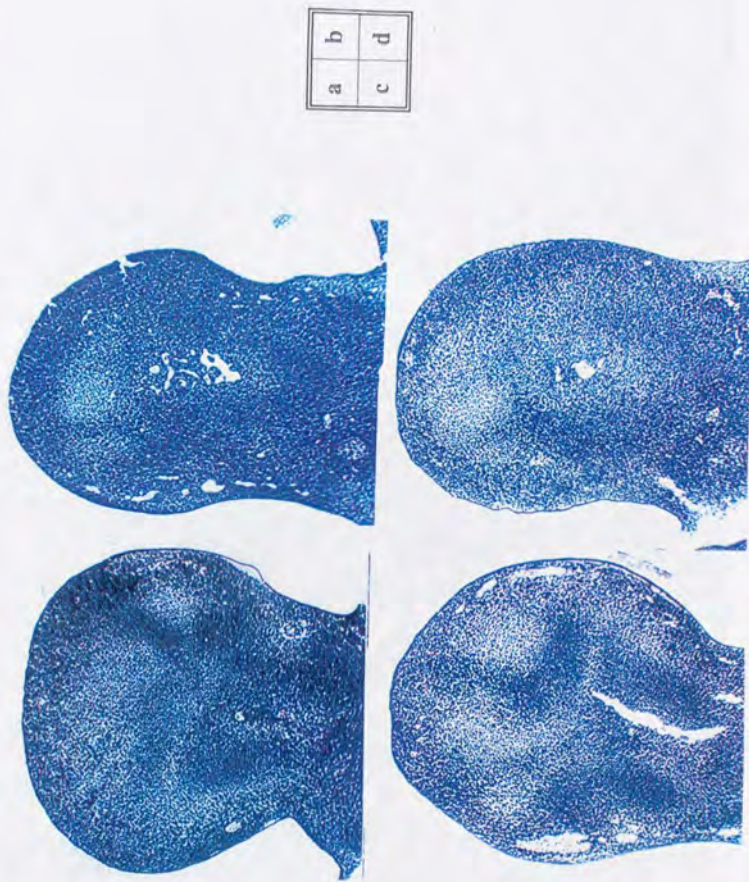


Fig. III-3. Light micrographs of mouse E11 and E11.5 limb bud sections parallel to the plane.

a	b
c	d

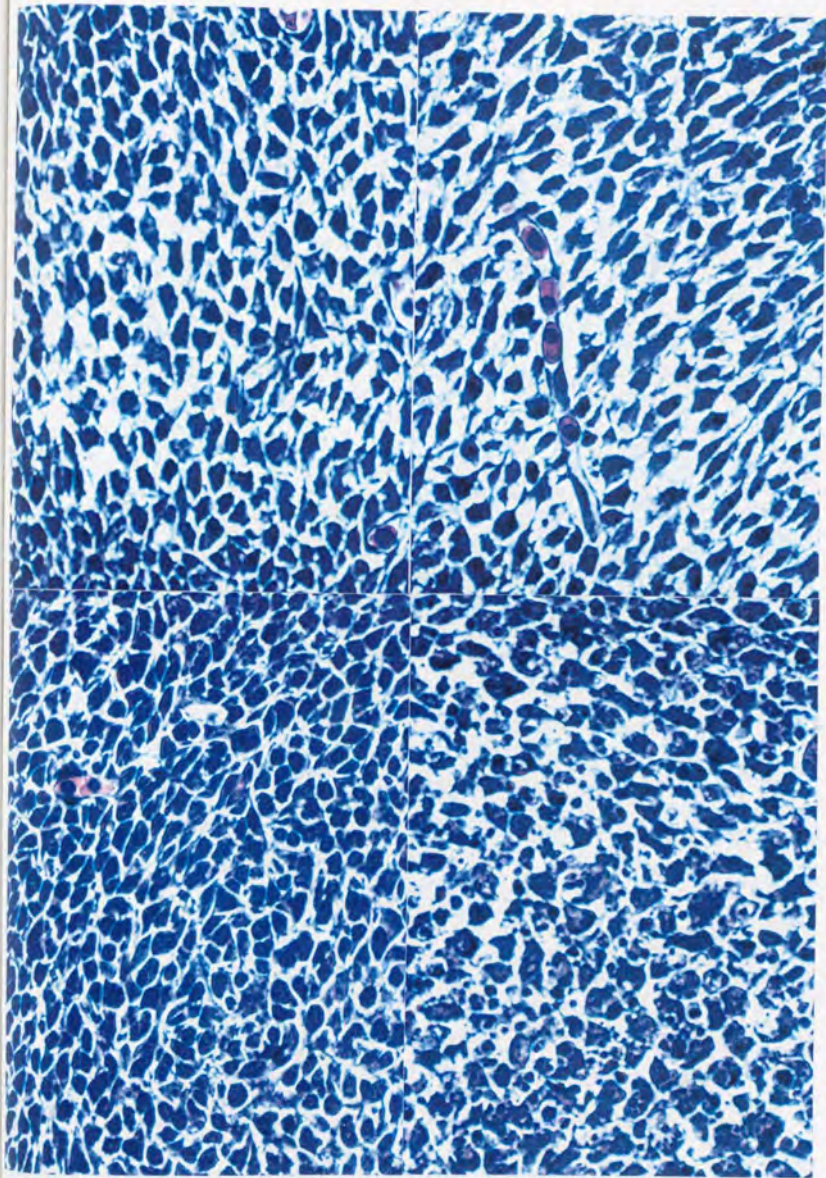


Fig. III-4. Higher magnification light micrographs of mouse E11 forelimb bud sections parallel to the plane.

a	b
c	d

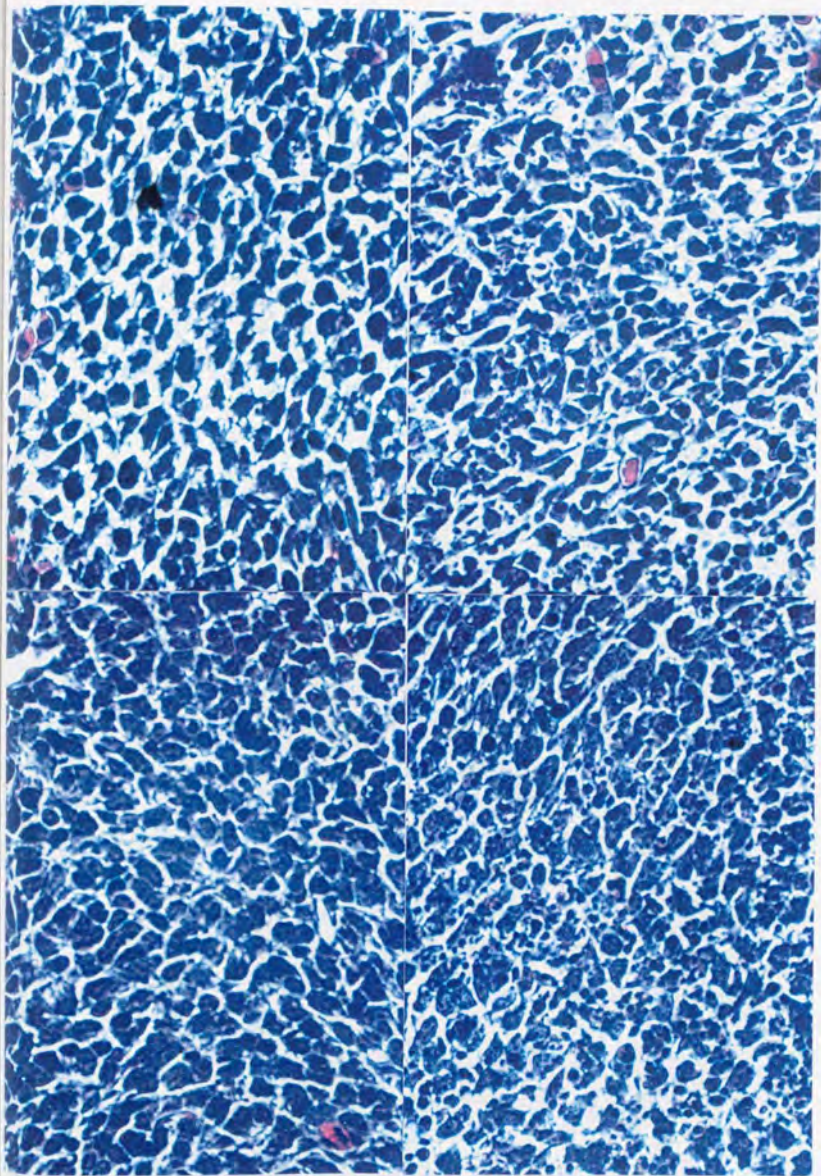


Fig. III-5. Higher magnification light micrographs of mouse E11 hindlimb bud sections parallel to the plane.

a	b
c	d

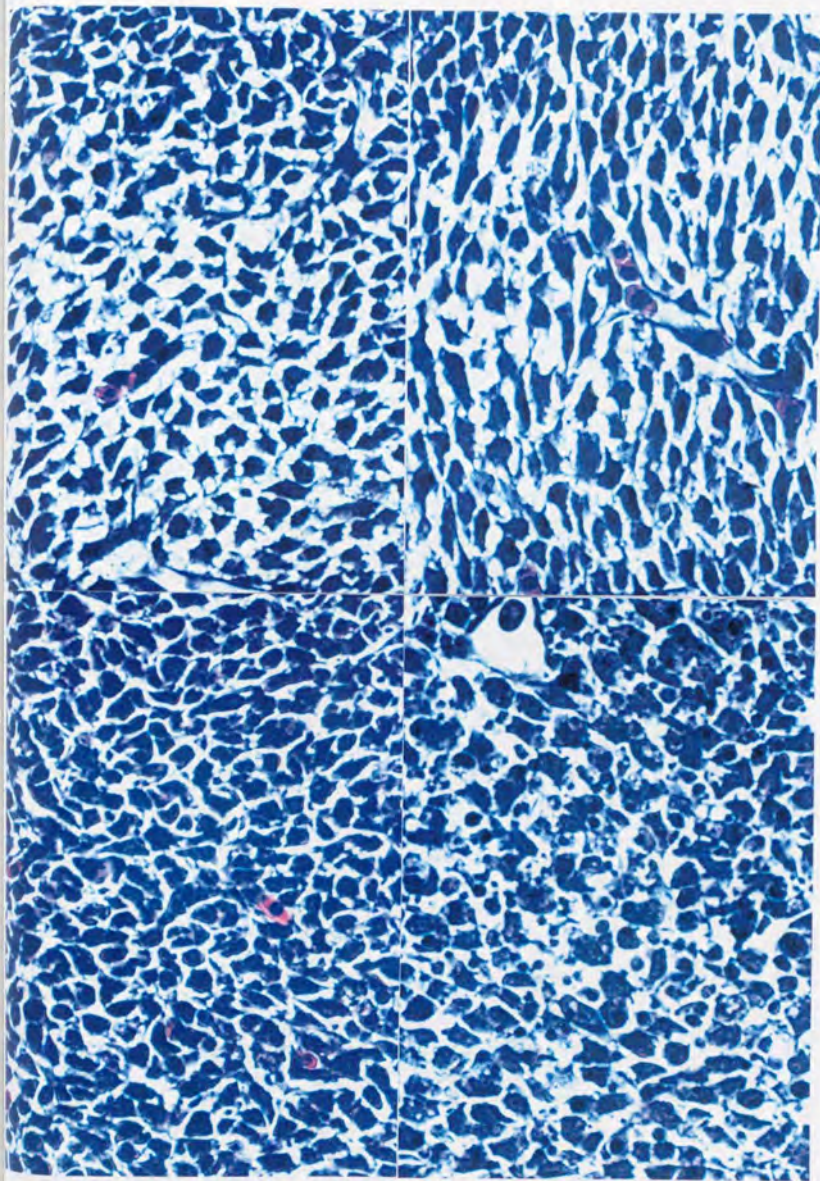


Fig. III-6. Higher magnification light micrographs of mouse E11.5 forelimb bud sections parallel to the plane.

a	b
c	d

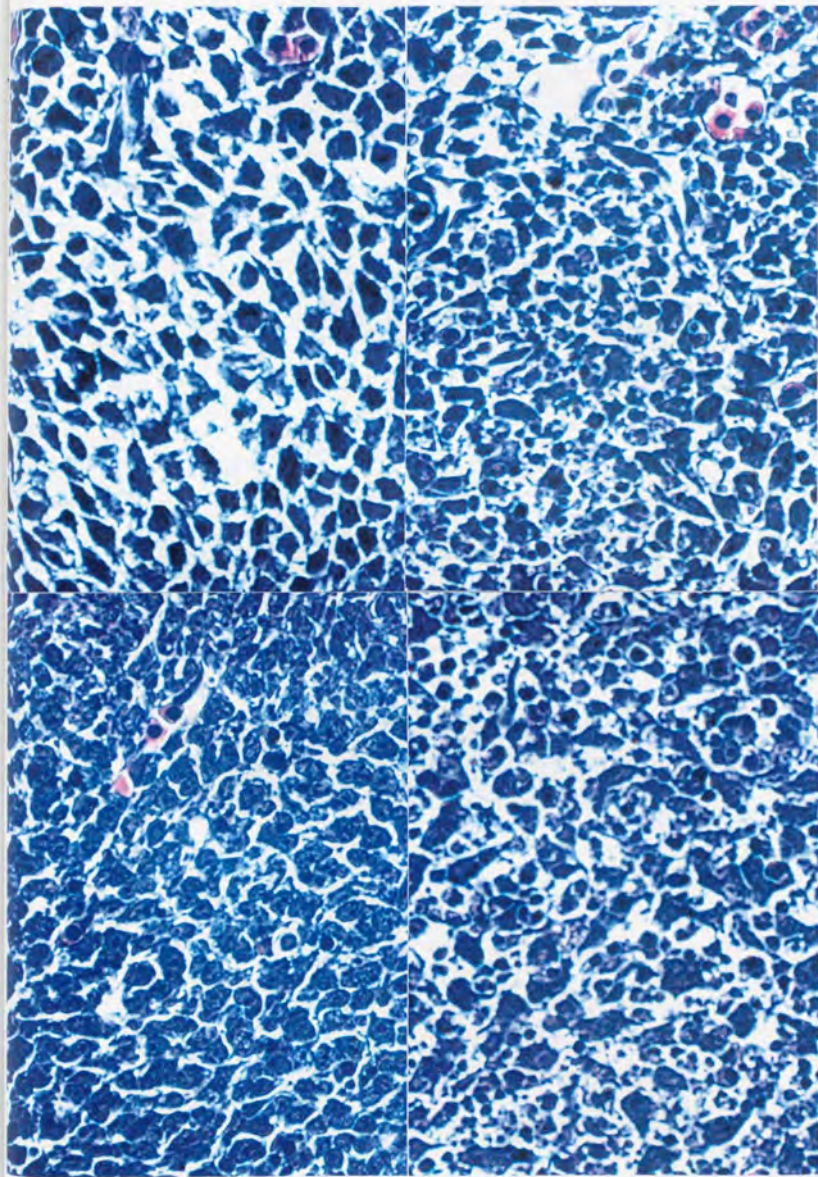
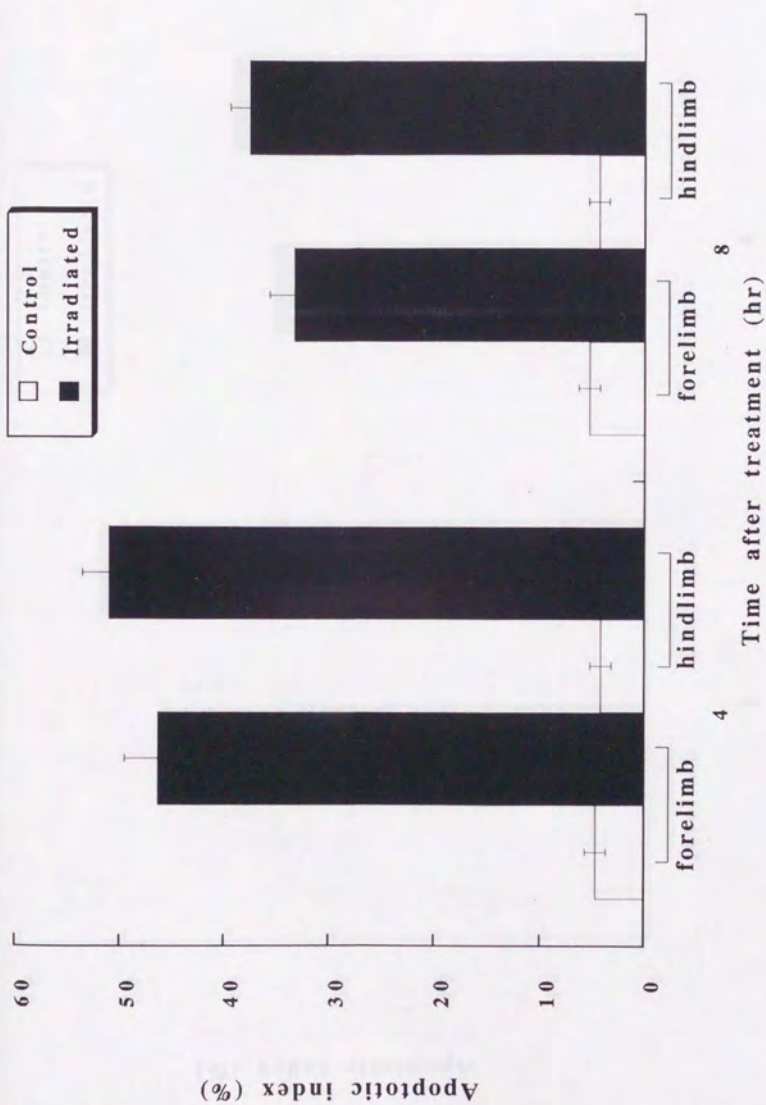
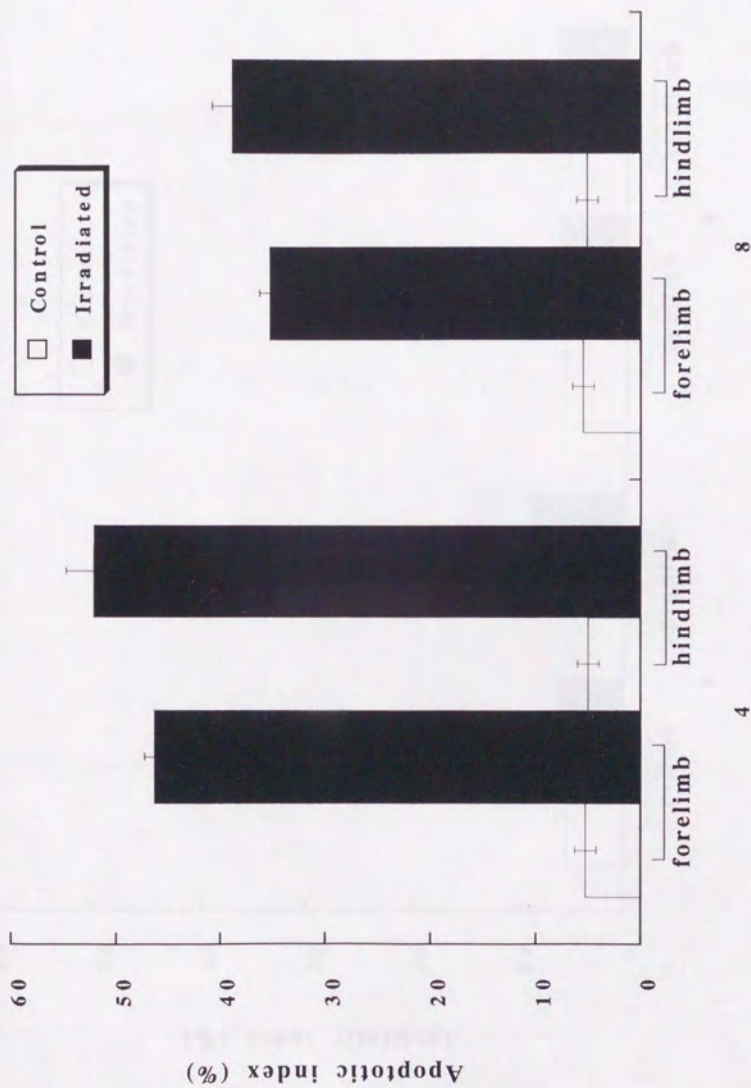


Fig. III-7. Higher magnification light micrographs of mouse E11.5 hindlimb bud sections parallel to the plane.



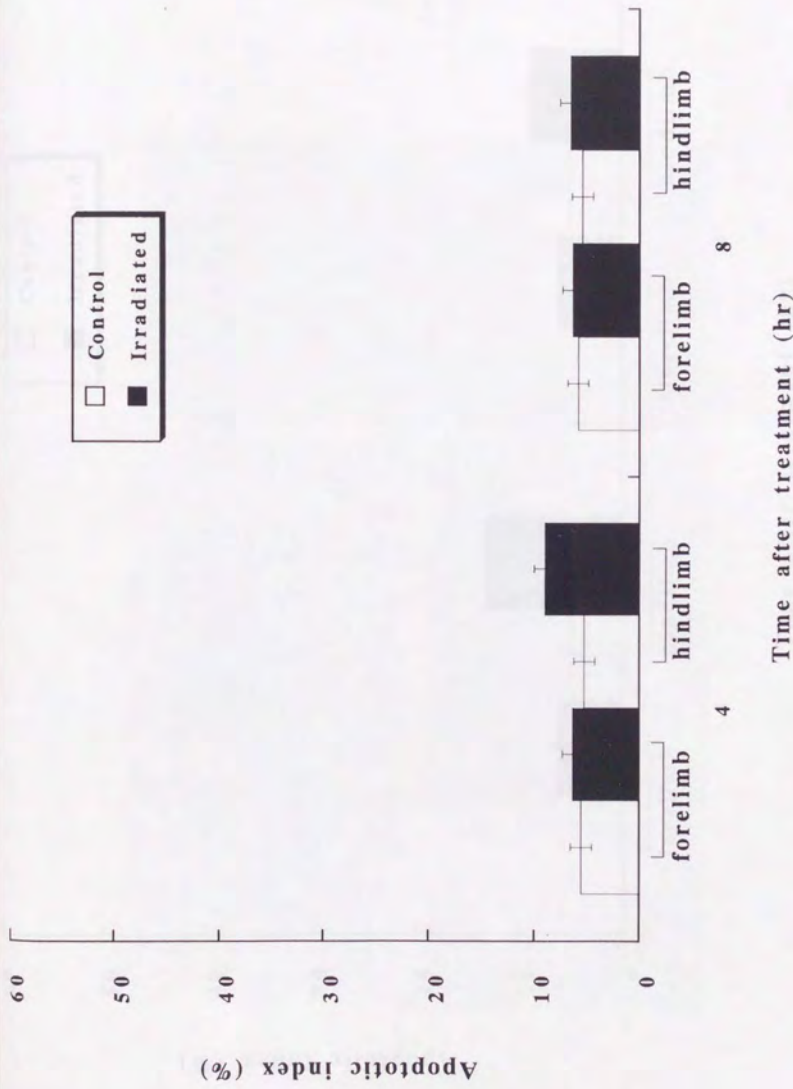
a. Pre-digital mesenchymal tissues of E11 limb buds

Fig. III-8. Apoptosis induction by 5 Gy of X-rays in the pre-digital regions of mouse limb buds.



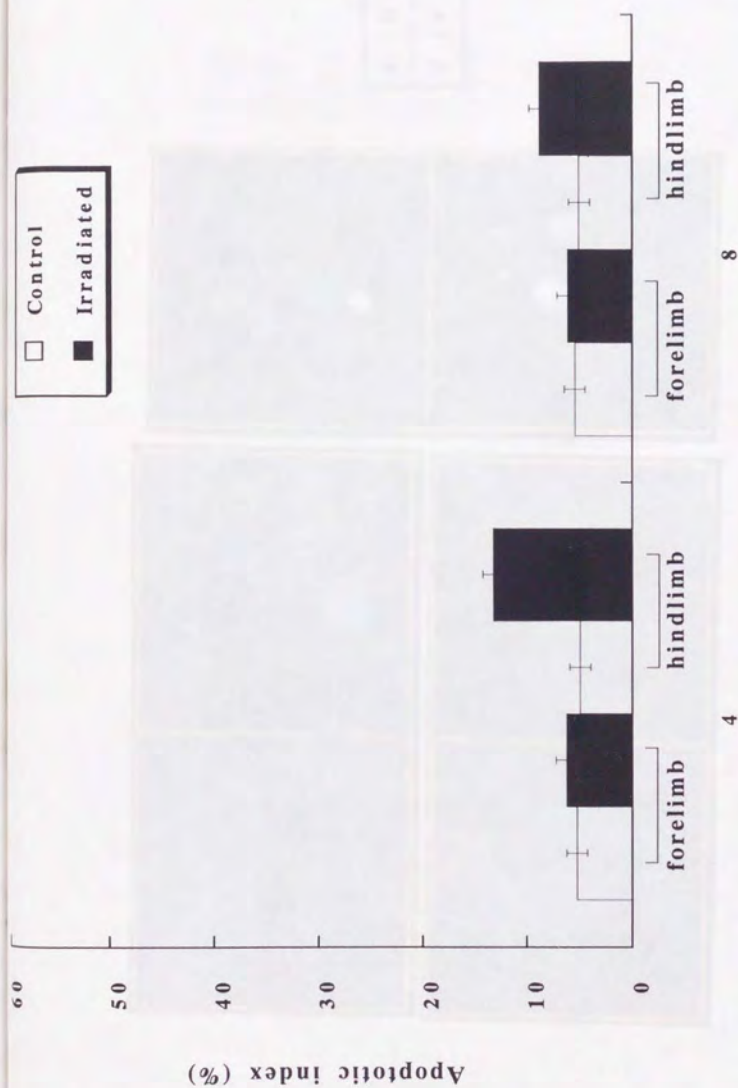
b. Pre-digital mesenchymal tissues of E11.5 limb buds

Fig. III-8. Apoptosis induction by 5 Gy of X-rays in the pre-digital regions of mouse limb buds.



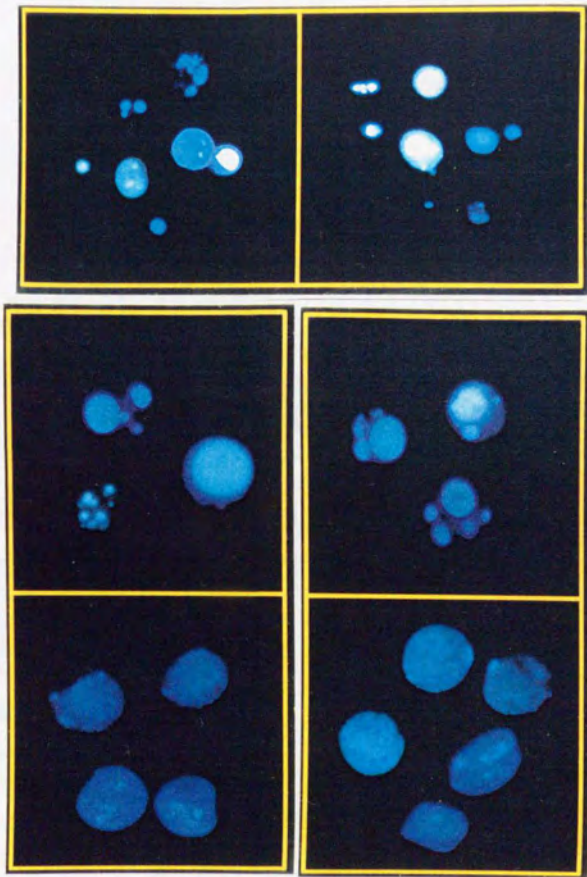
a. Pre-interdigital mesenchymal tissues of E11 limb buds

Fig. III-9. Apoptosis induction by 5 Gy of X-rays in the pre-interdigital regions of mouse limb buds.



b. Pre-interdigital mesenchymal tissues of E11.5 limb buds
 Time after treatment (hr)

Fig. III-9. Apoptosis induction by 5 Gy of X-rays in the pre-interdigital regions of mouse limb buds.



a	b	c
d	e	f

Fig. III-10. Morphological observation of cell nuclei by fluorescent microscopy.

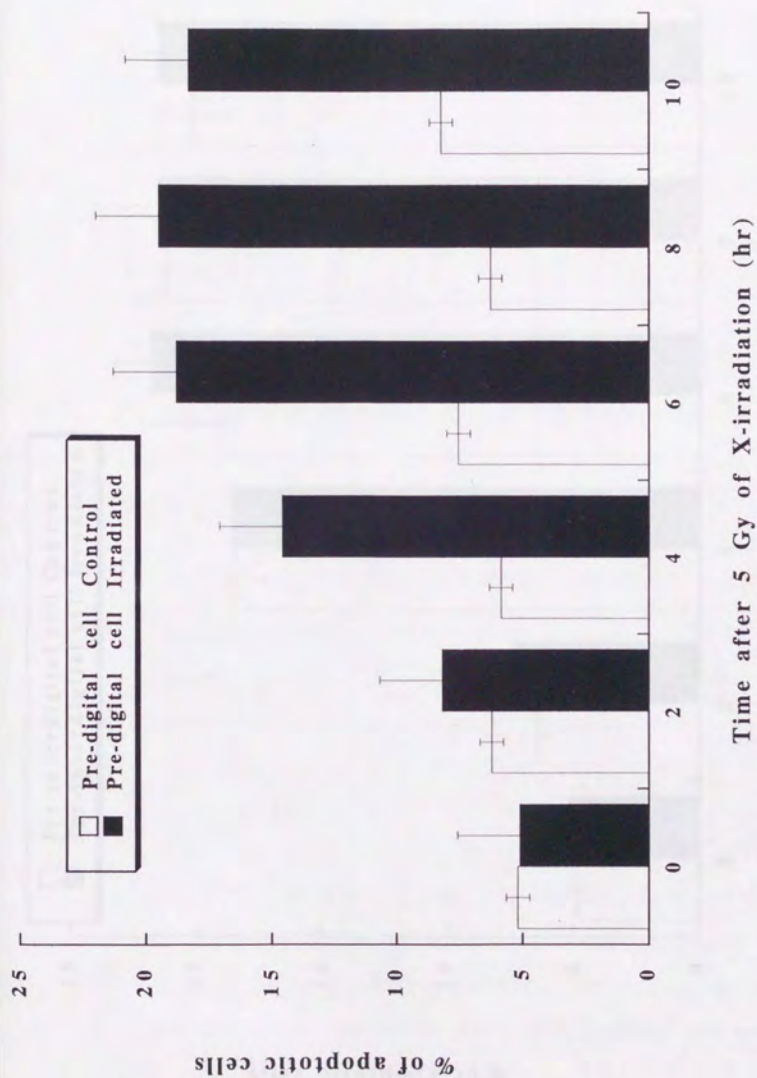


Fig. III-11. Time course curve of apoptotic fractions in the culture of tissues from pre-digital regions of E12 forelimb buds.

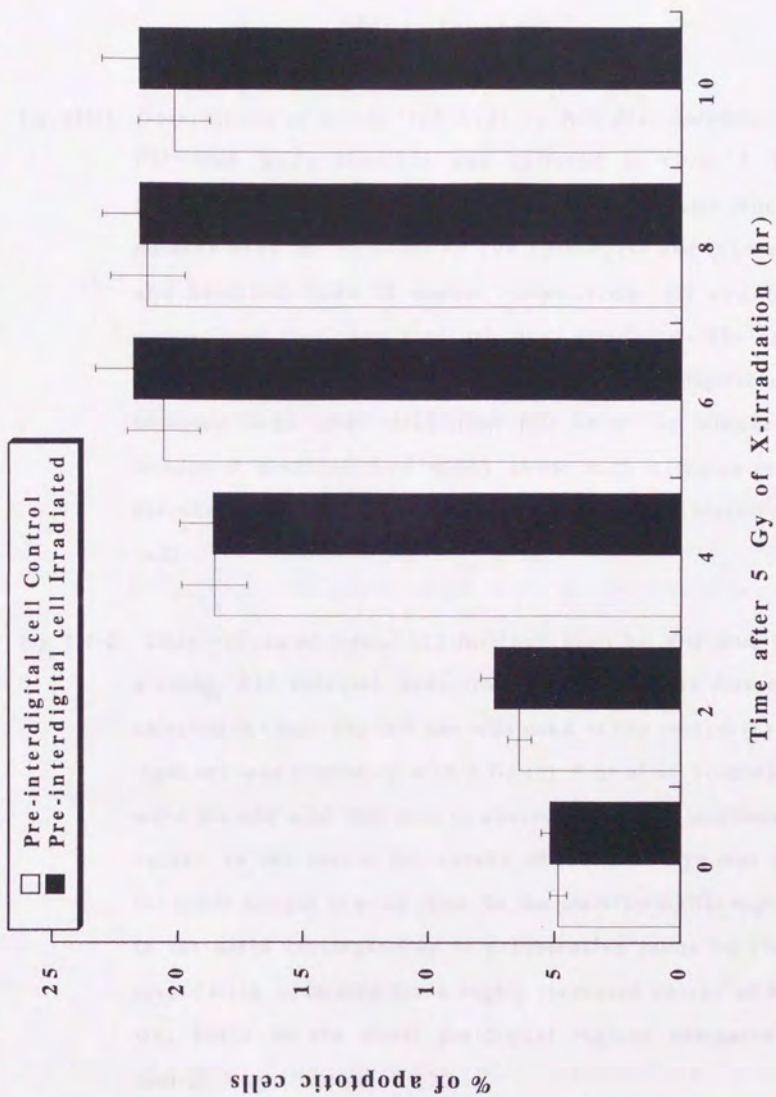


Fig. III-12. Time course curve of apoptotic fractions in the culture of tissues from pre-interdigital regions of E12 forelimb buds.

Figure legends

Fig. III-1. Observations of mouse limb buds by Nile Blue Sulphate staining. E11 limb buds dissected and cultured in vitro. 4 hr after irradiation with 5 Gy, limb buds were stained with Nile Blue to observe dead cell locations by dye uptake. (a) and (b) were fore- and hindlimb buds of control, respectively. (c) and (d) were respectively fore- and hindlimb buds irradiated. The uptake of Nile Blue dye distributed mainly in the distal pre-digital regions of forelimb buds after irradiation (c), while the uptake in the irradiated hindlimb bud didn't show such a region-associated distribution but a relative uniformly distribution. Magnification at $\times 32$.

Fig. III-2. Observations of mouse E12 forelimb buds by Nile Blue Sulphate staining. E12 forelimb buds from the same fetus dissected and cultured in vitro. The left one was used as the control (a) and the right one was irradiated with 5 Gy (b). 4 hr after irradiation, they were stained with Nile Blue to observe dead cell locations by dye uptake. In the control (a), uptake of Nile Blue dye was found in the ulnar margin of hand plate, in the pre-interdigital regions, and in the areas corresponding to presumptive joints on the digital rays. In the irradiated (b), a highly increased uptake of Nile Blue was found in the distal pre-digital regions compared to the control. Magnification at $\times 30$.

Fig. III-3. Light micrographs of mouse E11 and E11.5 limb bud sections parallel to the plane. Limb bud sections were stained with Heamatoxylin and Eosin. (a) E11 forelimb bud, (b) E11 hindlimb bud, (c) E11.5 forelimb bud, and (d) E11.5 hindlimb bud. Magnification was at $\times 80$.

Fig. III-4. Higher magnification ($\times 800$) light micrographs of mouse E11 forelimb bud sections parallel to the plane. Sections were stained with Heamatoxylin and Eosin. (c) pre-digital region, and (d) pre-interdigital sections 4 hr after irradiation with 5 Gy, and (a) and (b) were their controls, respectively.

Fig. III-5. Higher magnification ($\times 800$) light micrographs of mouse E11 hindlimb bud sections parallel to the plane. Sections were stained with Heamatoxylin and Eosin. (c) pre-digital region, and (d) pre-interdigital sections 4 hr after irradiation with 5 Gy, and (a) and (b) were their controls, respectively.

Fig. III-6. Higher magnification ($\times 800$) light micrographs of mouse E11.5 forelimb bud sections parallel to the plane. Sections were stained with Heamatoxylin and Eosin. (c) pre-digital region, and (d) pre-interdigital sections 4 hr after irradiation with 5 Gy, and (a) and (b) were their controls, respectively.

Fig. III-7. Higher magnification ($\times 800$) light micrographs of mouse E11.5 hindlimb bud sections parallel to the plane. Sections were stained

with Heamatoxylin and Eosin. (c) pre-digital region, and (d) pre-interdigital sections 4 hr after irradiation with 5 Gy, and (a) and (b) were their controls, respectively.

Fig. III-8. Apoptosis induction by 5 Gy of X-rays in the pre-digital regions of mouse E11 (a) and E11.5 (b) limb buds.

Fig. III-9. Apoptosis induction by 5 Gy of X-rays in the pre-interdigital regions of mouse E11 (a) and E11.5 (b) limb buds.

Fig. III-10. Morphological observation of cell nuclei by fluorescent microscopy. Images of normal pre-digital and pre-interdigital cells were (a) and (d). 2 hr (b and e) and 4 hr (c and f) after irradiation, some typical apoptotic cells were visualized by Hoechst 33342 fluorescent dye staining. Apoptotic cell was defined morphologically as those cells with densely condensed chromatin.

Fig. III-11. Time course curve of apoptotic fractions in the culture of tissues from pre-digital regions of E12 forelimb buds. Apoptotic cells was scored by cell suspension preparation and its fluorescent microscopy using Hoechst 33342 staining. An increase in number of cells with nucleus chromatin condensation was found 2 hr after radiation with 5 Gy. The apoptotic fractions (%) peaked at 8 hr after radiation and then decreased. In the control, the apoptotic fractions (%) scored a relatively stable value showing a slightly increase trend.

Fig. III-12. Time course curve of apoptotic fractions in the culture of tissues from pre-interdigital regions of E12 forelimb buds. Apoptotic cells was scored by cell suspension preparation and its fluorescent microscopy using Hoechst 33342 staining. An increase in the number of apoptotic cells was found from 2 hr after radiation. The apoptotic fractions (%) reached the maximum about 6 hr after radiation and maintained at a level of 22%. In the control, the apoptotic fractions (%) also showed an increase. There was no difference between the control and the irradiated at any checked time points ($p>0.05$).

References

- Barrach H. J. and D. Neubert. Significance of organ culture techniques for evaluation of prenatal toxicology. *Arch. Toxicol.*, 1980; 45: 161-187.
- Clarke P. G. H. Developmental cell death: Morphological diversity and multiple mechanisms. *Anat. Embryol.*, 1990; 181: 195-213.
- Councouvanis E. C., Martin G. R., and J. H. Nadeau. Genetic approaches for studying programmed cell death during development of laboratory mouse. *Method. Cell Biol.*, 1995; 46: 387 - 440.
- Desbiens X., Revillion-Carette F., Meunier L., and A. Bart. New in vitro procedures for experimental studies on the development of 11-day mouse embryo fore limb buds. *Biol. Cell*, 1987; 60: 145-150.
- Ellis R. E., Yuan J. Y., and H. R. Horvitz. Mechanisms and functions of cell death. *Annu. Rev. Cell Biol.*, 1991; 7: 663-698.
- Fallon J. F. and J. W. Saunders Jr. In vitro analysis of the control of cell death in a zone of prospective necrosis from the chick wing bud. *Dev. Biol.*, 1968; 18: 553-570.
- Friedman L. Teratological research using in vitro systems. II. Rodent limb bud culture system. *Environ. Health Perspect.* 1987; 72: 211-219.
- Fritz-Niggli H. 100 years of radiobiology: implications for biomedicine and future. *Experientia.* 1995; 51(7): 652-64.
- Hurle J. M. Cell death in the developing systems. *Methods Achiev. Exp. Pathol.*, 1988; 13: 55-86.
- Lessmollmann U., Hinz N., and D. Neubert. In vitro system for toxicological studies on the development of mammalian limb buds in a chemically defined medium. *Arch. Toxicol.*, 1976; 36: 169-176.

- Li Y., Sharov V. G., Jiang N., Zaloga C., Sabbah H. N., and M. Chopp. Ultrastructural and light microscopic evidence of apoptosis after middle cerebral artery occlusion in the rat. *Am. J. Pathol.*, 1995; 146(5): 1045-1051.
- Michel C. Radiation embryology. *Experientia*, 1989; 45: 69-77.
- Milare J. and J. Mulnard. Histogenesis in 11-day mouse embryo limb buds explanted in organ culture. *J. Exp. Zool.*, 1984; 232: 359-377.
- Mori C., Nakamura N., Kimura S., Irie H., Takigawa T., and K. Shiota. Programmed cell death in the interdigital tissue of the fetal mouse limb is apoptosis with DNA fragmentation. *Anat. Record*, 1995; 242: 103-110.
- Saunders J. W. Jr. and J. F. Fallon. Cell death in morphogenesis. In: *Major problem in developmental biology*. Ed. M. Locke. Academic Press. New York 1967, pp 289-314.
- Tone S., Tanaka S., and Y. Kato. The inhibitory effect of 5-bromodeoxyuridine on the programmed cell death in the chick limb. *Develop., Growth and Differ.*, 1983; 25(4): 381-391.
- Tone S. Limb bud organ and tissue culture. In: *The latest experimental methods for apoptosis research*. Ed. Tsujimoto Y., Tone S., and Yamada T. Youdosya Press. Tokyo, 1995. pp 124-129.
- UNSCEAR. UNSCEAR report: Sources and effects of ionizing radiation. Annex J. Developmental effects of radiation in utero. United Nations, New York 1977. pp 655-725.
- Wyllie A. H., Kerr J. F. K., and A. R. Currie. Cell death: The significance of apoptosis. *Int. Rev. Cytol.*, 1980; 68: 215-316.
- Zakeri Z. F. and H. S. Ahuja. Apoptotic cell death in the limb and its relationship to pattern formation. *Biochem. Cell Biol.*, 1994; 72:603-613.

General discussion and conclusion

Apoptosis plays a key role in morphogenesis and in the regulation of cell populations in embryos (Sanders and Wride 1995). Its significance is highlighted by alterations of cell death that create numerous developmental abnormalities. The normal development of mouse limbs and spontaneous cell death during morphogenesis have been widely studied (Zakeri and Ahuja 1994). The limb is an excellent model to study the mechanisms of radiation teratogenesis during development.

In order to clarify the role and mechanisms of apoptosis in the radiation-induced teratogenesis in ICR mouse limb bud irradiated at the day 11 (E 11) and 11.5 (E11.5), I used three different systems in the present study: micromass culture system (Chapter I), limb buds *in utero* (Chapter II), and organ and tissue culture system (Chapter III).

Experiments using the cell micromass culture system showed that radiation inhibited cellular differentiation (ID50, 5.2 Gy) more effectively than cellular proliferation (ID50, 6.1 Gy). Cells irradiated died typically via apoptosis, which was identified both biochemically and morphologically. Induction of apoptosis by X-irradiation was dose-dependent. Cells from different embryonic ages underwent spontaneous and radiation-induced apoptosis with different time courses. X-irradiation induced a higher level of p53 protein in the irradiated cells, on the other hand, such a high p53 level was not found in cells underwent spontaneous apoptosis.

Results indicated that (1) extensive apoptosis was induced by radiation in addition to the spontaneous apoptosis in the mouse limb buds, (2) the existence of cells with different radiosensitivities in the limb buds, (3) the

cells at E11 were more sensitive to radiation-induced apoptosis than the cells at E 11.5 and (4) mechanisms for the radiation-induced apoptosis were different from that for spontaneous apoptosis in limb buds.

In the limb bud irradiated *in utero*, radiation induced apoptosis was identified morphologically, histochemically and biochemically. Two kinds of morphologically different cells were found in the pre-digital and pre-interdigital mesenchymal tissue areas in forelimb bud sections. Spontaneous apoptosis occurred mainly in the pre-interdigital areas. A significant increase in number of the apoptotic cells was found, which located in the pre-digital areas of the irradiated forelimb and hindlimb buds, while there was only a slight increase in apoptotic cells in the pre-interdigital areas of the irradiated forelimb bud. Increase in apoptotic cells in pre-interdigital area was significantly lower than that for the pre-digital regions in hindlimb buds. A significantly higher percentage of p53 protein positively stained cells were found in the pre-digital areas of the forelimb buds after radiation.

All fetuses that survived after exposure to 5 Gy of X-rays at E11 and E11.5 showed congenital limb malformation on E19. The teratogenic effect of radiation was much greater on hindlimbs (mainly ectrodactyly) than that on forelimbs (mainly aplangy). The severity difference of malformation between the fore- and the hindlimb buds might be due to the difference in developmental stage at the time of irradiation. There was relatively higher percentage of the cells that had not yet been committed to undergo spontaneous apoptosis in the hindlimb buds than that of the forelimb buds at the time of radiation exposure. The above-mentioned results were schematically illustrated in Figure showing the locations of radiation-induced apoptosis and spontaneous apoptosis as well as the final defects of limbs.

For the limb bud organ culture system, the dissected E11 and E11.5 limb buds or E12 limb bud tissues were cultured on the filters in chemically defined medium for half a day. Nile Blue staining showed an increase in dye-stained cells that were distributed mainly in the distal areas of pre-digital mesenchymal tissues of forelimb buds after irradiation. Experimental results obtained from this organ culture system confirmed the findings obtained with the *in utero* experiments mentioned above.

The tissue culture experiments showed that pre-digital mesenchymal cells were highly radiosensitive. No significant effect by radiation was found on the induction of apoptosis in the pre-interdigital mesenchymal tissue cultures.

All these results indicated that (1) Radiation exerted its teratogenic effect on the limb bud morphogenesis during embryogenesis via induction of apoptosis. (2) Cells of different developmental stages possessed different radiosensitivities. (3) a cell population located in the pre-digital mesenchymal tissues of forelimb buds were radiosensitive and they underwent easily radiation-induced apoptosis. These cells probably would undergo proliferation and differentiation in the subsequent developmental stages. (4) Cells that located in pre-interdigital mesenchymal tissues of limb buds were composed of many radioresistant cells and hardly underwent radiation-induced apoptosis. They were probably committed to undergo spontaneous apoptosis when irradiated. (5) Spontaneous apoptosis and the radiation-induced apoptosis may involve different molecular mechanisms since an overproduction of p53 protein occurred only in the radiation-induced apoptosis but not in the spontaneous apoptosis.

Radiation-induced apoptosis gave a further explanation to the well-

known rule of Bergonié and Tribondeau: Radiation induced apoptotic cell death, preferably to the cells that would undergo proliferation and differentiation but not to the cells of which DNA synthesis and differentiation were stopped. This led to radiation killing of cells relates proportionally to cellular proliferation activity and inversely to degree of cellular differentiation.

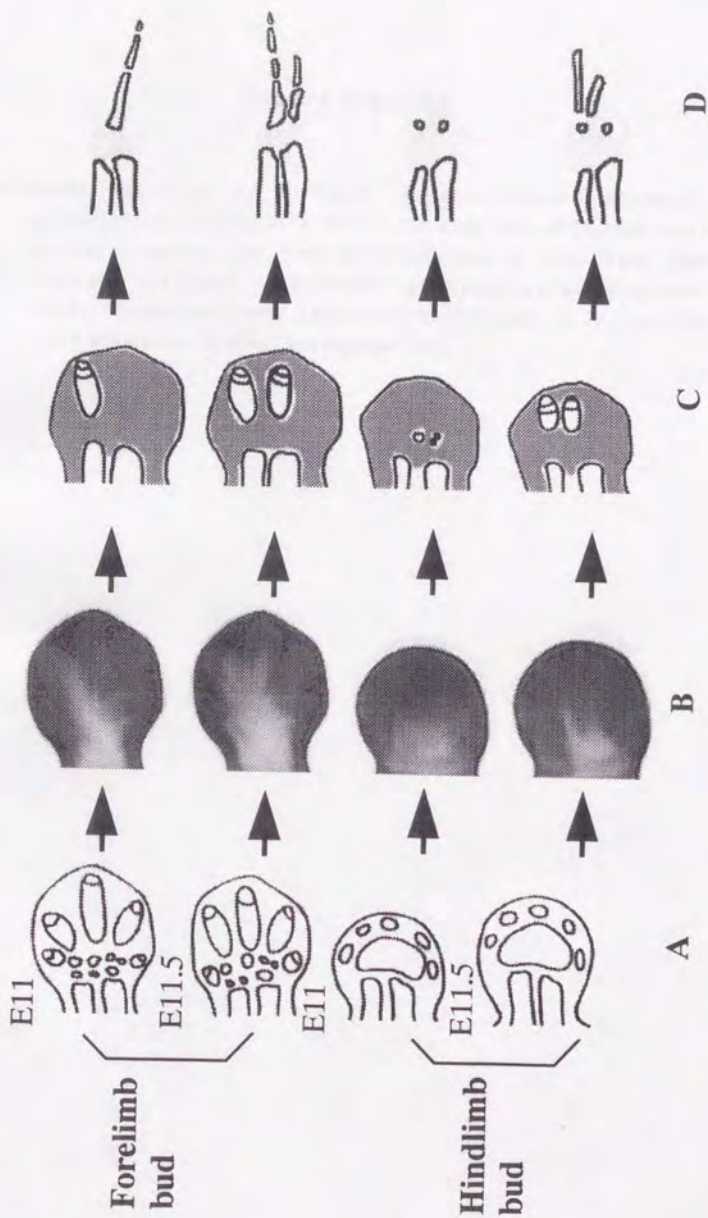
The most important result of the present study was cellular level findings explaining radiation teratogenesis in the mouse limb buds in the followings: (1) Radiation-induced apoptosis occurred, preferably in the pre-digital mesenchymal cells of limb buds during its morphogenesis. (2) The mesenchymal cells died via radiation-induced apoptosis in the pre-digital regions led to the failure of normal digital morphogenesis. The severity depended on both the limb bud developmental stage when being irradiated and the radiation dosage. (3) Radiation-induced apoptosis was responsible for the congenital limb malformations.

Results also provided us with an interesting paradox for further understanding of the mechanisms of radiation effects on the development and of radiation teratogenesis. When the embryos were exposed to radiation at their pre-implantation period and early period of organogenesis, a high incidence of prenatal death could be induced (Russell and Russell 1957). Recent studies indicated that these prenatal deaths were due to radiation-induced a high rate of apoptotic cell death in the embryos (Norimura *et al.* 1996). Because radiation induced a high rate of prenatal death via induction of apoptosis, it showed a preventive function against the incidence of congenital malformation. When the embryos were exposed to radiation at their late organogenesis period, paradoxically, radiation-induced apoptosis

could lead to congenital malformations.

References

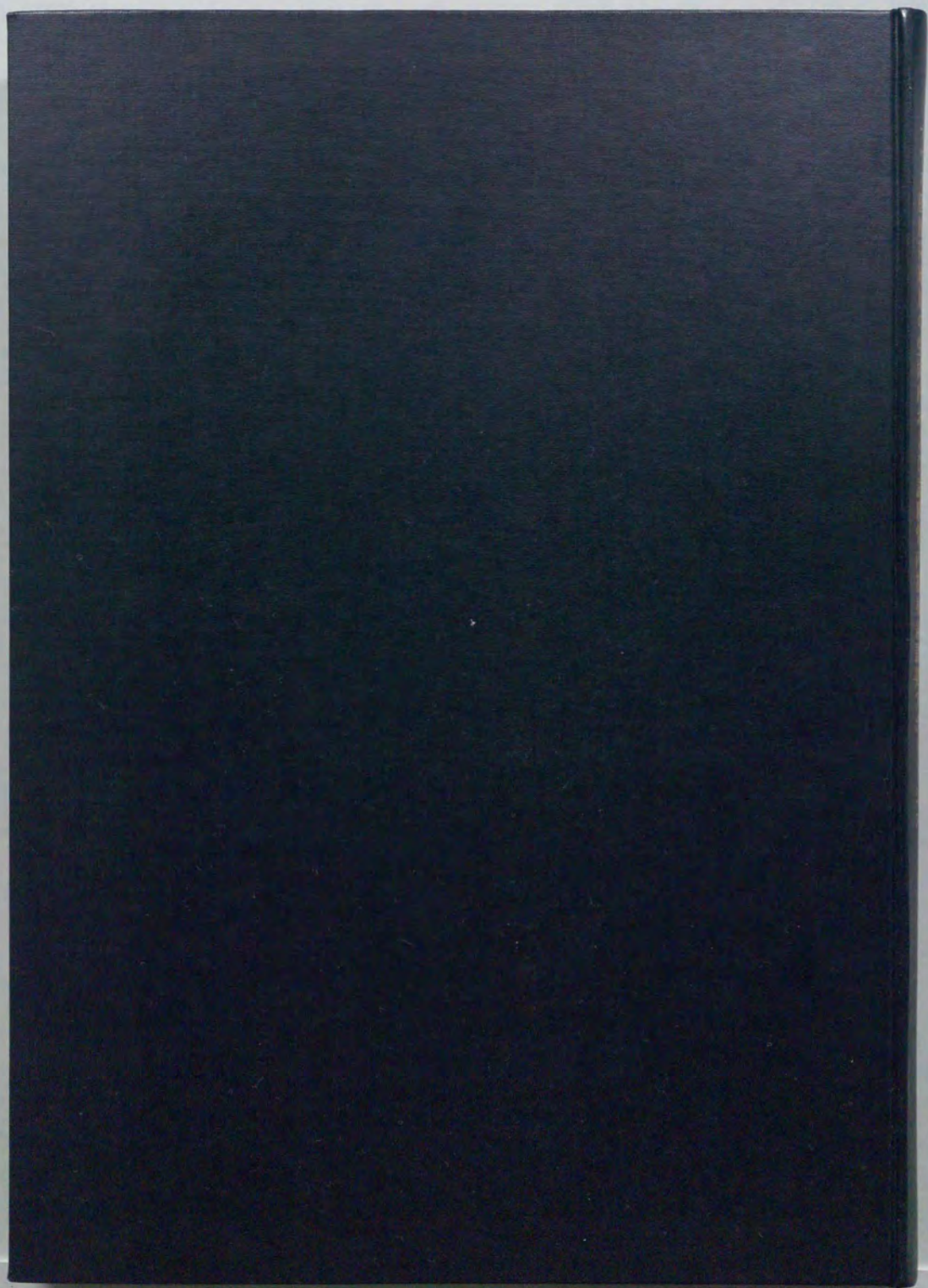
- Norimura T., Nomoto S., Katsuki M., Gondo Y., and S. Kondo. p53-dependent apoptosis suppresses radiation-induced teratogenesis. *Nature Med.*, 1996; 2(5): 577-580.
- Russell L. B. and W. L. Russell. An analysis of the changing radiation response of the developing mouse embryo. *J. Cell Physiol.*, 1957; 43(suppl 1): 1030-1049.
- Sanders E. J. and M. A. Wride. Programmed cell death in development. *Int. Rev. Cytol.*, 1995; 163: 105-173.
- Zakeri Z. F. and H. S. Ahuja. Apoptotic cell death in the limb and its relationship to pattern formation. *Biochem. Cell Biol.* 1994; 72:603-613.



Figure

Figure legends

Fig. Schematic drawings of locations of radioinduced apoptosis and spontaneous apoptosis in limb buds and final defects of the limbs. A: Fate maps at the time of irradiation. B: Cell death. Dots and shadow indicated distribution of spontaneous apoptosis and radioinduced apoptosis, respectively. C: Defects in the presumptive limb elements. D: Final malformations.





Kodak Color Control Patches

Blue Cyan Green Yellow Red Magenta White 3/Color Black

Kodak Gray Scale

A 1 2 3 4 5 6 M 8 9 10 11 12 13 14 15 B 17 18 19



© Kodak, 2007 TM Kodak